A MOLECULAR PRINTBOARD ON GLASS

PROEFSCHRIFT

ter verkrijging van

de graad van doctor aan de Universiteit Twente,

op gezag van de rector magnificus,

prof. dr. F. A. Van Vught,

volgens besluit van het College voor Promoties

in het openbaar te verdedigen

op vrijdag 8 oktober 2004 om 16.45 uur

door

Steffen Onclin

geboren op 11 februari 1975

te Groningen

Dit proefschrift is goedgekeurd door:

Promotor: Prof. dr. ir. D. N. Reinhoudt
Assistent-promotor: Dr. B. J. Ravoo

Contents

Chapter 3

Molecular printboards: Monolayers of *β*-cyclodextrins on silicon oxide

Chapter 4

Patterning of *β*-cyclodextrin monolayers with divalent fluorescent guests   **71**

Chapter 5

Immobilized dendrimer boxes for the encapsulation of anionic dyes   **91**

Chapter 1

Introduction

Nanotechnology is not a discipline, like chemistry or physics, but rather a tool kit for manipulating matter at its smallest scale.[1] It is fueled by the constant drive for miniaturization, which is believed will revolutionize fields like electronics[2,3] and biotechnology[4-6] in the near future. For decades, miniaturization has meant reducing the size of devices using existing technologies, the so-called top-down approach. It is expected that this trend will be broken in the coming decades, as conventional lithographic techniques reach their physical and economical limits.[7,8]

Nature practices the opposite trend. Starting from the smallest defined building blocks, atoms and molecules, increasingly complex systems are built. Inspired by this, researchers in fields like supramolecular chemistry, polymer chemistry, and biomolecular chemistry are able nowadays to assemble synthetic molecular systems with dimensions that start to overlap with the levels of miniaturization, suggesting that

bottom-up approaches to nanofabrication will soon be able to compete with the top-down approach.[9]

To create working devices that can be linked to the outside world, connection to a surface is usually required. Recent developments have led to the fabrication of molecular circuits,[3,10] and nanoscale bioarrays[11-13] on surfaces. Therefore, the ability to organize functional molecular assemblies on surfaces will have a prominent place in bottom-up techniques. One straightforward way to engineer surfaces is by employing self-assembled monolayers (SAMs).[14] SAMs are monomolecular layers that form spontaneously on a surface and possess a high degree of ordering. SAMs on surfaces like gold[15] and SiO_2[16] have been investigated intensely in recent years and have reached a high level of sophistication, enabling the use of SAMs as platforms for nanofabrication.[17,18]

The research described in this thesis is aimed at the use of functional SAMs on SiO_2 surfaces as well-defined platforms onto which molecules can be assembled. The immobilization of functional molecules onto these SAMs is based on non-covalent, supramolecular interactions. More specifically, the host-guest binding motif of β-cyclodextrins with suitable guest molecules is employed. The main advantages of this supramolecular approach are the high specificity of the interactions, and the ability to tune the interaction strength of immobilized molecules with host monolayers by the chemical design of the guest molecules.

Chapter 2 describes a literature overview of SAMs on SiO_2 and covers the aspects of monolayer formation and subsequent derivatization. Specific attention is given to the application of SAMs on SiO_2 in nanotechnology.

In Chapter 3, the preparation and characterization of β-cyclodextrin host monolayers on SiO_2 is described. These host monolayers have been employed to assemble functional molecules on a surface, based on specific supramolecular interactions. The binding properties of β-cyclodextrin monolayers on SiO_2 have been examined by desorption experiments using a fluorescent guest molecule.

Chapter 4 introduces the use of β-cyclodextrin monolayers as a molecular printboard. Utilizing readily accessible lithographic techniques such as microcontact printing and dip-pen nanolithography the assembly of patterns of fluorescent guest molecules on this molecular printboard has been examined. Working on the SiO_2 surface allows direct visualization of the fluorescent patterns by laser-scanning confocal microscopy. Using this technique, the stability of the generated patterns is

discussed. In addition, fluorescence spectroscopy allows for quantification of the amount of guest molecules at a surface. Assembly from solution has been compared to deposition by microcontact printing.

Chapter 5 describes the immobilization of dendrimer molecules on the molecular printboard. Dendrimer molecules are known to encapsulate suitable guests in their interior. Here, the encapsulation behavior has been studied on a surface using anionic dyes as guest molecules and the immobilized dendrimers as molecular boxes. Several characteristics of the encapsulation process have been explored and monitored by laser-scanning confocal microscopy. In addition, single molecule spectroscopy measurements on individual immobilized dendrimer molecules, filled with anionic dyes, have been performed.

In Chapter 6, the immobilization of dendrimer molecules is used to template the electroless deposition of metals. Dendrimers have been employed to ligate metal ions, which upon reduction form dendrimer-stabilized metal colloids that could catalyze electroless deposition. Two strategies have been explored to prepare dendrimer-stabilized colloid patterns on the molecular printboard. Subsequent electroless deposition resulted in micrometer-sized metal patterns on an insulating surface.

Chapter 7 describes the application of SAMs in microfluidics networks. Monolayer-functionalized microfluidics devices have been used for optical sensing of acidity. Rhodamine B-derivatized monolayers, which were able to switch reversibly between a fluorescent and a non-fluorescent state depending on the acidity of the organic solution inside the microchannel, have been immobilized onto the walls of glass-fabricated microchannels. In addition, a hybrid system, consisting of glass and PDMS, has been employed to attach an Oregon Green dye to the glass surface. This system responded to changes of the pH of *aqueous* solutions by changing its fluorescent properties.

1.1   References

[1]   Service, R. F. *Science* **2004,** *304*, 1732-1734.

[2]   Gittens, D. I.; Bethell, D.; Schriffrin, D. J.; Nichols, R. J. *Nature* **2000,** *408*, 67-69.

[3]   Service, R. F. *Science* **2001,** *294*, 2442-2443.

[4]   Niemeyer, C. M. *Science* **2002,** *297*, 62-63.

[5]   Roco, M. C. *Curr. Opin. Biotechnol.* **2003,** *14*, 337-346.

[6]   Sarikaya, M.; Tamerler, C.; Jen, A. K. Y.; Schulten, K.; Baneyx, F. *Nat. Mater.* **2003,** *2*, 577-585.

[7]   Wallraf, G. M.; Hinsberg, W. D. *Chem. Rev.* **1999,** *99*, 1801-1821.

[8]   Ito, T.; Okazaki, S. *Nature* **2000,** *406*, 1027-1031.

[9]   Gimzewski, J. K.; Joachim, C. *Science* **1999,** *283*, 1683-1688.

[10]   Collier, C. P.; Mattersteig, G.; Wong, E. W.; Luo, Y.; Beverly, K.; Sampaio, J.; Raymo, F. M.; Stoddart, J. F.; Heath, J. R. *Science* **2000,** *289*, 1172-1175.

[11]   Lee, K.-B.; Park, S.-J.; Mirkin, C. A.; Smith, J. C.; Mrksich, M. *Science* **2002,** *295*, 1702-1705.

[12]   Zhang, H.; Lee, K. B.; Li, Z.; Mirkin, C. A. *Nanotechnology* **2003,** *14*, 1113-1117.

[13]   Lynch, M.; Mosher, C.; Huff, J.; Nettikadan, S.; Johnson, J.; Henderson, E. *Proteomics* **2004,** *4*, 1695-1702.

[14]   Ulman, A. *An Introduction to Ultrathin Organic Films*. Academic Press: Boston, 1991.

[15]   Nuzzo, R. G.; Allara, D. L. *J. Am. Chem. Soc.* **1983,** *105*, 4481-4483.

[16]   Sagiv, J. *J. Am. Chem. Soc.* **1980,** *102*, 92-98.

[17]   Liu, S.; Maoz, R.; Sagiv, J. *Nano Lett.* **2004,** *4*, 845-851.

[18]   Rawlett, A. M.; Hopson, T. J.; Amlani, I.; Zhang, R.; Tresek, J.; Nagahara, L. A.; Tsui, R. K.; Goronkin, H. *Nanotechnology* **2003,** *14*, 377-384.

Chapter 2

Engineering the Silicon Oxide Surface

using Self-Assembled Monolayers

2.1   Introduction

Self-assembled monolayers (SAMs) are monomolecular thin films of adsorbates assembled at an appropriate surface. The most well-known adsorbate/substrate combinations are sulfur-containing molecules on gold,[1] and alkylsilanes on silicon oxide (SiO_2) surfaces.[2] Of these two the first combination has received by far the most attention, presumably because the preparation of these SAMs is simple, reproducible, and tolerates a large number of functional groups for further derivatization. However, alkylsilane SAMs on SiO_2 constitute a class of monolayers that possess some advantageous features. Due to the covalent nature of the assembly process they display superior stability, which allows extensive handling and post-modification steps without deterioration of the monolayer. In addition, these SAMs

are compatible with silicon technology and allow for the use of optical techniques, like fluorescence spectroscopy, as read-out methods.

Since the pioneering work of Sagiv and co-workers in the 1980s,[2-11] the field of SAMs on SiO_2 surfaces has grown tremendously. In little more than two decades studies have progressed from a basic understanding of the self-assembly process to the application of SAMs in many fields like (bio)chemical sensing and nanotechnology. This chapter will review the modification of SiO_2 surfaces with alkylsilane molecules. Chapter 2.2 will discuss the mechanism of the assembly process in detail. An overview of functional groups that have been introduced and reactions that were performed on SAMs will be given in Chapter 2.3, together with the application of SAMs in (bio)chemical sensing. Finally, an overview of techniques that are available to engineer the modified SiO_2 surface is presented in Chapter 2.4.

2.2 SAMs on SiO_2

2.2.1 Mechanism of formation

There has been much debate on how SAMs on SiO_2 are formed. Especially in the late 1980s and 1990s, when the field started to grow rapidly, many fundamental studies were performed in order to present a clear picture of the mechanism of monolayer formation and to achieve procedures that could guarantee reproducibility. It soon became apparent that several parameters are important in monolayer formation and especially the role of water has been investigated thoroughly. The first SAM of octadecyltrichlorosilane (OTS) molecules was reported by Sagiv.[2] He recognized that water on the surface was necessary to hydrolyze the chlorosilane molecules and assumed that the hydrolyzed molecules would undergo condensation reactions with the surface hydroxyl groups[12] and other OTS molecules to form a polymerized network of molecules in which each OTS molecule is covalently anchored to the surface. This view on the self-assembly process had to be adjusted when Finklea and co-workers discovered that organized monolayers of OTS could also be formed on the gold surface, a surface devoid of hydroxyl groups.[13] They concluded that the self-assembly took place on the adsorbed water film on the gold substrate, the silyl head groups being incorporated into a two-dimensional cross-linked network of Si-O-Si bonds. Later, this was confirmed by Allara *et al.*[14] Also the observation of a lower roughness of silanized wafers than that of unmodified wafers, as observed in X-ray

reflectivity experiments by Silberzan and co-workers, indicated that not all molecules are individually linked to the surface, but rather form a cross-polymerized net of molecules with only a few bonds to the surface.[15] This theory was supported by the IR studies of Tripp and Hair.[16,17] In a low-frequency study they found that the adsorbed species form few, if any, Si-O-Si bonds with the surface.

A general consensus exists that trace amounts of water are essential for the formation of well-packed monolayers. Several studies even reported that the quality of SAMs increases with the degree of hydration of the substrate.[16,18-21] SAMs formed on dry SiO₂ surfaces are generally of poor quality. IR data suggested that a uniform film containing disordered alkyl chains was formed.[18] Tripp and Hair showed that OTS in carbon tetrachloride does not react at all with the surface in the absence of moisture.[16,22] Rye and co-workers compared the saturation coverage of octadecyldimethylchlorosilane (ODMS) and OTS.[23] For hydrated surfaces, the ODMS coverage was approximately a third of the OTS coverage. In contrast, when the substrates were vacuum-baked prior to self-assembly the saturation coverages were comparable. They attributed this to coupling reactions being limited to the surface hydroxyl groups.

The same authors proposed a model of a growing crystallite resulting from the reaction of an alkyltrichlorosilane with oxidized silicon having a thin water layer.[23,24] The model is shown in Figure 2.1. It shows alkane chains that are forced into close proximity by the covalent bonds of the Si-O-Si framework and not by the alkane chain interaction. A Si-Si nearest neighbor distance of 3.5 Å was used in the construction of the model and the circles around the hydrocarbon chains represent the 2 Å Van der Waals radius for linear hydrocarbon chains. They claim that the steric crowding, imposed on the alkane chains could be reduced by tilting relative to the surface normal. However, in a modeling study by Stevens it was shown that cross-polymerization, which had been thought to be an essential element in the formation of stable SAMs on SiO₂, cannot occur for fully covered monolayers.[25] The reason for this is of a steric nature. One problem with the organization in a monolayer, as shown in Figure 2.1, is that the covalent bonds are substantially shorter than the Van der Waals diameters. The maximum distance between Si atoms of the Si-O-Si bond is 3.2 Å, while the Van der Waals diameter for C is 3.5 Å. When the hydrogens of the hydrocarbon chain are also taken into account, the overlap is even larger. The nearest neighbor hydrogen atoms are 1.5 Å apart, while the Van der Waals diameter for H

bonded to C is 2.5 Å. Moreover, cross-polymerization would yield an area per chain of around 11 Å^2, which is not observed. Instead, the experimentally observed area per chain of 21-25 Å^2 [26-31] is more consistent with the area per chain of 20-24 Å^2 that was found for hexagonally close-packed OTS Langmuir-Blodgett layers,[32,33] indicating that SAMs on SiO$_2$ are closely related to Langmuir-Blodgett layers. The same authors conducted a comparative study between OTS monolayers prepared by the Langmuir method and the chemisorption method.[34] Their findings were that OTS molecules in the Langmuir monolayer were less tilted (ca. 8-10˚) than their chemisorbed analogs (15-17˚) and also slightly better ordered, as concluded from the spacing of the molecules. Summarizing, it seems reasonable to conclude that SAMs on SiO$_2$ are very similar to Langmuir-Blodgett layers and that the reduced ordering could be explained by a certain degree of cross-polymerization. This most likely accounts for the fact that no long-range order is observed.
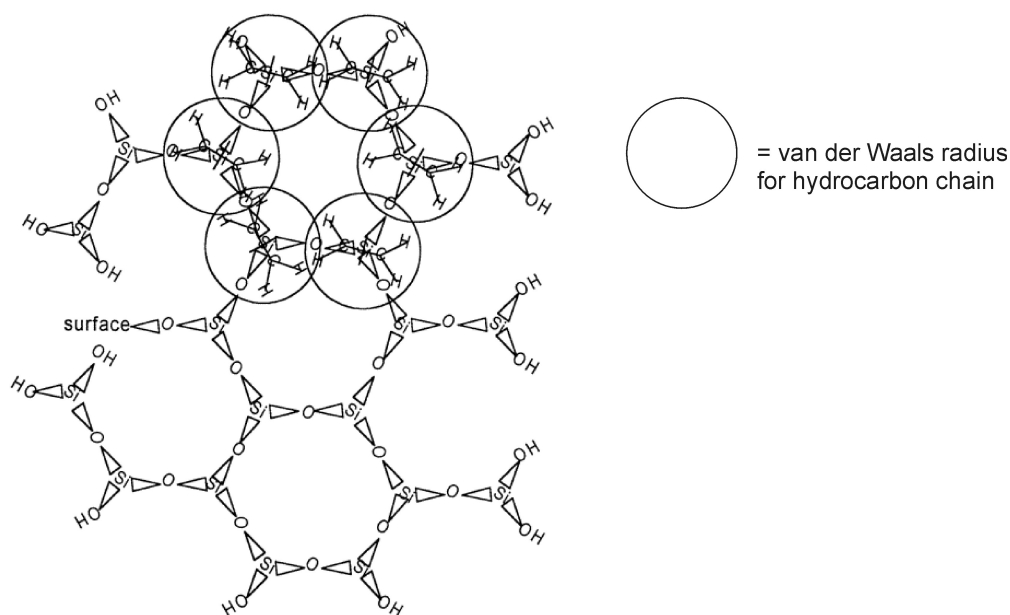
Figure 2.1 *Model of a growing monolayer crystallite resulting from reaction of an alkyltrichlorosilane with oxidized silicon.*[24]

Recently, Wang and co-workers reported a method to grow ultrasmooth OTS monolayers on native SiO$_2$.[35] By comparing the deposition of OTS under 'dry' and 'wet' conditions, they concluded that growth occurs by different mechanisms. Using dry hydrophobic solvents, where water was only present as a thin layer on the surface and not in solution, true monolayers could be grown with an RMS roughness of ~ 1 Å

in 2 days, a much longer deposition time than usually applied. Instead, under 'wet' conditions OTS formed flat aggregates in solution, which subsequently adsorbed onto the substrate. Because the aggregates were preformed in solution, they covered the substrate much faster than under 'dry' conditions, but were not able to form a smooth monolayer. The role of solvents on the self-assembly process was systematically investigated by McGovern *et al.*[36] They found that aromatic solvents like toluene, which are able to extract significant amounts of water from the substrate, yielded the densest OTS films in 1 h and postulated that hydrolysis of OTS took place in solution rather than at the surface, which was commonly assumed until then.

The study of partially formed monolayers is important for better understanding the self-assembly process and it was a topic of controversy during the 1980s and early 1990s. Sagiv and co-workers suggested that monolayers are formed through island structures, as suggested by Fourier transform infrared (FT-IR) data on partially formed SAMs,[6,9] while others concluded that disordered homogeneous incomplete monolayers are formed.[26,28,37-39] Both processes are schematically shown in Figure 2.2.
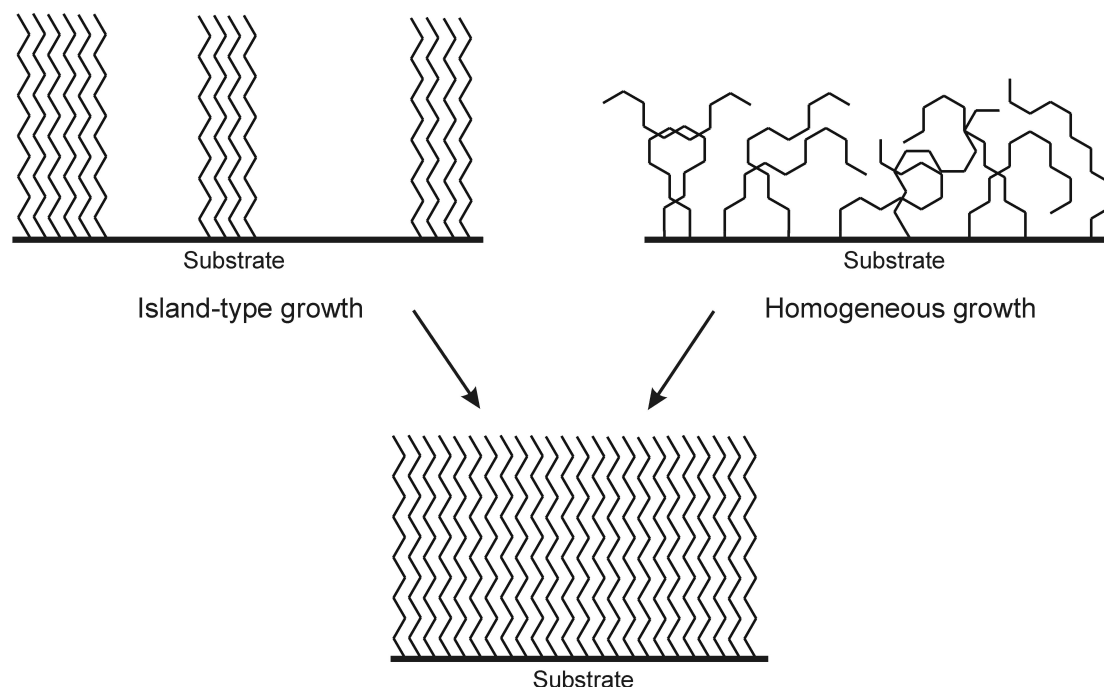
Figure 2.2 Schematic representation of island-type growth and homogeneous growth.

Eventually, it was shown by AFM that OTS monolayers grow via islands, virtually perpendicular to the substrate surface.[40] Also, perfluorinated trichlorosilanes grow via island formation.[41] In contrast, shorter-chain molecules do not show island growth behavior.[40] Several AFM studies revealed that the deposition process strongly depends on parameters like solvent,[42] solution age,[43-45] water content,[35,43,44,46] deposition time,[45-47] and temperature.[48-50] Vallant and co-workers observed both homogeneous growth and island-type growth depending on the water content and age of the silane solution.[43] With increasing water content or age of the solution, island-type was found to be strongly favored, indicative of the formation of larger preorganized aggregates of silanol molecules in solution. However, Wang *et al.* recently showed that even in the absence of water traces in solution, the self-assembly process still proceeds via island-type growth.[35] The reason that this was not observed in other studies is probably the slow kinetics. In the absence of water Wang *et al.* claim that they observed monolayer islands after 18 hours of deposition time, while usually deposition times of only seconds to a few hours are applied. Figure 2.3 shows a tapping-mode AFM image of a partial OTS film on oxidized silicon, which clearly shows the growth of an OTS monolayer via islands.
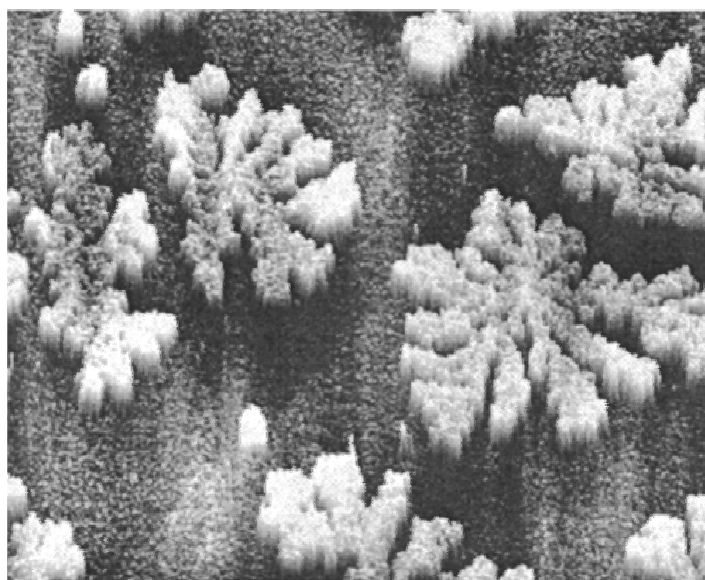
Figure 2.3 *TM-AFM image (20 × 20 μm²) of partial OTS film on oxidized silicon.*[50]

Following the monolayer formation in time revealed different stages. A combined LFM and sum-frequency generation (SFG) spectroscopy study by Liu and

co-workers showed OTS adsorption from solution and the beginning of island formation during the initial stage. This was followed by a dramatic change in alkyl chain conformation within the film from a disordered to an ordered, mainly all-trans conformation, while only a small increase in surface coverage occurred.[46] The final stage is a much slower adsorption process to form a complete monolayer. Balgar *et al.* observed two regimes: one with a nearly linear growth up to a coverage of ca. 75 %, followed by slow saturation at higher coverages.[47] Despite the complex mechanism of monolayer formation, and its dependence on many parameters, several studies reported first-order Langmuir adsorption kinetics using analytical techniques like in situ attenuated total reflection infrared spectroscopy (ATR-IR),[51] in situ AFM,[44] and X-ray reflectivity.[52] Recently, a simple two-dimensional model was developed for the growth of alkylsilane monolayers on hydroxylated surfaces.[53] The model, which takes into account the weak and strong bonding interactions of the aggregating species, was able to reproduce characteristics like island-type growth and first-order Langmuir adsorption kinetics. In addition, it could even provide an explanation for the observed deviations from the first-order Langmuir adsorption kinetics, observed in various ex situ studies.[47,54]

The first observation that monolayer formation depends on the temperature was made by Silberzan *et al.*[15] They found that lower temperatures favor the grafting process, something that seems paradoxical at first. Several groups have studied this phenomenon by monitoring the surface tension and suggested that a critical temperature, close to ambient temperature for OTS, is necessary for the formation of high-quality films.[55-57] As the critical temperature was found to depend on the alkyl chain length, these studies related the critical temperature to the triple point observed in the phase diagram of Langmuir layers at the water-air interface. Later, the group of Silberzan confirmed the analogy to Langmuir films by AFM studies.[48,54] Island-type growth was found to take place below the critical temperature, while islands were not observed for depositions above the critical temperature. However, Rye reported that a much simpler and more straightforward correlation exists between the melting points of alkanes and the observed critical temperature.[24] Time-resolved AFM studies by Carraro and co-workers indicated three distinct mechanisms, dependent on deposition temperature: island growth at low temperatures, homogeneous growth at high temperatures, and a mixed regime at intermediate temperatures.[49] Later, they reported a clever experiment that showed reversible structural change of the same partial OTS

monolayer as a function of temperature at constant coverage.[50] They concluded that the highly mobile monolayer exists in a hydrogen-bonded state at the surface and is closely related to the equilibrium state of Langmuir films at the air-water interface.

2.2.2 Stability of the SAMs

Part of the attractiveness of SAMs on SiO_2 stems from their stability, which is a vital issue in potential applications. The stability is caused by partial in-plane polymerization of the molecules and possible covalent anchoring to the substrate. In air, SAMs of OTS were found to be stable up to ca 150 °C,[9,58-61] after which irreversible changes occur in the monolayer structure. Perfluorinated SAMs appear to be even more resistant toward thermal treatment.[59,62] Srinisavan *et al.* reported that 1H,1H,2H,2H-perfluorodecyltrichlorosilane coatings remain intact even up to 400 °C.[59] The stability toward chemicals is remarkable: OTS SAMs can be washed with organic solvents, hot (tap) water, and detergent solutions without detectable damage to the layer.[63,64] The stability to boiling solvents like chloroform and water is good,[65] but when exposed to 2.5 M sulfuric acid in boiling dioxane or 48% aqueous HF the layers were damaged significantly, as witnessed by reduced ellipsometric thicknesses.[66] Wasserman and co-workers used tetradecyltrichlorosilane for stability studies and found that exposure to 0.1 N HCl for more than 40 h did not affect the monolayer, but when immersed in 0.1 N NaOH immediate degradation took place.[67] This lack of stability in basic media was attributed to the hydrolysis of Si-O bonds near the surface.

One of the first applications where SAMs on SiO_2 were thought to play a key role was in boundary lubrication in e.g. magnetic storage devices. As early as in 1993, the tribological properties of alkylsilane films on solid substrates were investigated.[68] It was found that the friction of coated interfaces was lower compared to the friction of bare interfaces, and the lifetime of the lubricated interfaces increased with increasing chain length.[68,69] Srinivasan and co-workers examined the potential of SAMs for the purpose of adhesion reduction in microelectromechanical systems.[59] They found a reduction in adhesion by more than 3 orders of magnitude upon applying an OTS coating, while fluorinated SAMs reduced it further by a factor of 4. The mechanical strength of octadecyltriethoxysilane (OTE) layers on mica has been investigated by scratching with an AFM tip.[70] No mechanical wear was observed for

loads up to 300 nN when a large tip radius was used. When sharper tips were used a load of ca. 10 nN was enough to displace the OTE monolayer. Using the same sharp tip, *n*-alkanethiols on Au were removed with a smaller force (ca. 5 nN). However, a more recent study questioned the mechanical stability of OTS SAMs on SiO₂.[71] It reported lower friction coefficients for monolayer-coated surfaces, but also a poor load-carrying capacity and antiwear ability. They concluded that OTS SAMs could only be potential boundary lubricants at low loads.

2.3   Chemical diversity of SAMs on SiO₂

SAMs provide molecularly defined platforms for chemical derivatization. Potential applications range from the control of surface properties to the fabrication of sensors, biochips, and their use in nanotechnology. Progress in the development of these fields partly depends upon the ability to functionalize surfaces with suitable groups. Given the ability to readily form stable self-assembled films on SiO₂, two issues determine the utility of such assemblies for the creation of functionalized surfaces: (1) the range of functionalities that can be tolerated in the self-assembly process to yield stable and ordered SAMs, and (2) the scope of chemical postmodifications of the monolayer that can be achieved.

A straightforward reaction in solution is not necessarily successful on a substrate. The reactivity of immobilized reactants can be significantly reduced as a consequence of steric constraints, transport limitations, solvation effects, charge, and dipole effects.[72] Therefore, the extent of reaction depends strongly on the location of the reaction center. When it is located at the incoming reagent, the transition state does not experience much steric limitation, while if it is confined to the surface the reaction center is severely crowded by immobilized neighbors. Also, acid/base properties of surface-confined molecules can differ significantly from those in solution.[73-75] Influencing factors are thought to be the polarity of the surface, interfacial electrostatic fields, and the local structure of the solvent.

2.3.1 Self-assembly of functionalized alkylsilanes and chemical transformations at the monolayer surface

The most straightforward way to prepare a functionalized SAM is by using an ω-substituted alkylsilane. However, the reactivity of alkoxysilanes and especially of

chlorosilanes limits the range of functional groups that can be introduced in this manner. The first functionalized SAM was reported by the group of Sagiv, and contained vinyl groups that could be transformed into terminal hydroxyl groups by hydroboration and oxidation.[3] Other reactions on these layers generated carboxylic acid-, and bromo-terminated films.[67] A nice example of surface chemistry with these carboxylic acid monolayers was shown by the group of Sagiv.[76] The carboxylic acids were used to form a bilayer with octadecylamine, based on electrostatic/hydrogen bonding interactions. Exposure of the bilayer to microwaves resulted in imide formation (Scheme 2.1). More recently, vinyl SAMs have proved useful for the covalent coupling of zwitterionic phosphorylcholine groups to a surface.[77] Such monolayers are biocompatible and prohibit the deposition of enzymes and proteins. In addition, vinyl monolayers can be modified with adenine, and zeolite crystals exposing thymine were assembled at that surface through adenine-thymine hydrogen bonding.[78] Tillman and co-workers prepared monolayers incorporating phenoxy groups and methylesters, of which the latter were reduced to the corresponding alcohols by LiAlH$_4$.[63,64,79] Other functional groups incorporated into monolayers include methylether,[80] acetate,[80] thiocyanate,[81] α-haloacetate,[82] (trimethylsilyl)ethynyl,[83] and thioacetate,[81] of which the last has been reduced to terminal thiol groups.[84]
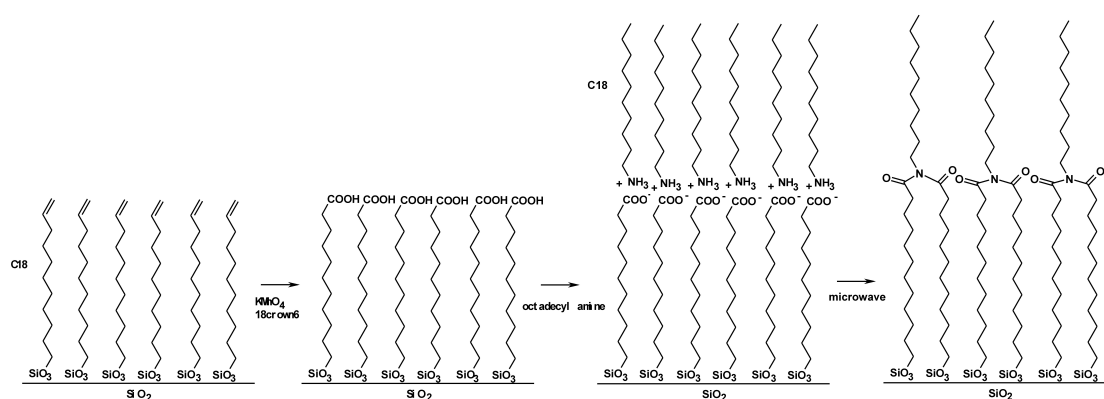
Scheme 2.1 *Microwave-induced imide formation.*[76]

A convenient starting point to perform chemistry on monolayers is provided by bromo-terminated SAMs.[51,80,85] Bromides can be quantitatively replaced by azide groups, which in turn have been reduced to ω-amino SAMs,[81,86] or can be used to

tether to a fullerene molecule.[87] In addition, bromides have also been replaced by other anionic nucleophiles such as thiocyanate and thiolate,[88] although these reactions did not go to completion, most likely due to steric congestion and the fact that they are not as nucleophilic as azides.

A second method to obtain amino-terminated SAMs, is via self-assembly of cyanide monolayers.[51,81] These SAMs can be reduced in one step using LiAlH₄ or BH₃.[81] Amino SAMs form an important platform for reaction with functionalized molecules. When amino SAMs are prepared via reduction of azides or cyanides, ordered and well-defined layers are obtained.[81,86,89] Aminosilane films prepared in one step, on the other hand, are completely disordered.[90] XPS and IR measurements indicated that this is probably due to interaction of the amino group with the surface.[90,91] Nevertheless, aminosilanes, and particularly 3-aminopropyl-trialkoxysilanes (APS), have been used extensively as adhesion promoters and the well-known reactivity of amines has been exploited for the introduction of various functionalized molecules. APS layers were used to covalently bind fullerenes,[92,93] chromophores,[94,95] and fluorescent groups,[96,97] and to coordinate to a zinc-porphyrin.[98] In addition, photoresponsive spiropyran molecules were covalently attached to an APS layer and used as a system to induce reversible changes in wettability upon switching to a more polar zwitterionic merocyanine isomer, triggered by the absorption of UV light.[99,100] More surface reactions on amino-terminated SAMs will be discussed in Chapter 2.3.3 and 2.3.4.

SAMs exposing thiol groups are potentially interesting because of their ability to coordinate to noble metals. The self-assembly of (mercaptopropyl)trimethoxysilane (MPTMS) has been reported,[72,101] and the preparation of colloidal gold multilayers using MPTMS as a linker molecule has been investigated.[102] This layer-by-layer growth method was found to yield uniform colloidal Au multilayers. More recently, MPTMS layers have been oxidized to produce sulfonic acid-functionalized silica that can be used as a catalyst in esterification reactions,[103] and MPTMS monolayers have also been used for electroless plating of Ag.[104]

Homogeneous epoxy-terminated SAMs have been reported by Luzinov and co-workers to serve as a template for chemical tethering of polymer layers.[105] These layers can serve as a useful functionalized surface to react with various amino-derivatized molecules. Kulak *et al.* attached an APS layer to zeolite crystals and found that the modified crystals assembled as monolayers on an epoxy SAM.[106] The zeolite

layer remained intact after sonication, indicating that strong linkages were formed between each crystal and the substrate. Furthermore, epoxy layers were used to immobilize per-6-amino β-cyclodextrin onto a surface, thus creating a surface exposing host molecules.[107]

Immobilization of polymers at a surface is a convenient way to tailor the surface properties of inorganic materials. One promising approach to accomplish this is by the immobilization of initiators for the in situ generation of grafted polymers. Using SAMs carrying azo initiators, the group of Rühe prepared layers of polystyrene and a perfluorinated polymer in a controlled manner and with high graft densities.[108,109] A different approach involves electrochemical polymerization of thiophene-capped SAMs on indium tin oxide. It was shown that the thiophene monolayer could nucleate growth of polythiophene at potentials below the oxidation potential of monomeric thiophene in solution.[110,111] Also without polymers SAMs are widely used to tailor inorganic surfaces for specific properties. Well-known examples are the use of fluorinated silanes to generate surfaces with very low surface free energy,[41,80,112,113] and poly(ethylene glycol) carrying silanes to produce SAMs that resist non-specific adsorption of biomolecules.[114]

Recently, functionalized molecules were immobilized without first depositing a silane coupling agent, avoiding chemistry and difficult characterization at the surface. Although this offers an advantage, it is not likely that well-ordered monolayers are formed because of the bulky substituents. Striking examples are the immobilization of redox-active silane compounds on a platinum surface,[115] and photofunctional siloxane-based calix[4]arenes on SiO_2.[116]

2.3.2 Multilayer formation

Whereas a SAM is only a few nanometers thick, many practical devices require the formation of high-quality, close-packed, and highly ordered films with thicknesses of a few hundred nanometers to several micrometers.[64] In order to add this third dimension to the two-dimensional structure of SAMs, the growth of highly ordered multilayers is necessary. Multilayer formation was studied for the first time by the group of Sagiv.[3] They described the conversion of an olefin-terminated SAM into an alcohol bearing surface, which could be used to deposit a second layer of olefinic silanes. However, the hydroboration of the olefin was not quantitative,

leading to increasing disorder in the subsequent layers. An improvement of the same strategy was reported involving a more effective multilayer construction system based on the reduction of methyl esters to alcohols by LiAlH$_4$.[64] This approach succeeded in the construction of assemblies of up to 25 discrete monolayers. Later, a new methodology to produce hydroxyl-terminated, siloxane-anchored SAMs and multilayers was reported.[117] This work explored the photolysis of a nitrate-bearing SAM as a route to surface hydroxyl formation, which does not require any reagents. This photoconversion allowed the photopatterning of film functionalization and subsequent multilayer construction.

An alternative procedure to yield multilayer assemblies involves the immobilization of a boronate-protected trichlorosilane, which has been hydrolyzed conveniently with water/ethanol to a diol-terminated group, after which the process was repeated.[118] A completely different approach was reported by Yam *et al*,[119] which involved acid-base hydrolytic chemistry of aminosilanes with dihydroxy-terminated molecules. The layer-by-layer construction methodology used Si(NEt$_2$)$_4$ and rigid rod-like dihydroxy molecules, and led to relatively close-packed multilayered structures.

Instead of covalent coupling, also hydrogen bonds can be used to stabilize the three-dimensional structure of the multilayer. Maoz and co-workers oxidized an olefinic SAM to the corresponding carboxylic acid before the next layer was assembled on top.[120-122] Lateral coupling of the silane head-groups provided structural robustness and self-healing capability of the films. Non-covalent multilayers were also reported by the group of Mallouk.[123,124] They used the strong electrostatic and coordinative interaction between phosphonates and Zr^{4+} for multilayer formation. Marks *et al.* prepared thin-film nonlinear optical (NLO) materials in which self-assembled chromophore-containing multilayer structures were built.[125-131] They reported the formation of an acentric monolayer by self-assembly of a trimethoxysilane-functionalized azobenzene-based chromophore from solution. Subsequently, a siloxane capping layer was formed, which stabilized the structure by crosslinking and provided hydroxyl groups to start a new cycle. This process is schematically shown in Figure 2.4.
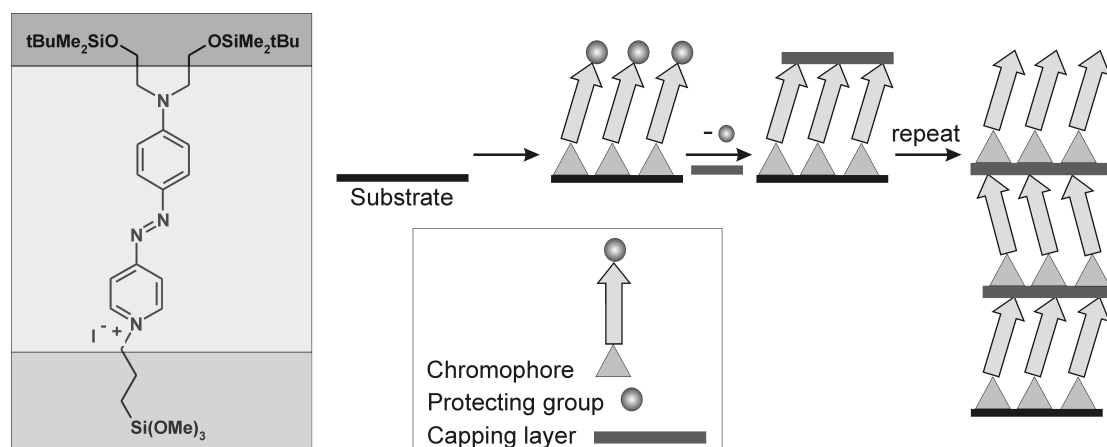
Figure 2.4 *Schematic representation of the self-assembly of chromophoric superlattices.*[131]

2.3.3 Sensing layers

One field of increasing interest in which SAMs are employed extensively is (bio)chemical sensing. Immobilization of sensor systems implies the transition from solution to the solid state, offering an easier way to couple sensing systems to the macroscopic world through read-out functions. The major part of sensor functionalities in SAMs has been developed for gold surfaces, using read-out techniques like electrochemistry, surface plasmon resonance, and AFM.[132] However, as a transduction mechanism for molecular recognition, fluorescence spectroscopy has advantages over electrochemical methods, as there is no need for reference electrodes or additional electrolytes.[133] In addition, molecules labeled with fluorescent probes are easily prepared or commercially available and can be visualized even individually. Fluorescence spectroscopy is extensively used in biological sensing (see Chapter 2.3.4), where it is applied in e.g. DNA chips and protein microarrays to gain information at a nucleic acid or protein level. The reason for the limited use of fluorescence spectroscopy on gold lies in the strong quenching effect of the gold substrate on the fluorescence of nearby molecules, making oxide surfaces like SiO_2 the surface of choice for the immobilization of fluorescent sensing molecules.[134-137]

One of the first immobilized sensor systems was reported by De Silva *et al.*[138] The sensing system consisted of a covalently connected anthracene fluorophore that could behave as a pH probe, depending on the protonation state of the amino group. Porphyrins linked to an APS layer was reported by McCallien and co-workers.[139] After attachment to the substrate, zinc was inserted and the interaction of the zinc-

porphyrins with amino ligands was investigated by UV-Vis spectroscopy. Porphyrins could also be immobilized through reaction of a vinyl or hydroxyethyl group of a porphyrin with a thiol-terminated monolayer, providing a simple and direct method for attaching porphyrins onto solid substrates.[140] UV-Vis measurements were used to monitor the coordination of carbon monoxide to various metal porphyrins.

Host-guest interactions on the SiO₂ surface have been reported by several groups. Fullerenes were attached to silica gel to investigate binding affinities of potential hosts like calixarenes and cyclodextrins.[141] Cyclodextrin films were prepared to monitor the interactions with various guest molecules,[107,142,143] and in an elegant experiment Flink and co-workers monitored the interaction of *β*-cyclodextrin hosts with monolayers of dansyl adsorbates by polarity-dependent fluorescence.[144] A monolayer bearing preorganized binding sites for metal ions was reported by Van der Veen and co-workers and is shown in Scheme 2.2.[133] They used a calix[4]arene receptor modified with ligating groups and two pyrene fluorophores. The immobilized receptor site showed selectivity for Na^+ over other alkali metal ions and the complexation of Na^+ ions could be monitored by a decrease in monomer emission and an increase in excimer emission. Although the fluoroionophore, shown in Scheme 2.2, was found to be a good Na^+ receptor, the use of preorganized recognition sites brings forth certain disadvantages. It requires lengthy synthesis procedures and results in disordered monolayers due to the bulkiness of the receptor molecule. Therefore, a new approach was developed more recently.[145,146] It relies on the immobilization of ligating functionalities on an amino-terminated SAM, without any preorganization. A small library containing various simple ligating and reporter molecules was made, and the response to different metal ions was measured. Results showed that selectivity for different metal ions could be achieved, depending on the surface functionalization. The same approach was used by Brasola and co-workers to develop a fluorescence nanosensor for Cu^{2+} on silica particles, the only difference being the immobilization of ligating and reporter molecules in one step, without a preformed monolayer.[147]
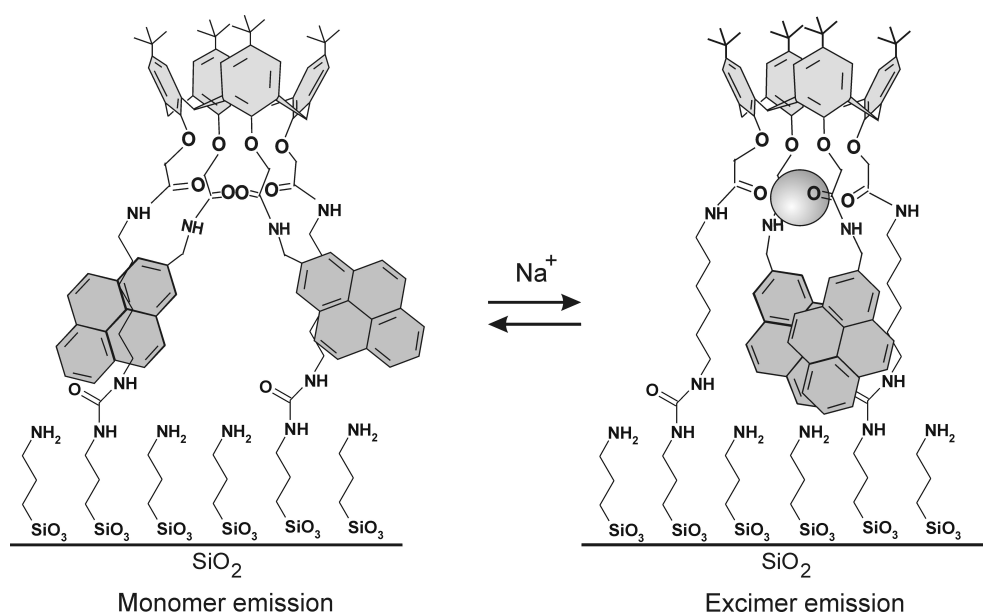
Scheme 2.2 *Immobilized preorganized Na$^+$ selective fluoroionophore showing a change from monomer emission to excimer emission upon complexation of Na$^+$.*[133]

2.3.4 Immobilization of biomolecules

The attachment of biologically important molecules to surfaces is of considerable importance for the development of biological microarrays, such as DNA chips and protein microarrays.[148,149] DNA chips are promising for obtaining information on nucleic acid levels and sequences in a fast, simple and cheap way, and are projected for use in large-scale genotyping and gene-expression profiling.[148] Protein microarray technology is valuable in the pharmaceutical industry for the acceleration of drug target and diagnostic biomarker discovery.[149] Crucial for the development of these small-molecule microarrays is the ability to selectively attach compounds to the surface under mild conditions and at the same time avoid non-specific interactions. Moreover, the reactions should be compatible with a wide variety of functional groups that occur in biologically relevant molecules. To meet these requirements, extensive research has been performed in order to expand the immobilization techniques on surfaces. Recently, an overview of different reactions that have been studied on monolayers on Au and SiO$_2$, with the emphasis on immobilization of biomolecules, was reported.[150]

The formation of amino-terminated SAMs on glass surfaces allows immobilization of biologically important molecules both in a covalent and a non-covalent way. Cells were found to bind to amino SAMs based on electrostatic

interactions between the positively charged ammonium groups and the negatively charged cell membrane.[151] This simple electrostatic adsorption has also been used to link short oligonucleotides to a positively charged amino SAM.[152] Applying this method produced a stable oligonucleotide monolayer at a density that approached a two-dimensional close-packed array.

Although reactions in solution cannot always be readily transferred to a surface, several mild methods have been developed to covalently couple biological molecules to the glass surface. Successful reactions include DCC coupling of pepsin,[72] EDC coupling of DNA,[153] the immobilization of p-nitrophenyl chloroformate activated dextrans,[154] reaction of compounds containing acidic protons with diazobenzilidene-functionalized glass slides,[155] and a photoaffinity reaction.[156] Many groups have employed a two-step approach, where after self-assembly the amino SAM was derivatized with a linker molecule to increase the reactivity of the monolayer. Heterobifunctional reagents such as *N*-succinimidyl 6-maleimidocaproate react with APS monolayers, exposing the maleimide functionality, which in turn can be used in a Michael addition with thiol-containing compounds.[157-159] A critical feature of this methodology is the resistance to non-specific adsorption, which was attributed to the hydrophilicity of the maleimide functionality.[159] It has also been shown that the same heterobifunctional molecule could be attached to a thiol-terminated SAM.[160] In this case it was utilized to link an amino-containing, fluorescently labeled oligodeoxynucleotide probe to the surface for hybridization experiments. A slightly different approach to attach DNA covalently to glass surfaces was reported by O'Donnel and co-workers.[161] They applied a heterobifunctional cross-linking agent to incorporate an iodoacetamido group, which was reacted with a reduced oligodeoxynucleotide presenting free thiol groups.

As was mentioned before, resistance to non-specific adsorption is a critical issue when designing microarrays. Sekal *et al.* described a method to prepare monolayers that are resistant to non-specific protein adsorption and present primary amino groups for derivatization.[162] By treating an APS layer with glutaraldehyde and subsequently with 2,2'-(ethylenedioxy)bis(ethylenediamine) they were able to incorporate ligands and protein-sensitive fluorescent reporter groups, and used these monolayers for the detection of protein-ligand interactions.

Problems regarding surface silylation reactions can involve inhomogeneous layer formation, poor surface coverage, and difficulties to withstand frequent

regeneration steps.[163] To overcome these problems, Benters and co-workers developed a method for generating highly homogeneous activated silica surfaces that can be applied for the efficient coupling of oligonucleotides to produce DNA microarrays.[163] The method involves the initial formation of an APS layer, which is activated by a homobifunctional linker such as 1,4-phenylenediisothiocyanate (DITC), and then allowed to react with a starburst dendrimer containing 64 primary amino groups at the periphery. Subsequently, the attached dendritic molecules are activated and crosslinked with a homobifunctional spacer to display a surface with high coverage, decreased steric hindrance, and that is resistant against repeated regeneration procedures. Recently, layers obtained by this procedure and APS layers were derivatized with appropriate phosphane groups to immobilize azido-functionalized biomolecules via Staudinger ligation.[164,165] This coupling strategy affords rapid immobilization and offers the advantage that it is compatible with unprotected functional groups, often required for interactions in biological systems.

Epoxy-terminated SAMs can react with molecules bearing amino groups. In this way it was possible to bind cyclopeptides to the glass surface, which could be used as a molecular receptor,[166] and to determine binding constants between an immobilized tripeptide and vancomycin using confocal fluorescence detection.[167] Hydrolyzing an epoxy SAM yields a diol, which was used to develop a biosensor that utilizes immobilized nucleic acid aptamers to detect nonlabeled targets such as proteins.[168]

Another relatively simple coupling strategy involves the reaction of aldehyde-modified glass surfaces with amine-presenting molecules. The aldehydes react readily with primary amines of proteins or DNA to form a Schiff's base linkage.[153,169] This strategy was applied to prepare libraries of peptidyl coumarins in microarrays. It was demonstrated that the bound peptides were accessible for proteolytic cleavage.[170]

Other reported strategies to attach biological molecules to SiO_2 surfaces involve the reactions of thiol-terminated SAMs with disulfide-modified oligonucleotides or hemeproteins,[171,172] iodopropyl monolayers with thiol-containing proteins,[173] alcohols with a silyl chloride surface,[174] and bromoacetamide SAMs with phosphorothioate-functionalized oligonucleotides.[175]

2.4 Engineering the SiO$_2$ surface using SAMs

Developing methods that allow chemistries of surfaces to be controlled on the 1-100 nm length scale is a fundamental challenge in nanoscience and nanotechnology because it opens new possibilities in the fields ranging from molecular electronics to biomedicine and catalysis.[176] SAMs offer an ideal platform for engineering on a molecular level, provided that techniques are developed to pattern or assemble SAMs on the nanoscale in a spatially resolved manner.

2.4.1 *Spacing of chemical functionalities*

Spatially patterning of terminal chemical groups on a surface is of technological importance, in order to, for example, localize adsorption. In the design of DNA- and protein-chips the density of probe molecules is a critical issue. A facile method to achieve spatial patterns is by preparing multicomponent SAMs so that chemical functionalities can be assembled in a matrix of other molecules, which might be unfunctionalized or carry a different functionality. Several approaches have been described in literature, of which the most widely used involves competitive chemisorption, i.e. the treatment of a surface with a mixture of reagents. Although the composition and properties of mixed monolayers are not at all straightforward, numerous binary monolayers have been prepared as listed by McCarthy and co-workers.[177] Fan *et al.* stimulated phase separation in a binary monolayer by using two very different alkylsilane amphiphiles, one with strong cohesive interactions and one able to form hydrogen bonds, to generate a surface with nano-islands of a chemical functionality.[178] The surface composition was analyzed by AFM, which showed pronounced differences in height and friction for the two components. The phase behavior of multicomponent SAMs could be used as an effective "latent image" to generate features in the surface by wet etching.[179] This difference in etch stability was achieved by the assembly of molecules with different chain length, and it was proposed that regions of more densely packed molecules were more etch resistant than regions of less coherent packing. Mixed SAMs can be conveniently used to control the surface free energy, as was shown in an elegant experiment by Lee and co-workers.[180] They used different ratios of –OH and –CH$_3$ groups to tailor the surface free energy of silicon substrates, and found that in this way they could control the growth modes of atomic layer deposition (ALD) of TiO$_2$.

An alternative approach for the preparation of "mixed surfaces" involves subsequent reaction of partially modified surfaces with another silane. As mentioned earlier, SAMs on SiO$_2$ grow via an island growth mechanism, offering the possibility to fill partial monolayers of one component with another. Recent examples have reported small domains of OTS islands filled with bromine-terminated,[181] and amino-terminated SAMs.[182] Fadeev and co-workers have used a very bulky silane for deposition, and found by size-exclusion contact angle hysteresis measurements that nanopores with a cross section of ~0.5 nm^2 were still present at the surface, accessible to probes of smaller dimension.[177] In this way uniformly mixed binary monolayers were generated, the procedure of which is schematically shown in Figure 2.5.
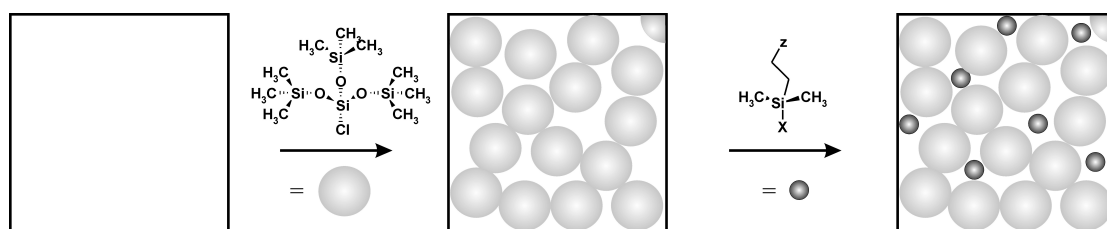
Figure 2.5 *Schematic representation of a two-step silanization procedure.[177]*

A different strategy to achieve spacing of chemical functionalities on a surface comprises the assembly of large molecules carrying only one functionality (Figure 2.6). Focally functionalized dendrons appear to be particularly suitable molecules for this method. Submonolayers, monolayers, and multilayers of SiCl$_3$-terminated carbosilane dendrons with a phenyl group in the focal point were reported by the group of Cai,[183,184] and self-assembly of dendrons through multiple ionic interactions yielded mesospacing between reactive amino groups.[185] In the latter case, dendrons bearing carboxyl groups at the periphery and a protected amine in the focal point were assembled on an amino-terminated SAM. AFM and fluorescence measurements indicated the formation of a close-packed layer with spacing between the amino functional groups of 24 – 34 Å.

Figure 2.6 *Cartoon illustration of the concept of using large molecules to control spacing between functional moieties at a surface.*

Surfaces patterned via above mentioned methods are relatively easily prepared, without the use of expensive machinery and via a flexible process that allows patterning on a large scale and is not restricted to flat areas. However, a 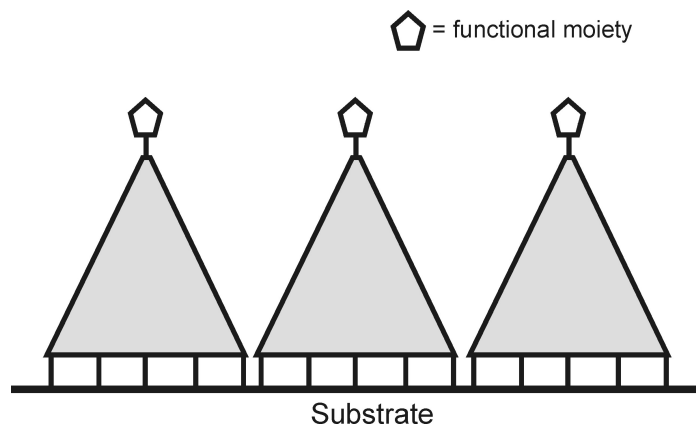significant drawback of these approaches is that only homogeneously patterned surfaces can be generated and the functionalities cannot be directed spatially, which is required for the building of nanosized functional entities.

2.4.2 Patterning SAMs with photons and particles

2.4.2.1 Photolithography

Photolithography on SAMs relies on the absorption of radiation in the exposed regions of the monolayer, which undergo photocleavage to yield surface residues. The use of less expensive equipment, compared to e.g. e-beam lithography makes this a widely used technique to create patterned SAMs, but the feature sizes that can be achieved are diffraction-limited.

Irradiation with deep-UV light has been used extensively to remove SAMs in exposed regions. This leaves an activated surface that can be used for numerous post-patterning processes. SAMs of different chemical functionalities were deposited for the immobilization of fluorophores,[186] for cell adhesion,[187] and to control the surface potential.[188,189] The remaining SAMs have been used as a mask for wet chemical etching to fabricate microstructures at Si substrates,[190,191] and as a template for Pd adhesion and subsequent electroless deposition of ZnO.[192] The exposed areas could be used as templates for electroless plating of Ni,[186,191] and for the deposition of TiO₂

films.[193] Recently, photocatalytic lithography of alkylsilane SAMs was reported using UV and TiO_2 to rapidly and homogeneously remove the SAM by the generation of highly reactive oxygen species.[194]

Instead of completely removing the monolayer, photolithography can also be used to create patterns with different chemical functionalities. Some groups have reported photodeprotection of protected amino groups, after which the exposed areas could be selectively developed by the adsorption of fluorescent particles.[195,196] A very elegant example is the combination of photolithography with immobilization of biomolecules for the generation of e.g. DNA chips.[197] Pioneering work in this field was conducted by the group of Fodor.[198-201] They used light-directed, spatially addressable parallel synthesis to build arrays for rapid DNA analysis. The pattern of illumination through a mask, using light to remove photolabile protecting groups from selected areas, determines which regions of the surface are activated for coupling. Then the first set of building blocks, each bearing a photolabile group, is exposed to the surface, but reacts only with the patterned areas. Subsequently the substrate is illuminated through another mask for deprotection and coupling with a second building block. The steps of masking/irradiation and coupling are repeated to build up various oligomers. The patterns of the masks and the sequence of reagents define the ultimate sequences synthesized, and their locations on the surface are known.

Other chemical transformations have been shown by the groups of Dressick and Sugimura. The first group was able to transform 4-chloromethylphenyl chromophores into phenylaldehyde groups, which in turn could be reduced to amines.[202] The latter group showed that OTS SAMs decomposed gradually upon vacuum UV light exposure, generating –COOH groups that were successfully reacted with functional and fluorinated silanes. Surface wettability could also be controlled using photolithographic methods. In a series of papers the group of Beebe reported cunning experiments to control liquid flow inside microchannels.[203-205] Surface free energies were patterned by use of SAMs in combination with photolithography, as shown in Scheme 2.3. They could confine the flow of aqueous liquids to the hydrophilic pathways, provided that the pressure was maintained below a critical value.
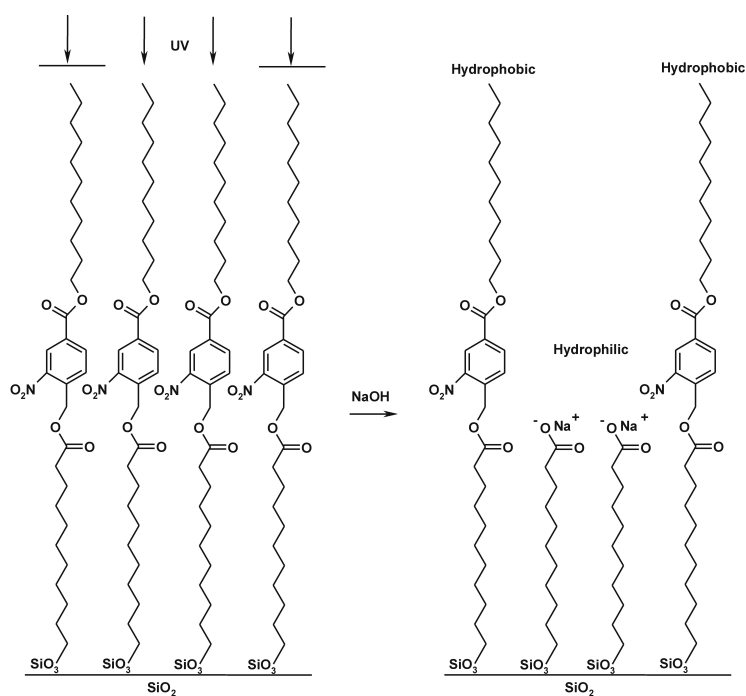
Scheme 2.3 *UV patterning to fabricate hydrophilic patterns inside microchannels.*[203]

2.4.2.2 Electron beam lithography

SAMs have been candidates for very high resolution resists in electron beam (e-beam) lithography. As the feature size generated with e-beam lithography depends on the thickness of the resist, the monomolecular thickness of SAMs could provide ultrahigh-resolution e-beam patterning. It has been shown that patterns of several tens of nm could be created in OTS and perfluorinated SAMs on SiO₂, and that the patterns could be transferred into the substrate by wet etching techniques.[206-208] Later, the same group showed that patterns smaller than 10 nm could be attained using a scanning electron microscope (SEM) with a small beam diameter.[209] A different development of the created patterns was reported by Marrian and co-workers.[210] Low voltage e-beam lithography was used to pattern films and the patterns were applied as templates for the electroless plating of thin Ni films. Linewidths down to ~20 nm were observed after plating.

There have been several reports that combine e-beam lithography with functionalized SAMs. The group of Craighead patterned amino-terminated SAMs and developed the patterns by exposing them to palladium colloids and coated polystyrene fluorescent spheres.[211] The colloids and spheres adhered only to unexposed areas of the monolayers. Other studies employed the deposition of amino-silanes through a

PMMA mask or an unfunctionalized SAM that was patterned by e-beam lithography.[212-214] In this way colloidal particles and carbon nanotubes were deposited selectively on the amine-modified parts of the substrate.

Recently, e-beam irradiation was used to induce chemical transformations in monolayers. The group of Park studied several procedures to prepare patterned amino- and bromo-terminated SAMs, and verified the reactivity by attaching biotin/streptavidin groups,[215] or amplified the patterns vertically by radical polymerization.[216] The transformations are shown in Scheme 2.4. In addition, sub-50-nm patterns were prepared in SAMs with embedded disulfide bonds.[217] Phenyl (3-trimethoxysilylpropyl)disulfide monolayers were patterned with e-beam lithography, which generated 3-4 Å deep and 30 nm wide trenches. XPS indicated the cleavage of the disulfide bonds to sulfhydryl groups, and the resulting chemical patterns could be developed by reaction with *N*-(1-pyrene)maleimide. Even smaller chemical patterns were attainable by a combination of e-beam lithography and gas-phase silanization.[218] It was shown that monolayers with varying chemical functionalities could be formed through nanoholes in a PMMA mask. After removing the mask a monolayer of different functionality was deposited, generating well-defined nanoislands as small as 20 nm of one chemical functionality in a matrix of another.

2.4.2.3 Ion beam- and X-ray lithography

Techniques that have been less frequently used to pattern SAMs are ion beam- and X-ray lithography. Patterning with low-energy ion beams usually employs shadow masks due to the difficulty of focusing such sources. However, using high-energy focused ion beams (FIBs) should result in the possibility to produce nanometer-scale patterns, as it is possible to attain beam diameters as small as 8 nm.[219] FIBs have already been used to write 10-nm-wide features in thin PMMA films.[220] A vinyl-terminated monolayer was selectively deposited in ion beam etched regions of a methyl-terminated SAM with a resolution of 1-3 μm.[221] Ada and co-workers have studied in detail the interaction of low-energy ions with organosilane SAMs, and were able to create 300 nm wide gaps employing FIB.[222] Smaller feature sizes were reported by exposing monolayers to low doses of slow, highly charged ions, like Xe^{41+} and Th^{73+}.[223] AFM images showed craters from single ion impacts with

diameters of 50-63 nm. Equally small features have also been reported by the group of Whitesides, utilizing neutral Cs atoms.[224]
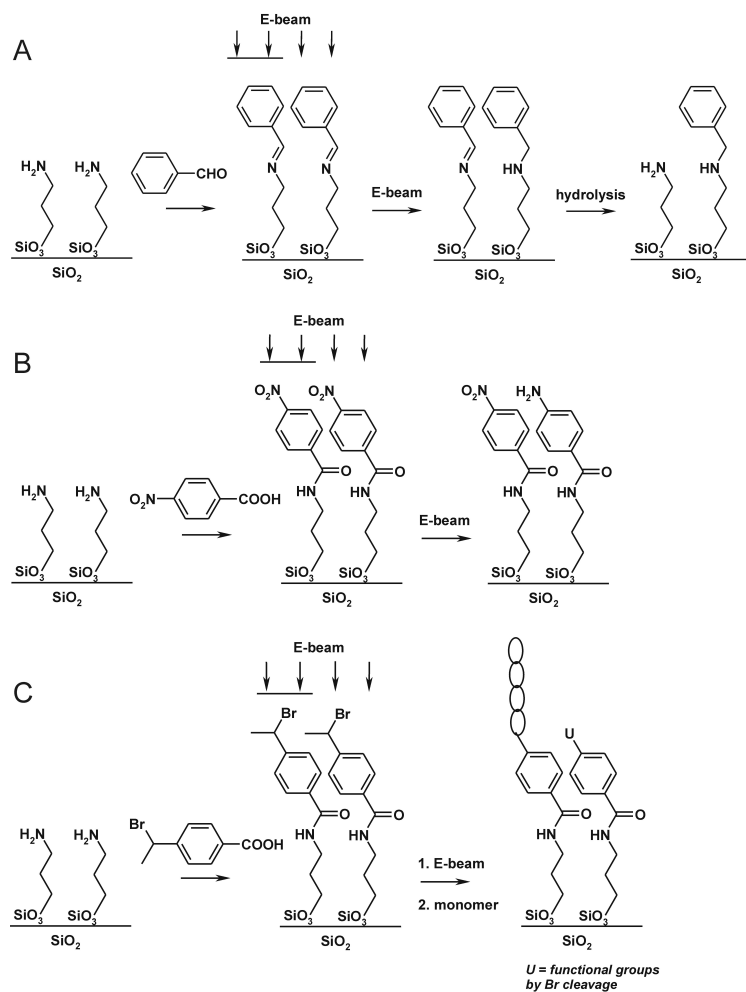
Scheme 2.4 *Chemical transformations with low-energy electron-beam.*[215,216]

Irradiation with soft X-rays through a mask can be a convenient method for chemical patterning of monolayers. Reported transformations include the loss of halogens in halogenmethylphenylsilyl layers,[225,226] and the cleavage of nitro groups in nitro-substituted aromatic SAMs.[227] Using masks with nm-sized features, La and co-workers were able to develop sub-100-nm patterns, as evidenced by AFM images.[228] The patterns could be derivatized by further linking fluorescently labeled oligonucleotides. Irradiation of OTS layers resulted in the formation of oxygen-containing groups like hydroxyls and aldehydes.[229] Pattern transfer of features with dimensions as small as 150 nm into the underlying substrate were obtained by reactive

ion etching using thin films of Ni, selectively deposited onto the exposed areas of the OTS SAM. Recently, it was shown that hybrid patterning strategies allow for the fabrication of defect-free nanopatterns of block copolymers.[230] A photoresist on top of a phenylethyl monolayer was patterned with 45-55 nm-sized features by extreme-UV interferometric lithography, and the pattern was transferred into the underlying SAM by chemical modification using soft X-rays. After removing the photoresist, poly(styrene-block-methylmethacrylate) (PS-b-PMMA) was spin-coated onto the patterned SAM and annealed. It was found that the PMMA block preferentially wetted the modified regions of the surface, and thus domain structures were formed analogous to the SAM patterns, as observed by scanning electron microscopy (SEM) (Figure 2.7).
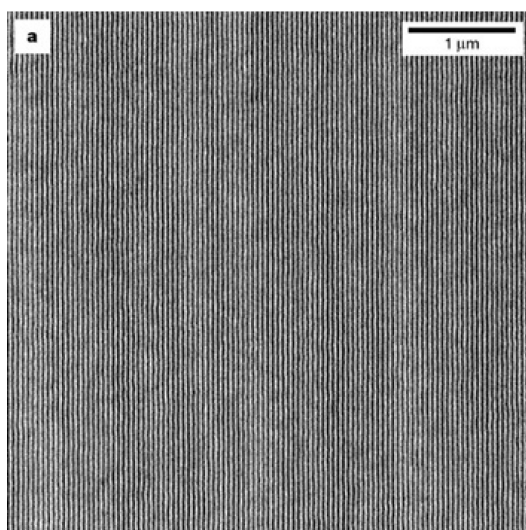
Figure 2.7 *SEM image showing 48 nm wide PS and PMMA domains.[230]*

2.4.3 Soft lithography

Soft lithography[231] is the collective name for a set of lithographic techniques including replica molding, mirocontact printing (μCP), and micromolding using a patterned elastomer as mold, stamp, or mask to transfer a pattern.[232] Soft lithography offers advantages over other lithographic methods concerning the patterning of nonplanar substrates, unusual materials, or large areas.[232] Of these techniques, μCP has been employed most frequently for the facile (sub)micron patterning of surfaces. μCP relies on the inking of an elastomeric (usually PDMS) stamp with suitable

molecules. When the stamp is brought into contact with a substrate, the molecules are transferred from the stamp to the substrate in the regions of contact. μCP was initially developed for the patterning of gold surfaces with alkanethiols, and still the bulk of the work in literature comprises patterning of this surface.

Reports regarding μCP on SiO$_2$ surfaces have been rather limited. This might be explained by the inherent sensitivity of trialkoxy- and especially trichlorosilanes, and the lower edge resolution of silanes on SiO$_2$ when compared with thiols on gold, that was described by the group of Whitesides.[233] While this paper reported that printed OTS SAMs were only partly etch resistant, later studies showed that printed patterns could be transferred into the underlying substrate,[234] even with feature sizes as small as 80 nm.[235] Detailed studies by the group of Nuzzo indicated that close-packed OTS monolayers were formed after 30 s of printing, in contrast to their solution analogs, which took minutes to form a densely packed layer.[236] They also found that stable SAMs were formed, but that patterning at dimensions less than a few microns resulted in spreading of OTS in regions that were not in contact with the stamp. Using docosyltrichlorosilane resulted in more accurate transfer to the substrate, and these films offered an improvement to serve as a wet etch resist.[237] Amplification of a printed pattern can also be achieved in a different manner. Harada and co-workers amplified a printed vinyl-terminated pattern by attaching selectively a Ru complex, which reacted with norborene derivatives to give thin polymer films.[238] Employing the contrast in wettability between clean SiO$_2$ and a printed OTS pattern enabled the confinement and alignment of molecules.[239] After printing, the remaining hydrophilic parts of the substrate were covered with a thin polyelectrolyte layer, onto which biological macromolecules and liquid crystals could be confined. This afforded a straightforward way to create microchannels on a surface.

The majority of the work concerning μCP and SAMs on SiO$_2$ involves deposition of metals. Printed monolayers can serve as a resist for copper chemical vapor deposition,[240] or SnCl$_2$ deposition from solution, which served as a nucleation point for electroless plating of Ag.[241] But instead of printing a monolayer, it is also possible to print onto a preformed monolayer. Hidber *et al.* used an amino-terminated SAM as an adhesion promoter to print (sub)micron patterns of Pd-colloids.[242] The immobilized colloids served as a catalyst for the electroless deposition of copper, yielding (sub)micron scaled copper lines on an insulating surface. More recently,

thiol-terminated MPTMS SAMs have also been used as adhesion promoters.[243] In this case a gold-coated stamp was used to transfer thin but stable gold layers onto the monolayer (Scheme 2.5). In a series of papers Delamarche and co-workers described an elegant process to produce NiB stuctures and metal nanowires on glass substrates.[244-248] They combined the adhesive properties of an amino-terminated SAM to bind Pd/Sn colloids, which were used to initiate electroless deposition of NiB. Then, electroplated copper was deposited and patterned by μCP using a protective layer of thiol molecules. The pattern was subsequently transferred into the copper and NiB by two wet etching techniques. This process was developed to provide a new and potentially cost-effective way for the fabrication of gate layers in thin-film transistor (TFT)-LCDs, and could even be applied on a macro (15 inch) scale.
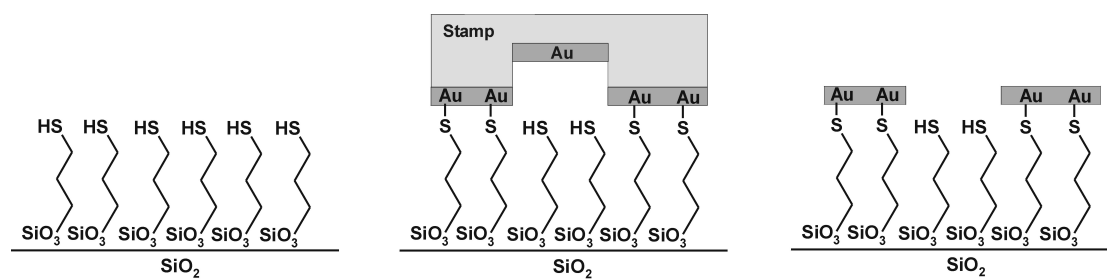
Scheme 2.5 *Metal structures prepared on adhesion SAMs by nanotransfer printing.[243]*

2.4.4 Scanning probe lithography

Scanning probe microscopy can visualize surfaces and surface properties at the submolecular level. In addition, probe tips can be used to manipulate atoms and molecules on surfaces, and in this mode the technique is often referred to as scanning probe lithography.[249] Sugimura *et al.* were among the first to combine a scanning probe tip with self-assembly on SiO_2 surfaces to create nanoscale patterns. They have used a scanning tunneling microscope (STM) tip for local anodization of a Si-H surface to SiO_2 in the presence of an organosilane vapor.[250] This resulted in the formation of monolayer features of 20 nm that showed a resistance to chemical etching. Other studies from the same author reported patterning of a homogeneous monolayer by applying a bias voltage to the probe tip, effectively removing the monolayer from the probe-scanned regions. Next, the exposed regions were filled with SAMs of different chemical composition to regulate the surface potential or

selectively assemble proteins at a spatial resolution on the nm scale.[251,252] A different method for nm-scale patterning was obtained by field-induced oxidation (FIO) using a conductive cantilever.[253] When FIO was employed locally on an oxide surface in a dry nitrogen atmosphere, surface hydroxyl groups, necessary for monolayer formation, were removed and monolayer formation was suppressed. In this way, a line structure of an OTS SAM as narrow as 22 nm could be fabricated. In contrast, when FIO was performed under humid conditions, OTS SAMs formed on the entire surface.

2.4.4.1 Constructive nanolithography

Constructive nanolithography was first reported by the group of Sagiv.[254] It involves non-destructive surface patterning by means of an electrical bias to a conducting AFM tip operated under ambient conditions, followed by template controlled self-assembly. The versatility of this approach was demonstrated in several systems where they could locally electrooxidize vinyl-terminated and OTS SAMs for the preparation of patterned bilayers,[255] self-assembled metal islands,[254,256] metal nanoparticles,[257-259] and nanowires.[258] Using this method, features with sub-50 nm dimensions could be fabricated. A schematical representation of the organosilane template pattern and the self-assembly of [Au$_{55}$] clusters on the template is displayed in Scheme 2.6. This methodology could be taken from the nm to mm dimension range by employing electrooxidation using a rigid metallic stamp.[260] Recently, another group applied local probe oxidation of OTS SAMs for functionalization with cationic gold nanoparticles, quaternary ammonium salts, and a polymer grafting reaction.[261]

A few years before Sagiv and co-workers introduced constructive nanolithography, a similar approach was presented by Schultz *et al.* making use of a catalytic probe.[262] In this elegant experiment an alkylazide monolayer was reduced to its corresponding amine by a catalytic Pt coated AFM tip. The amino groups were then covalently modified with fluorescently labeled beads and imaged under a confocal microscope.
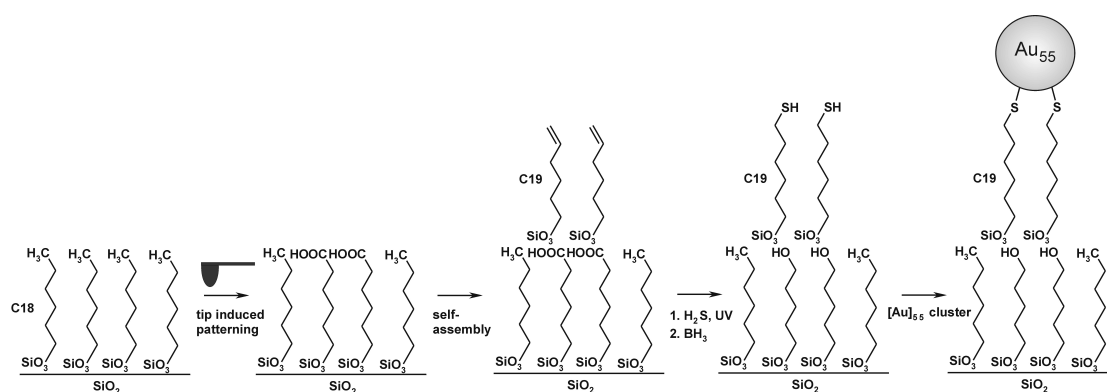
Scheme 2.6 *Schematic representation of constructive nanolithography, employing tip-induced electrooxidation and subsequent self-assembly on the written template. In this case [Au$_{55}$] clusters were assembled.*[257]

2.4.4.2 Dip-pen nanolithography

Dip-pen nanolithography (DPN)[176,263] uses an inked AFM tip to deposit molecules on a substrate. This technique, which is believed to rely on the transport of molecules from the tip to a surface through a water meniscus, has been used to generate structures with line widths as small as ~10 nm. The process is depicted schematically in Figure 2.8A. Reported examples have dealt almost exclusively with the writing of thiol inks on gold substrates, or the use of metal salts for the electrostatical assembly on appropriately biased silicon substrates. Thus far, silane-based inks have rarely been used, mainly because of the incompatibility of chloro- and alkoxysilane groups with the water meniscus mentioned above. The group of Mirkin used hexamethyldisilazane to write organic patterns on SiO$_2$ with sub-100 nm dimensions.[264] Two recent articles, however, demonstrated that it is possible to write with trialkoxysilane-based inks. Pena *et al.* wrote APTES and MPTMS lines of nm dimensions, but were not able to further derivatize the formed structures.[265] They explained this lack of reactivity by the formation of multilayers through hydrogen bonding. These results were contradicted by a study of Jung and co workers.[266] They claimed that DPN with reactive silanes is possible if proper measures against polymerization are taken. Writing at low humidity resulted in the formation of 110 nm wide MPTMS lines, which were successfully reacted with biotin and fluorescently labeled streptavidin.
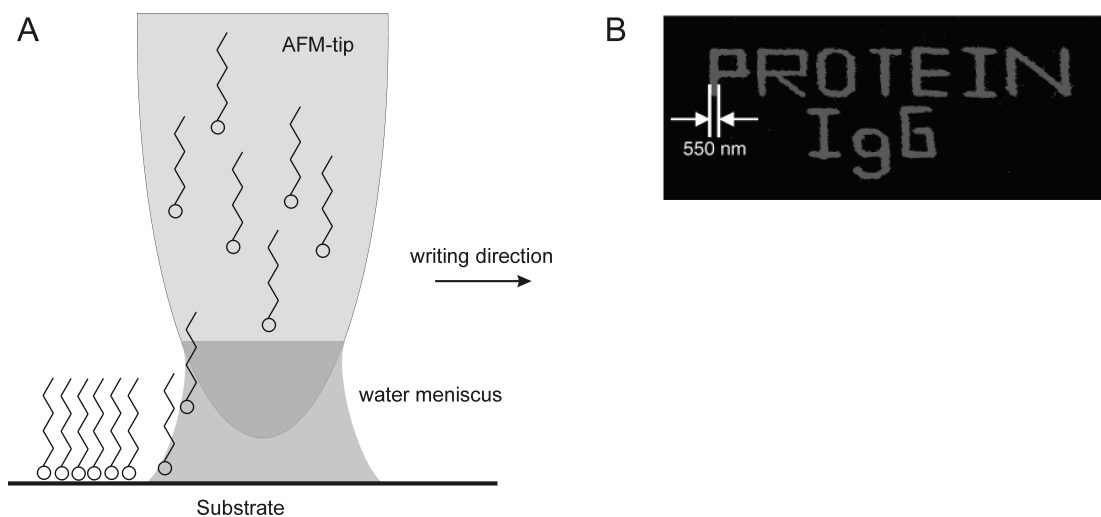
Figure 2.8 *(a) Schematic representation of DPN process. (b) Fluorescence image of DPN-generated labeled antirabbit IgG structure on SiO₂.*[267]

An alternative method to write functionalized structures on the SiO₂ surface constitutes writing on preformed functional monolayers. Covalently anchored nanoscale patterns of oligonucleotides were written onto preformed MPTMS SAMs.[268] Feature sizes from micrometers to sub-100 nm were written with acrylamide bearing oligonucleotides, and exhibited sequence-specific binding properties as witnessed by epifluorescence micrographs. The same group also reported the direct writing of proteins on modified SiO₂ surfaces.[267] A negatively charged surface was used to bind proteins electrostatically (Figure 2.8B), and proteins were covalently bound employing writing on a preformed aldehyde-terminated monolayer. Some modifications to the writing process had to be made. First, a poly(ethylene glycol) (PEG) coated AFM-tip was used in order to minimize protein adsorption and to reduce the activation energy required for protein transport from tip to surface. In addition, it protects the protein from denaturation on the tip surface. Second, it was found that high humidity is a prerequisite for writing with high-molecular weight molecules. Patterning was performed at relative humidities between 60 and 90 %, whereas for writing with low-molecular weight trialkoxysilanes low humidities were sufficient.

2.5 Concluding remarks

The formation of self-assembled monolayers on SiO_2 constitutes a powerful tool for the successful functionalization of this surface. It has been sufficiently shown that stable and well-ordered monomolecular layers can be formed, displaying a wide range of functionalities that are available for further derivatization.

In particular the rise of nanotechnology has boosted the use of monolayers to engineer surfaces on a molecular level, as they form an ideal two-dimensional platform. The development of a variety of techniques for the formation and manipulation of nanometer-scale monolayer patterns brings forth opportunities to add the third dimension to the platform. These techniques should eventually lead to the development of functional nanostructures at a surface.

In this thesis functional self-assembled monolayers of host molecules on planar surfaces are described, which can be patterned based on specific supramolecular interactions, using techniques discussed in Chapter 2. Functional monolayers have also been prepared in microchannels for monitoring changes in acidity of fluids inside the channels with fluorescence spectroscopy.

2.6 References

[1]   Nuzzo, R. G.; Allara, D. *J. Am. Chem. Soc.* **1983,** *105*, 4481-4483.

[2]   Sagiv, J. *J. Am. Chem. Soc.* **1980,** *102*, 92-98.

[3]   Netzer, L.; Sagiv, J. *J. Am. Chem. Soc.* **1983,** *105*, 674-676.

[4]   Netzer, L.; Iscovici, R.; Sagiv, J. *Thin Solid Films* **1983,** *99*, 235-241.

[5]   Netzer, L.; Iscovici, R.; Sagiv, J. *Thin Solid Films* **1983,** *100*, 67-76.

[6]   Maoz, R.; Sagiv, J. *J. Colloid Interface Sci.* **1984,** *100*, 465-496.

[7]   Gun, J.; Iscovici, R.; Sagiv, J. *J. Colloid Interface Sci.* **1984,** *101*, 201-213.

[8]   Gun, J.; Sagiv, J. *J. Colloid Interface Sci.* **1986,** *112*, 457-472.

[9]   Cohen, S. R.; Naaman, R.; Sagiv, J. *J. Phys. Chem.* **1986,** *90*, 3054-3056.

[10]   Maoz, R.; Sagiv, J. *Langmuir* **1987,** *3*, 1034-1044.

[11]   Maoz, R.; Sagiv, J. *Langmuir* **1987,** *3*, 1045-1051.

[12]   Zhuravlev, L. T. *Langmuir* **1987,** *3*, 316-318.

[13]   Finklea, H. O.; Robinson, L. R.; Blackburn, A.; Richter, B.; Allara, D.; Bright, T. *Langmuir* **1986,** *2*, 239-244.

[14]   Allara, D. L.; Parikh, A. N.; Rondelez, F. *Langmuir* **1995,** *11*, 2357-2360.

[15]   Silberzan, P.; Leger, L.; Ausserre, D.; Benattar, J. J. *Langmuir* **1991,** *7*, 1647-1651.

[16]   Tripp, C. P.; Hair, M. L. *Langmuir* **1992,** *8*, 1120-1126.

[17]   Tripp, C. P.; Hair, M. L. *Langmuir* **1995,** *11*, 1215-1219.

[18]   Angst, D. L.; Simmons, G. W. *Langmuir* **1991,** *7*, 2236-2242.

[19]   Legrange, J. D.; Markham, J. L.; Kurkjian, C. R. *Langmuir* **1993,** *9*, 1749-1753.

[20]   Fairbank, R. W. P.; Wirth, M. J. *J. Chromatogr., A* **1999,** *830*, 285-291.

[21]   Wang, R. W.; Wunder, S. L. *Langmuir* **2000,** *16*, 5008-5016.

[22]   Hair, M. L.; Tripp, C. P. *Colloids Surf., A* **1995,** *105*, 95-103.

[23]   Rye, R. R.; Nelson, G. C.; Dugger, M. T. *Langmuir* **1997,** *13*, 2965-2972.

[24]   Rye, R. R. *Langmuir* **1997,** *13*, 2588-2590.

[25]   Stevens, M. J. *Langmuir* **1999,** *15*, 2773-2778.

[26]   Wasserman, S. R.; Whitesides, G. M.; Tidswell, I. M.; Ocko, B. M.; Pershan, P. S.; Axe, J. D. *J. Am. Chem. Soc.* **1989,** *111*, 5852-5861.

[27]   Banga, R.; Yarwood, J.; Morgan, A. M.; Evans, B.; Kells, J. *Thin Solid Films* **1996,** *285*, 261-266.

[28]   Tidswell, I. M.; Ocko, B. M.; Pershan, P. S.; Wasserman, S. R.; Whitesides, G. M.; Axe, J. D. *Phys. Rev. B* **1990,** *41*, 1111-1128.

[29]   Tidswell, I. M.; Rabedeau, T. A.; Pershan, P. S.; Kosowsky, S. D.; Folkers, J. P.; Whitesides, G. M. *J. Chem. Phys.* **1991,** *95*, 2854-2861.

[30]   Fujii, M.; Sugisawa, S.; Fukada, K.; Kato, T.; Seimiya, T. *Langmuir* **1995,** *11*, 405-407.

[31]   Fujii and co-workers reported an occupied area of 0.43 nm^2 per OTS chain, but extensively dried the substrate prior to self-assembly. This could explain the high surface area per OTS chain and the observed low ellipsometric thickness.

[32]   Barton, S. W.; Goudot, A.; Rondelez, F. *Langmuir* **1991,** *7*, 1029-1030.

[33]   Kojio, K.; Ge, S. R.; Takahara, A.; Kajiyama, T. *Langmuir* **1998,** *14*, 971-974.

[34]   Kojio, K.; Takahara, A.; Omote, K.; Kajiyama, T. *Langmuir* **2000,** *16*, 3932-3936.

[35]   Wang, Y. L.; Lieberman, M. *Langmuir* **2003,** *19*, 1159-1167.

[36]   McGovern, M. E.; Kallury, K. M. R.; Thompson, M. *Langmuir* **1994,** *10*, 3607-3614.

[37]   Ohtake, T.; Mino, N.; Ogawa, K. *Langmuir* **1992,** *8*, 2081-2083.

[38]   Mathauer, K.; Frank, C. W. *Langmuir* **1993,** *9*, 3002-3008.

[39]   Mathauer, K.; Frank, C. W. *Langmuir* **1993,** *9*, 3446-3451.

[40]   Bierbaum, K.; Grunze, M.; Baski, A. A.; Chi, L. F.; Schrepp, W.; Fuchs, H. *Langmuir* **1995,** *11*, 2143-2150.

[41]   Banga, R.; Yarwood, J.; Morgan, A. M.; Evans, B.; Kells, J. *Langmuir* **1995,** *11*, 4393-4399.

[42]   Rozlosnik, N.; Gerstenberg, M. C.; Larsen, N. B. *Langmuir* **2003,** *19*, 1182-1188.

[43]   Vallant, T.; Brunner, H.; Mayer, U.; Hoffmann, H.; Leitner, T.; Resch, R.; Friedbacher, G. *J. Phys. Chem. B* **1998,** *102*, 7190-7197.

[44]   Leitner, T.; Friedbacher, G.; Vallant, T.; Brunner, H.; Mayer, U.; Hoffmann, H. *Mikrochim. Acta* **2000,** *133*, 331-336.

[45]   Reiniger, M.; Basnar, B.; Friedbacher, G.; Schleberger, M. *Surf. Interface Anal.* **2002,** *33*, 85-88.

[46]   Liu, Y.; Wolf, L. K.; Messmer, M. C. *Langmuir* **2001,** *17*, 4329-4335.

[47]   Balgar, T.; Bautista, R.; Hartmann, N.; Hasselbrink, E. *Surf. Sci.* **2003,** *532*, 963-969.

[48]   Davidovits, J. V.; Pho, V.; Silberzan, P.; Goldmann, M. *Surf. Sci.* **1996,** *352*, 369-373.

[49]   Carraro, C.; Yauw, O. W.; Sung, M. M.; Maboudian, R. *J. Phys. Chem. B* **1998,** *102*, 4441-4445.

[50]   Sung, M. M.; Carraro, C.; Yauw, O. W.; Kim, Y.; Maboudian, R. *J. Phys. Chem. B* **2000,** *104*, 1556-1559.

[51]   Vallant, T.; Kattner, J.; Brunner, H.; Mayer, U.; Hoffmann, H. *Langmuir* **1999,** *15*, 5339-5346.

[52]   Richter, A. G.; Yu, C. J.; Datta, A.; Kmetko, J.; Dutta, P. *Colloids Surf., A* **2002,** *198*, 3-11.

[53]   Bautista, R.; Hartmann, N.; Hasselbrink, E. *Langmuir* **2003,** *19*, 6590-6593.

[54]   Goldmann, M.; Davidovits, J. V.; Silberzan, P. *Thin Solid Films* **1998,** *329*, 166-171.

[55]   Brzoska, J. B.; Shahidzadeh, N.; Rondelez, F. *Nature* **1992,** *360*, 719-721.

[56]   Brzoska, J. B.; Benazouz, I.; Rondelez, F. *Langmuir* **1994,** *10*, 4367-4373.

[57]   Parikh, A. N.; Allara, D. L.; Azouz, I. B.; Rondelez, F. *J. Phys. Chem.* **1994,** *98*, 7577-7590.

[58]   CalistriYeh, M.; Kramer, E. J.; Sharma, R.; Zhao, W.; Rafailovich, M. H.; Sokolov, J.; Brock, J. D. *Langmuir* **1996,** *12*, 2747-2755.

[59]   Srinivasan, U.; Houston, M. R.; Howe, R. T.; Maboudian, R. *JMEMS* **1998,** *7*, 252-260.

[60]   Wang, R. W.; Baran, G.; Wunder, S. L. *Langmuir* **2000,** *16*, 6298-6305.

[61]   Wang, R. W.; Wunder, S. L. *J. Phys. Chem. B* **2001,** *105*, 173-181.

[62]   Devaprakasam, D.; Sampath, S.; Biswas, S. K. *Langmuir* **2004,** *20*, 1329-1334.

[63]   Tillman, N.; Ulman, A.; Schildkraut, J. S.; Penner, T. L. *J. Am. Chem. Soc.* **1988,** *110*, 6136-6144.

[64]   Tillman, N.; Ulman, A.; Penner, T. L. *Langmuir* **1989,** *5*, 101-111.

[65]   Linford, M. R.; Chidsey, C. E. D. *J. Am. Chem. Soc.* **1993,** *115*, 12631-12632.

[66]   Linford, M. R.; Fenter, P.; Eisenberger, P. M.; Chidsey, C. E. D. *J. Am. Chem. Soc.* **1995,** *117*, 3145-3155.

[67]   Wasserman, S. R.; Tao, Y. T.; Whitesides, G. M. *Langmuir* **1989,** *5*, 1074-1087.

[68]   Ruhe, J.; Novotny, V. J.; Kanazawa, K. K.; Clarke, T.; Street, G. B. *Langmuir* **1993,** *9*, 2383-2388.

[69]   Xiao, X. D.; Hu, J.; Charych, D. H.; Salmeron, M. *Langmuir* **1996,** *12*, 235-237.

[70]   Xiao, X. D.; Liu, G. Y.; Charych, D. H.; Salmeron, M. *Langmuir* **1995,** *11*, 1600-1604.

[71]   Ren, S.; Yang, S. R.; Zhao, Y. P.; Zhou, J. F.; Xu, T.; Liu, W. M. *Tribol. Lett.* **2002,** *13*, 233-239.

[72]   Kurth, D. G.; Bein, T. *Langmuir* **1993,** *9*, 2965-2973.

[73]   Li, T. T.-T.; Weaver, M. J. *J. Am. Chem. Soc.* **1984,** *106*, 6107-6108.

[74]   Zhao, B.; Mulkey, D.; Brittain, W. J.; Chen, Z. H.; Foster, M. D. *Langmuir* **1999,** *15*, 6856-6861.

[75]   Gershevitz, O.; Sukenik, C. N. *J. Am. Chem. Soc.* **2004,** *126*, 482-483.

[76]   Maoz, R.; Cohen, H.; Sagiv, J. *Langmuir* **1998,** *14*, 5988-5993.

[77]   Wang, Y. L.; Su, T. J.; Green, R.; Tang, Y. Q.; Styrkas, D.; Danks, T. N.; Bolton, R.; Liu, J. R. *Chem. Commun.* **2000**, 587-588.

[78] Park, J. S.; Lee, G. S.; Lee, Y. J.; Park, Y. S.; Yoon, K. B. *J. Am. Chem. Soc.* **2002,** *124*, 13366-13367.

[79] Tillman, N.; Ulman, A.; Elman, J. F. *Langmuir* **1989,** *5*, 1020-1026.

[80] Chaudhury, M. K.; Whitesides, G. M. *Science* **1992,** *255*, 1230-1232.

[81] Balachander, N.; Sukenik, C. N. *Langmuir* **1990,** *6*, 1621-1627.

[82] Lee, Y. W.; Reedmundell, J.; Sukenik, C. N.; Zull, J. E. *Langmuir* **1993,** *9*, 3009-3014.

[83] Ogawa, K.; Mino, N.; Tamura, H.; Hatada, M. *Langmuir* **1990,** *6*, 1807-1809.

[84] Wenzler, L. A.; Moyes, G. L.; Raikar, G. N.; Hansen, R. L.; Harris, J. M.; Beebe, T. P.; Wood, L. L.; Saavedra, S. S. *Langmuir* **1997,** *13*, 3761-3768.

[85] Chupa, J. A.; Xu, S. T.; Fischetti, R. F.; Strongin, R. M.; McCauley, J. P.; Smith, A. B.; Blasie, J. K.; Peticolas, L. J.; Bean, J. C. *J. Am. Chem. Soc.* **1993,** *115*, 4383-4384.

[86] Lee, M. T.; Ferguson, G. S. *Langmuir* **2001,** *17*, 762-767.

[87] Tsukruk, V. V.; Lander, L. M.; Brittain, W. J. *Langmuir* **1994,** *10*, 996-999.

[88] Fryxell, G. E.; Rieke, P. C.; Wood, L. L.; Engelhard, M. H.; Williford, R. E.; Graff, G. L.; Campbell, A. A.; Wiacek, R. J.; Lee, L.; Halverson, A. *Langmuir* **1996,** *12*, 5064-5075.

[89] Onclin, S.; Mulder, A.; Huskens, J.; Ravoo, B. J.; Reinhoudt, D. N. *Langmuir* **2004**, 5460-5466.

[90] Bierbaum, K.; Kinzler, M.; Woll, C.; Grunze, M.; Hahner, G.; Heid, S.; Effenberger, F. *Langmuir* **1995,** *11*, 512-518.

[91] Zhdanov, S. P.; Kosheleva, L. S.; Titova, T. I. *Langmuir* **1987,** *3*, 960-967.

[92] Chen, K. M.; Caldwell, W. B.; Mirkin, C. A. *J. Am. Chem. Soc.* **1993,** *115*, 1193-1194.

[93] Li, D. Q.; Swanson, B. I. *Langmuir* **1993,** *9*, 3341-3344.

[94] Heiney, P. A.; Gruneberg, K.; Fang, J. Y.; Dulcey, C.; Shashidhar, R. *Langmuir* **2000,** *16*, 2651-2657.

[95] Fang, J. Y.; Chen, M. S.; Shashidhar, R. *Langmuir* **2001,** *17*, 1549-1551.

[96] Flink, S.; Van Veggel, F. C. J. M.; Reinhoudt, D. N. *J. Phys. Org. Chem.* **2001,** *14*, 407-415.

[97] Krasnoslobodtsev, A. V.; Smirnov, S. N. *Langmuir* **2002,** *18*, 3181-3184.

[98] Zhang, Z.; Hu, R.; Liu, Z. *Langmuir* **2000,** *16*, 1158-1162.

[99] Rosario, R.; Gust, D.; Hayes, M.; Jahnke, F.; Springer, J.; Garcia, A. A. *Langmuir* **2002,** *18*, 8062-8069.

[100] Bunker, B. C.; Kim, B. I.; Houston, J. E.; Rosario, R.; Garcia, A. A.; Hayes, M.; Gust, D.; Picraux, S. T. *Nano Lett.* **2003,** *3*, 1723-1727.

[101] Hu, M. H.; Noda, S.; Okubo, T.; Yamaguchi, Y.; Komiyama, H. *Appl. Surf. Sci.* **2001,** *181*, 307-316.

[102] Tseng, J. Y.; Lin, M. H.; Chau, L. K. *Colloids Surf., A* **2001,** *182*, 239-245.

[103] Cano-Serrano, E.; Campos-Martin, J. M.; Fierro, J. L. G. *Chem. Commun.* **2003**, 246-247.

[104] Liu, Z. C.; He, Q. G.; Xiao, P. F.; Liang, B.; Tan, J. X.; He, N. Y.; Lu, Z. H. *Mater. Chem. Phys.* **2003,** *82*, 301-305.

[105] Luzinov, I.; Julthongpiput, D.; Liebmann-Vinson, A.; Cregger, T.; Foster, M. D.; Tsukruk, V. V. *Langmuir* **2000,** *16*, 504-516.

[106] Kulak, A.; Lee, Y. J.; Park, Y. S.; Yoon, K. B. *Angew. Chem., Int. Ed.* **2000,** *39*, 950-953.

[107] Busse, S.; DePaoli, M.; Wenz, G.; Mittler, S. *Sens. Actuators, B* **2001,** *80*, 116-124.

[108] Prucker, O.; Ruhe, J. *Macromolecules* **1998,** *31*, 592-601.

[109] Jung, D. H.; Park, I. J.; Choi, Y. K.; Lee, S. B.; Park, H. S.; Ruhe, J. *Langmuir* **2002,** *18*, 6133-6139.

[110] Sullivan, J. T.; Harrison, K. E.; Mizzell, J. P.; Kilbey, S. M. *Langmuir* **2000,** *16*, 9797-9803.

[111] Kang, J. F.; Perry, J. D.; Tian, P.; Kilbey, S. M. *Langmuir* **2002,** *18*, 10196-10201.

[112] Lindner, E.; Arias, E. *Langmuir* **1992,** *8*, 1195-1198.

[113] Tripp, C. P.; Veregin, R. P. N.; Hair, M. L. *Langmuir* **1993,** *9*, 3518-3522.

[114] Papra, A.; Gadegaard, N.; Larsen, N. B. *Langmuir* **2001,** *17*, 1457-1460.

[115] Long, Y. T.; Herrwerth, S.; Eck, W.; Grunze, M. *Phys. Chem. Chem. Phys.* **2002,** *4*, 522-526.

[116] Van der Boom, T.; Evmenenko, G.; Dutta, P.; Wasielewski, M. R. *Chem. Mater.* **2003,** *15*, 4068-4074.

[117] Collins, R. J.; Bae, I. T.; Scherson, D. A.; Sukenik, C. N. *Langmuir* **1996,** *12*, 5509-5511.

[118] Kato, S.; Pac, C. *Langmuir* **1998,** *14*, 2372-2377.

[119]   Yam, C. M.; Kakkar, A. K. *Langmuir* **1999,** *15*, 3807-3815.

[120]   Maoz, R.; Sagiv, J.; Degenhardt, D.; Mohwald, H.; Quint, P. *Supramol. Sci.* **1995,** *2*, 9-24.

[121]   Maoz, R.; Matlis, S.; DiMasi, E.; Ocko, B. M.; Sagiv, J. *Nature* **1996,** *384*, 150-153.

[122]   Maoz, R.; Sagiv, J. *Adv. Mater.* **1998,** *10*, 580-584.

[123]   Lee, H.; Kepley, L. J.; Hong, H. G.; Mallouk, T. E. *J. Am. Chem. Soc.* **1988,** *110*, 618-620.

[124]   Lee, H.; Kepley, L. J.; Hong, H. G.; Akhter, S.; Mallouk, T. E. *J. Phys. Chem.* **1988,** *92*, 2597-2601.

[125]   Li, D. Q.; Ratner, M. A.; Marks, T. J.; Zhang, C. H.; Yang, J.; Wong, G. K. *J. Am. Chem. Soc.* **1990,** *112*, 7389-7390.

[126]   Kakkar, A. K.; Yitzchaik, S.; Roscoe, S. B.; Kubota, F.; Allan, D. S.; Marks, T. J.; Lin, W. P.; Wong, G. K. *Langmuir* **1993,** *9*, 388-390.

[127]   Yitzchaik, S.; Roscoe, S. B.; Kakkar, A. K.; Allan, D. S.; Marks, T. J.; Xu, Z. Y.; Zhang, T. G.; Lin, W. P.; Wong, G. K. *J. Phys. Chem.* **1993,** *97*, 6958-6960.

[128]   Roscoe, S. B.; Yitzchaik, S.; Kakkar, A. K.; Marks, T. J. *Langmuir* **1994,** *10*, 1337-1339.

[129]   Yitzchaik, S.; Marks, T. J. *Acc. Chem. Res.* **1996,** *29*, 197-202.

[130]   Roscoe, S. B.; Kakkar, A. K.; Marks, T. J.; Malik, A.; Durbin, M. K.; Lin, W. P.; Wong, G. K.; Dutta, P. *Langmuir* **1996,** *12*, 4218-4223.

[131]   Van der Boom, M. E.; Evmenenko, G.; Yu, C. J.; Dutta, P.; Marks, T. J. *Langmuir* **2003,** *19*, 10531-10537.

[132]   Flink, S.; Van Veggel, F. C. J. M.; Reinhoudt, D. N. *Adv. Mater.* **2000,** *12*, 1315-1328.

[133]   Van der Veen, N. J.; Flink, S.; Deij, M. A.; Egberink, R. J. M.; Van Veggel, F. C. J. M.; Reinhoudt, D. N. *J. Am. Chem. Soc.* **2000,** *122*, 6112-6113.

[134]   Chance, R.; Prock, A.; Silbey, R. *Adv. Chem. Phys.* **1978,** *37*, 1-65.

[135]   Kummerlen, J.; Leitner, A.; Brunner, H.; Aussenegg, F. R.; Wokaun, A. *Mol. Phys.* **1993,** *80*, 1031-1046.

[136]   Enderlein, J. *Chem. Phys.* **1999,** *247*, 1-9.

[137]   Reese, S.; Fox, M. A. *J. Phys. Chem. B* **1998,** *102*, 9820-9824.

[138] Ayadim, M.; Jiwan, J. L. H.; DeSilva, A. P.; Soumillion, J. P. *Tetrahedron Lett.* **1996,** *37*, 7039-7042.

[139] McCallien, D. W. J.; Burn, P. L.; Anderson, H. L. *J. Chem. Soc., Perkin Trans. 1* **1997**, 2581-2586.

[140] Pilloud, D. L.; Moser, C. C.; Reddy, K. S.; Dutton, P. L. *Langmuir* **1998,** *14*, 4809-4818.

[141] Bianco, A.; Gasparrini, F.; Maggini, M.; Misiti, D.; Polese, A.; Prato, M.; Scorrano, G.; Toniolo, C.; Villani, C. *J. Am. Chem. Soc.* **1997,** *119*, 7550-7554.

[142] Li, D. Q.; Ma, M. *Sens. Actuators, B* **2000,** *69*, 75-84.

[143] Rudzinski, C. M.; Young, A. M.; Nocera, D. G. *J. Am. Chem. Soc.* **2002,** *124*, 1723-1727.

[144] Flink, S.; Van Veggel, F. C. J. M.; Reinhoudt, D. N. *Chem. Commun.* **1999**, 2229-2230.

[145] Crego-Calama, M.; Reinhoudt, D. N. *Adv. Mater.* **2001,** *13*, 1171-1174.

[146] Basabe-Desmonts, L.; Beld, J.; Zimmerman, R. S.; Hernando, J.; Mela, P.; Garcia Parajo, M. F.; Van Hulst, N. F.; Van den Berg, A.; Reinhoudt, D. N.; Crego-Calama, M. *J. Am. Chem. Soc.* **2004,** *126*, 7293-7299.

[147] Brasola, E.; Mancin, F.; Rampazzo, E.; Tecilla, P.; Tonellato, U. *Chem. Commun.* **2003**, 3026-3027.

[148] Pirrung, M. C. *Angew. Chem., Int. Ed.* **2002,** *41*, 1276-1289.

[149] Wilson, D. S.; Nock, S. *Angew. Chem., Int. Ed.* **2003,** *42*, 494-500.

[150] Sullivan, T. P.; Huck, W. T. S. *Eur. J. Org. Chem.* **2003**, 17-29.

[151] Margel, S.; Sivan, O.; Dolitzky, Y. *Langmuir* **1991,** *7*, 2317-2322.

[152] Belosludtsev, Y.; Iverson, B.; Lemeshko, S.; Eggers, R.; Wiese, R.; Lee, S.; Powdrill, T.; Hogan, M. *Anal. Biochem.* **2001,** *292*, 250-256.

[153] Zammatteo, N.; Jeanmart, L.; Hamels, S.; Courtois, S.; Louette, P.; Hevesi, L.; Remacle, J. *Anal. Biochem.* **2000,** *280*, 143-150.

[154] Tasker, S.; Matthijs, G.; Davies, M. C.; Roberts, C. J.; Schacht, E. H.; Tendler, S. J. B. *Langmuir* **1996,** *12*, 6436-6442.

[155] Barnes-Seeman, D.; Park, S. B.; Koehler, A. N.; Schreiber, S. L. *Angew. Chem., Int. Ed.* **2003,** *42*, 2376-2379.

[156] Kanoh, N.; Kumashiro, S.; Simizu, S.; Kondoh, Y.; Hatakeyama, S.; Tashiro, H.; Osada, H. *Angew. Chem., Int. Ed.* **2003,** *42*, 5584-5587.

[157] Hong, H. G.; Bohn, P. W.; Sligar, S. G. *Anal. Chem.* **1993,** *65*, 1635-1638.

[158] Hong, H. G.; Jiang, M.; Sligar, S. G.; Bohn, P. W. *Langmuir* **1994,** *10*, 153-158.

[159] MacBeath, G.; Koehler, A. N.; Schreiber, S. L. *J. Am. Chem. Soc.* **1999,** *121*, 7967-7968.

[160] Benoit, V.; Steel, A.; Torres, M.; Lu, Y. Y.; Yang, H. J.; Cooper, J. *Anal. Chem.* **2001,** *73*, 2412-2420.

[161] Odonnell, M. J.; Tang, K.; Koster, H.; Smith, C. L.; Cantor, C. R. *Anal. Chem.* **1997,** *69*, 2438-2443.

[162] Sekar, M. M. A.; Hampton, P. D.; Buranda, T.; Lopez, G. P. *J. Am. Chem. Soc.* **1999,** *121*, 5135-5141.

[163] Benters, R.; Niemeyer, C. M.; Wohrle, D. *ChemBioChem* **2001,** *2*, 686-694.

[164] Kohn, M.; Wacker, R.; Peters, C.; Schroder, H.; Soulere, L.; Breinbauer, R.; Niemeyer, C. M.; Waldmann, H. *Angew. Chem., Int. Ed.* **2003,** *42*, 5830-5834.

[165] Soellner, M. B.; Dickson, K. A.; Nilsson, B. L.; Raines, R. T. *J. Am. Chem. Soc.* **2003,** *125*, 11790-11791.

[166] Leipert, D.; Nopper, D.; Bauser, M.; Gauglitz, G.; Jung, G. *Angew. Chem., Int. Ed.* **1998,** *37*, 3308-3311.

[167] Elbs, M.; Brock, R. *Anal. Chem.* **2003,** *75*, 4793-4800.

[168] Potyrailo, R. A.; Conrad, R. C.; Ellington, A. D.; Hieftje, G. M. *Anal. Chem.* **1998,** *70*, 3419-3425.

[169] MacBeath, G.; Schreiber, S. L. *Science* **2000,** *289*, 1760-1763.

[170] Salisbury, C. M.; Maly, D. J.; Ellman, J. A. *J. Am. Chem. Soc.* **2002,** *124*, 14868-14870.

[171] Pilloud, D. L.; Rabanal, F.; Gibney, B. R.; Farid, R. S.; Dutton, P. L.; Moser, C. C. *J. Phys. Chem. B* **1998,** *102*, 1926-1937.

[172] Rogers, Y. H.; Jiang-Baucom, P.; Huang, Z. J.; Bogdanov, V.; Anderson, S.; Boyce-Jacino, M. T. *Anal. Biochem.* **1999,** *266*, 23-30.

[173] Stayton, P. S.; Olinger, J. M.; Jiang, M.; Bohn, P. W.; Sligar, S. G. *J. Am. Chem. Soc.* **1992,** *114*, 9298-9299.

[174] Hergenrother, P. J.; Depew, K. M.; Schreiber, S. L. *J. Am. Chem. Soc.* **2000,** *122*, 7849-7850.

[175] Pirrung, M. C.; Davis, J. D.; Odenbaugh, A. L. *Langmuir* **2000,** *16*, 2185-2191.

[176] Ginger, D. S.; Zhang, H.; Mirkin, C. A. *Angew. Chem., Int. Ed.* **2004,** *43*, 30-45.

[177] Fadeev, A. Y.; McCarthy, T. J. *Langmuir* **1999,** *15*, 7238-7243.

[178] Fan, F. Q.; Maldarelli, C.; Couzis, A. *Langmuir* **2003,** *19*, 3254-3265.

[179] Finnie, K. R.; Nuzzo, R. G. *Langmuir* **2001,** *17*, 1250-1254.

[180] Lee, J. P.; Jang, Y. J.; Sung, M. M. *Adv. Funct. Mater.* **2003,** *13*, 873-876.

[181] Kumar, N.; Maldarelli, C.; Steiner, C.; Couzis, A. *Langmuir* **2001,** *17*, 7789-7797.

[182] Buseman-Williams, J.; Berg, J. C. *Langmuir* **2004,** *20*, 2026-2029.

[183] Xiao, Z. D.; Cai, C. Z.; Mayeux, A.; Milenkovic, A. *Langmuir* **2002,** *18*, 7728-7739.

[184] Yam, C. M.; Mayeux, A.; Milenkovic, A.; Cai, C. Z. *Langmuir* **2002,** *18*, 10274-10278.

[185] Hong, B. J.; Shim, J. Y.; Oh, S. J.; Park, J. W. *Langmuir* **2003,** *19*, 2357-2365.

[186] Dulcey, C. S.; Georger, J. H.; Krauthamer, V.; Stenger, D. A.; Fare, T. L.; Calvert, J. M. *Science* **1991,** *252*, 551-554.

[187] Stenger, D. A.; Georger, J. H.; Dulcey, C. S.; Hickman, J. J.; Rudolph, A. S.; Nielsen, T. B.; McCort, S. M.; Calvert, J. M. *J. Am. Chem. Soc.* **1992,** *114*, 8435-8442.

[188] Saito, N.; Hayashi, K.; Sugimura, H.; Takai, O.; Nakagiri, N. *Chem. Phys. Lett.* **2001,** *349*, 172-177.

[189] Hayashi, K.; Saito, N.; Sugimura, H.; Takai, O.; Nakagiri, N. *Langmuir* **2002,** *18*, 7469-7472.

[190] Sugimura, H.; Ushiyama, K.; Hozumi, A.; Takai, O. *Langmuir* **2000,** *16*, 885-888.

[191] Sugimura, H.; Hanji, T.; Takai, O.; Masuda, T.; Misawa, H. *Electrochim. Acta* **2001,** *47*, 103-107.

[192] Saito, N.; Haneda, H.; Sekiguchi, T.; Ohashi, N.; Sakaguchi, I.; Koumoto, K. *Adv. Mater.* **2002,** *14*, 418-421.

[193] Masuda, Y.; Seo, W. S.; Koumoto, K. *Langmuir* **2001,** *17*, 4876-4880.

[194] Lee, J. P.; Sung, M. M. *J. Am. Chem. Soc.* **2004,** *126*, 28-29.

[195] Jonas, U.; del Campo, A.; Kruger, C.; Glasser, G.; Boos, D. *Proc. Natl. Acad. Sci. U. S. A.* **2002,** *99*, 5034-5039.

[196] Nakagawa, M.; Ichimura, K. *Colloids Surf., A* **2002,** *204*, 1-7.

[197] Pirrung, M. C. *Chem. Rev.* **1997,** *97*, 473-488.

[198] Fodor, S. P. A.; Read, J. L.; Pirrung, M. C.; Stryer, L.; Lu, A. T.; Solas, D. *Science* **1991,** *251*, 767-773.

[199] Pease, A.; Solas, D.; Sullivan, E.; Cronin, M.; Holmes, C.; Fodor, S. *Proc. Natl. Acad. Sci. U. S. A.* **1994,** *91*, 5022-5026.

[200] McGall, G.; Labadie, J.; Brock, P.; Wallraff, G.; Nguyen, T.; Hinsberg, W. *Proc. Natl. Acad. Sci. U. S. A.* **1996,** *93*, 13555-13560.

[201] McGall, G. H.; Barone, A. D.; Diggelmann, M.; Fodor, S. P. A.; Gentalen, E.; Ngo, N. *J. Am. Chem. Soc.* **1997,** *119*, 5081-5090.

[202] Brandow, S. L.; Chen, M. S.; Aggarwal, R.; Dulcey, C. S.; Calvert, J. M.; Dressick, W. J. *Langmuir* **1999,** *15*, 5429-5432.

[203] Zhao, B.; Moore, J. S.; Beebe, D. J. *Science* **2001,** *291*, 1023-1026.

[204] Zhao, B.; Moore, J. S.; Beebe, D. J. *Anal. Chem.* **2002,** *74*, 4259-4268.

[205] Zhao, B.; Viernes, N. O. L.; Moore, J. S.; Beebe, D. J. *J. Am. Chem. Soc.* **2002,** *124*, 5284-5285.

[206] Lercel, M. J.; Tiberio, R. C.; Chapman, P. F.; Craighead, H. G.; Sheen, C. W.; Parikh, A. N.; Allara, D. L. In *Self-assembled monolayer electron-beam resists on GaAs and SiO$_2$*, Proceedings of the 16th international symposium on electron, ion, and photon beams, San Diego, California (USA), 1993.

[207] Lercel, M. J.; Redinbo, G. F.; Pardo, F. D.; Rooks, M.; Tiberio, R. C.; Simpson, P.; Craighead, H. G.; Sheen, C. W.; Parikh, A. N.; Allara, D. L. *J. Vac. Sci. Technol., B* **1994,** *12*, 3663-3667.

[208] St.John, P. M.; Craighead, H. G. *J. Vac. Sci. Technol., B* **1996,** *14*, 69-74.

[209] Lercel, M. J.; Craighead, H. G.; Parikh, A. N.; Seshadri, K.; Allara, D. L. *Appl. Phys. Lett.* **1996,** *68*, 1504-1506.

[210] Marrian, C. R. K.; Perkins, F. K.; Brandow, S. L.; Koloski, T. S.; Dobisz, E. A.; Calvert, J. M. *Appl. Phys. Lett.* **1994,** *64*, 390-392.

[211] Harnett, C. K.; Satyalakshmi, K. M.; Craighead, H. G. *Appl. Phys. Lett.* **2000,** *76*, 2466-2468.

[212] Sato, T.; Hasko, D. G.; Ahmed, H. *J. Vac. Sci. Technol., B* **1997,** *15*, 45-48.

[213] Choi, K. H.; Bourgoin, J. P.; Auvray, S.; Esteve, D.; Duesberg, G. S.; Roth, S.; Burghard, M. *Surf. Sci.* **2000,** *462*, 195-202.

[214] Krupke, R.; Malik, S.; Weber, H. B.; Hampe, O.; Kappes, M. M.; von Lohneysen, H. *Nano Lett.* **2002,** *2*, 1161-1164.

[215] Jung, Y. J.; La, Y. H.; Kim, H. J.; Kang, T. H.; Ihm, K.; Kim, K. J.; Kim, B.; Park, J. W. *Langmuir* **2003,** *19*, 4512-4518.

[216] Maeng, I. S.; Park, J. W. *Langmuir* **2003,** *19*, 4519-4522.

[217] Wang, X. J.; Hu, W. C.; Ramasubramaniam, R.; Bernstein, G. H.; Snider, G.; Lieberman, M. *Langmuir* **2003,** *19*, 9748-9758.

[218] Pallandre, A.; Glinel, K.; Jonas, A. M.; Nysten, B. *Nano Lett.* **2004,** *4*, 365-371.

[219] Kubena, R. L.; Ward, J. W.; Stratton, F. P.; Joyce, R. J.; Atkinson, G. M. *J. Vac. Sci. Technol., B* **1991,** *9*, 3079-3083.

[220] Kubena, R. L.; Joyce, R. J.; Ward, J. W.; Garvin, H. L.; Stratton, F. P.; Brault, R. G. *J. Vac. Sci. Technol., B* **1988,** *6*, 353-356.

[221] Rieke, P. C.; Tarasevich, B. J.; Wood, L. L.; Engelhard, M. H.; Baer, D. R.; Fryxell, G. E.; John, C. M.; Laken, D. A.; Jaehnig, M. C. *Langmuir* **1994,** *10*, 619-622.

[222] Ada, E. T.; Hanley, L.; Etchin, S.; Melngailis, J.; Dressick, W. J.; Chen, M.-S.; Calvert, J. M. *J. Vac. Sci. Technol., B* **1995,** *13*, 2189-2196.

[223] Schenkel, T.; Schneider, M.; Hattass, M.; Newman, M. W.; Barnes, A. V.; Hamza, A. V.; Schneider, D. H.; Cicero, R. L.; Chidsey, C. E. D. *J. Vac. Sci. Technol., B* **1998,** *16*, 3298-3300.

[224] Younkin, R.; Berggren, K. K.; Johnson, K. S.; Prentiss, M.; Ralph, D. C.; Whitesides, G. M. *Appl. Phys. Lett.* **1997,** *71*, 1261-1263.

[225] Suh, D.; Simons, J. K.; Taylor, J. W.; Koloski, T. S.; Calvert, J. M. In *Soft x-ray photochemistry of chemisorbed self-assembled monolayers*, Proceedings of the 16th international symposium on electron, ion, and photon beams, San Diego, California (USA), 1993.

[226] Dressick, W. J.; Dulcey, C. S.; Brandow, S. L.; Witschi, H.; Neeley, P. F. *J. Vac. Sci. Technol., A* **1999,** *17*, 1432-1440.

[227] La, Y. H.; Kim, H. J.; Maeng, I. S.; Jung, Y. J.; Park, J. W.; Kim, K. J.; Kang, T. H.; Kim, B. *Langmuir* **2002,** *18*, 2430-2433.

[228] La, Y. H.; Jung, Y. J.; Kim, H. J.; Kang, T. H.; Ihm, K.; Kim, K. J.; Kim, B.; Park, J. W. *Langmuir* **2003,** *19*, 4390-4395.

[229] Yang, X. M.; Peters, R. D.; Kim, T. K.; Nealey, P. F.; Brandow, S. L.; Chen, M. S.; Shirey, L. M.; Dressick, W. J. *Langmuir* **2001,** *17*, 228-233.

[230] Kim, S. O.; Solak, H. H.; Stoykovich, M. P.; Ferrier, N. J.; de Pablo, J. J.; Nealey, P. F. *Nature* **2003,** *424*, 411-414.

[231] Xia, Y. N.; Whitesides, G. M. *Angew. Chem., Int. Ed.* **1998,** *37*, 551-575.

[232] Xia, Y. N.; Rogers, J. A.; Paul, K. E.; Whitesides, G. M. *Chem. Rev.* **1999,** *99*, 1823-1848.

[233] Xia, Y. N.; Mrksich, M.; Kim, E.; Whitesides, G. M. *J. Am. Chem. Soc.* **1995,** *117*, 9576-9577.

[234] John, P. M. S.; Craighead, H. G. *Appl. Phys. Lett.* **1996,** *68*, 1022-1024.

[235] Wang, D.; Thomas, S. G.; Wang, K. L.; Xia, Y.; Whitesides, G. M. *Appl. Phys. Lett.* **1997,** *70*, 1593-1595.

[236] Jeon, N. L.; Finnie, K.; Branshaw, K.; Nuzzo, R. G. *Langmuir* **1997,** *13*, 3382-3391.

[237] Finnie, K. R.; Haasch, R.; Nuzzo, R. G. *Langmuir* **2000,** *16*, 6968-6976.

[238] Harada, Y.; Girolami, G. S.; Nuzzo, R. G. *Langmuir* **2003,** *19*, 5104-5114.

[239] Pfohl, T.; Kim, J. H.; Yasa, M.; Miller, H. P.; Wong, G. C. L.; Bringezu, F.; Wen, Z.; Wilson, L.; Kim, M. W.; Li, Y.; Safinya, C. R. *Langmuir* **2001,** *17*, 5343-5351.

[240] Jeon, N. L.; Clem, P. G.; Payne, D. A.; Nuzzo, R. G. *Langmuir* **1996,** *12*, 5350-5355.

[241] Moran, C. E.; Radloff, C.; Halas, N. J. *Adv. Mater.* **2003,** *15*, 804-807.

[242] Hidber, P. C.; Helbig, W.; Kim, E.; Whitesides, G. M. *Langmuir* **1996,** *12*, 1375-1380.

[243] Loo, Y. L.; Willett, R. L.; Baldwin, K. W.; Rogers, J. A. *J. Am. Chem. Soc.* **2002,** *124*, 7654-7655.

[244] Delamarche, E.; Geissler, M.; Magnuson, R. H.; Schmid, H.; Michel, B. *Langmuir* **2003,** *19*, 5892-5897.

[245] Delamarche, E.; Geissler, M.; Vichiconti, J.; Graham, W. S.; Andry, P. A.; Flake, J. C.; Fryer, P. M.; Nunes, R. W.; Michel, B.; O'Sullivan, E. J.; Schmid, H.; Wolf, H.; Wisnieff, R. L. *Langmuir* **2003,** *19*, 5923-5935.

[246] Geissler, M.; Kind, H.; Schmidt-Winkel, P.; Michel, B.; Delamarche, E. *Langmuir* **2003,** *19*, 6283-6296.

[247] Geissler, M.; Wolf, H.; Stutz, R.; Delamarche, E.; Grummt, U. W.; Michel, B.; Bietsch, A. *Langmuir* **2003,** *19*, 6301-6311.

[248]   Delamarche, E.; Vichiconti, J.; Hall, S. A.; Geissler, M.; Graham, W.; Michel, B.; Nunes, R. *Langmuir* **2003,** *19*, 6567-6569.

[249]   Kramer, S.; Fuierer, R. R.; Gorman, C. B. *Chem. Rev.* **2003,** *103*, 4367-4418.

[250]   Sugimura, H.; Nakagiri, N.; Ichinose, N. *Appl. Phys. Lett.* **1995,** *66*, 3686-3688.

[251]   Sugimura, H.; Nakagiri, N. *J. Am. Chem. Soc.* **1997,** *119*, 9226-9229.

[252]   Sugimura, H.; Hanji, T.; Hayashi, K.; Takai, O. *Adv. Mater.* **2002,** *14*, 524-526.

[253]   Inoue, A.; Ishida, T.; Choi, N.; Mizutani, W.; Tokumoto, H. *Appl. Phys. Lett.* **1998,** *73*, 1976-1978.

[254]   Maoz, R.; Frydman, E.; Cohen, S. R.; Sagiv, J. *Adv. Mater.* **2000,** *12*, 424-429.

[255]   Maoz, R.; Cohen, S. R.; Sagiv, J. *Adv. Mater.* **1999,** *11*, 55-61.

[256]   Maoz, R.; Frydman, E.; Cohen, S. R.; Sagiv, J. *Adv. Mater.* **2000,** *12*, 725-731.

[257]   Liu, S. T.; Maoz, R.; Schmid, G.; Sagiv, J. *Nano Lett.* **2002,** *2*, 1055-1060.

[258]   Hoeppener, S.; Maoz, R.; Cohen, S. R.; Chi, L. F.; Fuchs, H.; Sagiv, J. *Adv. Mater.* **2002,** *14*, 1036-1041.

[259]   Liu, C. S.; Maoz, R.; Sagiv, J. *Nano Lett.* **2004,** *4*, 845-851.

[260]   Hoeppener, S.; Maoz, R.; Sagiv, J. *Nano Lett.* **2003,** *3*, 761-767.

[261]   Wouters, D.; Schubert, U. S. *Langmuir* **2003,** *19*, 9033-9038.

[262]   Muller, W. T.; Klein, D. L.; Lee, T.; Clarke, J.; McEuen, P. L.; Schultz, P. G. *Science* **1995,** *268*, 272-273.

[263]   Piner, R. D.; Zhu, J.; Xu, F.; Hong, S. H.; Mirkin, C. A. *Science* **1999,** *283*, 661-663.

[264]   Ivanisevic, A.; Mirkin, C. A. *J. Am. Chem. Soc.* **2001,** *123*, 7887-7889.

[265]   Pena, D. J.; Raphael, M. P.; Byers, J. M. *Langmuir* **2003,** *19*, 9028-9032.

[266]   Jung, H.; Kulkarni, R.; Collier, C. P. *J. Am. Chem. Soc.* **2003,** *125*, 12096-12097.

[267]   Lim, J. H.; Ginger, D. S.; Lee, K. B.; Heo, J.; Nam, J. M.; Mirkin, C. A. *Angew. Chem., Int. Ed.* **2003,** *42*, 2309-2312.

[268]   Demers, L. M.; Ginger, D. S.; Park, S.-J.; Li, Z.; Chung, S.-W.; Mirkin, C. A. *Science* **2002,** *296*, 1836-1838.

Chapter 3

Molecular Printboards: Monolayers of β-Cyclodextrins on Silicon Oxide Surfaces[*]

3.1   Introduction

Self-assembled monolayers[1,2] (SAMs) offer a unique way to confine molecules in two dimensions. When functionalized with suitable receptor adsorbates, SAMs can be used to monitor binding events at the interface, which is of considerable importance in, for example, biochemistry and sensor development. A well-known class of receptor molecules are the naturally occurring cyclodextrins (CDs) that consist of six (α), seven (β), or eight (γ) α-D-glucose units. These macrocycles are water-soluble molecules that contain a hydrophobic cavity, which enables complexation of organic molecules from aqueous solutions based on hydrophobic interactions.[1]

Immobilization of CDs on a gold surface and the complexation behavior of immobilized CDs have been investigated intensively in recent years.[3-18] Recently, our group introduced the term 'molecular printboard' for a host surface onto which guest molecules can be positioned by reversible interactions of tunable strength.[18] However, an inherent disadvantage when working with SAMs on gold is the difficulty to use fluorescence techniques. The reason for this is that the excited state of fluorescent molecules situated at or near the gold couples with the surface plasmons of the gold, resulting in energy transfer from the fluorescent dye to the surface without fluorescence emission. This quenching process is a well-known phenomenon for fluorescent molecules near metallic surfaces,[19,20] and for this reason fluorescence imaging is typically limited to oxide surfaces (e.g. SiO_2). Fluorescence spectroscopy and microscopy can be very sensitive characterization tools that allow for both qualitative and quantitative analysis of binding processes at the surface.[21] Therefore, receptor monolayers on SiO_2 could offer the advantage of employing fluorescence techniques to study binding events at the receptor interface.

Since their discovery in the early 1980s,[22] SAMs of trichloro- and trialkoxysilanes on hydroxyl-terminated surfaces (e.g. glass, oxidized silicon wafers) have been investigated extensively, as was reviewed in Chapter 2. However, the high reactivity of the trichloro- and trialkoxysilanes strongly limits the number of functional groups that can be directly introduced into these SAMs. As a result the chemical diversity of these monolayers has been rather limited when compared to SAMs on gold.[23] In accordance with the limited number of functional groups available on the glass surface, reports on the immobilization of CD molecules are rare. Li and coworkers have reported the covalent binding of *β*-CDs to the SiO_2 surface by using 1,6-bis(trichlorosilyl)hexane as a coupling layer.[24,25] However, hardly any characterization of these layers was given, and it is unlikely that ordered monolayers are formed as 1,6-bis(trichlorosilyl)hexane can backfold to react twice with the surface and is prone to form multilayers by polymerization. Nevertheless, attenuated total reflection infrared (ATR-IR) measurements suggested the successful attachment of functionalized *β*-CDs, and interactions of the layers with volatile organic compounds (VOCs) in the gas phase were studied by surface acoustic wave (SAW) measurements. Modifying *β*-CDs with trialkoxysilanes on both the primary and secondary side led to deposition of CD siloxane multilayer thin films.[26] Also these films were used to monitor interactions with VOCs. *β*-CDs with an unmodified

secondary side were immobilized by Wenz and Mittler, who reacted per-6-amino *β-*CD with an epoxy-terminated monolayer.[27] Although these layers gave reasonable interactions with VOCs, they were not characterized in detail.

This Chapter presents a new synthesis route toward stable, densely packed *β-*CD monolayers. The *β*-CD monolayers have been characterized in detail. Fluorescence spectroscopy was used to study the binding properties of these monolayers. Such a monolayer of receptor molecules can be used as a 'molecular printboard' to position molecules on a surface through well-defined supramolecular interactions.

3.2   Results and Discussion

3.2.1 *Monolayer synthesis*

The synthesis route to prepare *β*-CD monolayers on SiO_2 is outlined in Scheme 3.1. It starts with the formation of a cyano-terminated monolayer of 1-cyano-11-trichlorosilylundecane. SAMs were prepared on cleaned microscope glass slides or silicon wafers by immersion of the substrate in a cooled 0.1 vol% solution in toluene.[28] Following SAM formation the layers were reduced to the corresponding free amines using Red Al.[29] Red Al yielded better results than $LiAlH_4$ in THF, which has been reported before for this reaction.[30] This indirect way to obtain well-defined amino-terminated monolayers was preferred over direct functionalization with compounds like 3-aminopropyl-triethoxysilane as the monolayers made by the latter method suffer from a lack of well-defined structure in the siloxane networks formed.[31] More importantly, the monolayers formed by direct functionalization display only a limited stability in aqueous solution. A good stability is necessary, as binding studies at *β*-CD monolayers have to be performed in aqueous media.

Linking *β*-CDs to the SAM was accomplished by first reacting the free amino groups with 1,4-phenylene diisothiocyanate (DITC) to convert the surface amino groups to free isothiocyanate groups. The use of *p*-substituted phenylenes as linking molecules has been reported recently by Suter and co-workers.[32] They reacted a hydroxyl-terminated SAM on gold with 1,4-phenylene diisocyanate and found that only one of the isocyanate groups reacted with the monolayer, leaving the second available for further derivatization. The isocyanate-terminated surface could be modified by a number of reactions with amines or alcohols. In this case the reaction

with per-6-amino *β*-CD, which is poorly soluble in organic solvents, required working in aqueous solution. As isocyanates are unstable in water, the use of a different reacting group that is stable in aqueous solution and reactive toward free amines was necessary. For this reason isothiocyanates were used. Amino-terminated SAMs were modified with DITC in toluene, and the resulting isothiocyanates were reacted with an aqueous per-6-amino *β*-CD solution at pH 8.5 to yield a *β*-CD-terminated surface. Since the *β*-CD molecules will exclusively react through the amino groups on the primary side, it is expected that they are oriented with the wider, secondary side facing upward.
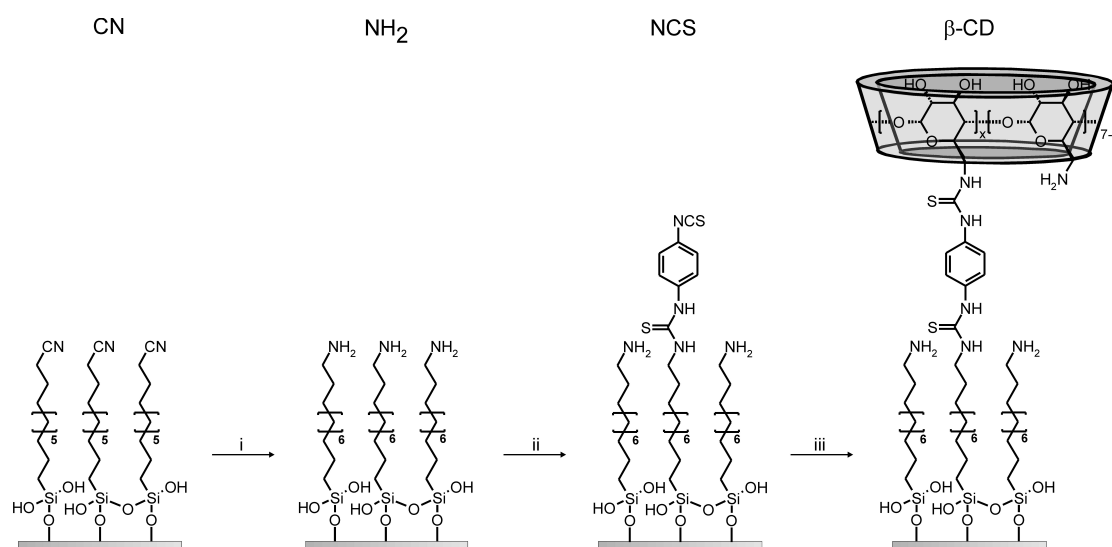
Scheme 3.1 *Synthesis scheme for the preparation of β-CD monolayers on SiO₂ surfaces: (i) Red Al, toluene, 40 ˚C; (ii) DITC, toluene, 50 ˚C; (iii) per-6-amino β-CD, H₂O, 50 ˚C.*

3.2.2 Monolayer characterization

Monolayer formation and subsequent surface reactions were monitored with a variety of techniques including contact angle goniometry, ellipsometry, Brewster-angle FT-IR, X-ray photoelectron spectroscopy (XPS), and time-of-flight secondary ion mass spectrometry (TOF-SIMS). Contact angle, ellipsometry, and XPS data are summarized in Table 3.1.

Table 3.1 *Advancing (θ$_a$) and receding (θ$_r$) water contact angles, ellipsometric thicknesses, and selected XPS data of SAMs shown in Scheme 3.1.*

SAM	θ$_a$ (°)	θ$_r$ (°)	Ell. thickness (nm)	C/N (XPS)	C/N (calc.)
CN	73 ± 1	60 ± 2	2.0 ± 0.1	11.5 ± 0.4	12
NH$_2$	60 ± 1	25 ± 2	2.0 ± 0.2	13.6 ± 0.7	12
SCN	68 ± 1	< 20	2.4 ± 0.2	8.5 ± 0.3	8.8[*]
β-CD	49 ± 1	< 20	3.2 ± 0.3	7.8 ± 0.6	7.9[*]

[*] Estimated value. See text for details.

SAMs formed from 1-cyano-11-trichlorosilylundecane had an advancing contact angle of 73°, consistent with a previously reported value,[30] and a hysteresis of 13° suggesting that the SAM is well-packed. Also the ellipsometric thickness of 2.0 nm is consistent with the anticipated length of a *trans*-extended conformation of this adsorbate. Furthermore, the C/N ratio of 11.5 found by XPS is in agreement with the molecular composition. Besides XPS, also TOF-SIMS was employed to analyze the chemical surface composition of the CN SAM. While reports on the use of TOF-SIMS as a characterization tool for SAMs on gold are numerous, TOF-SIMS studies on organosilicon compounds immobilized on oxide surfaces are rare.[33-36] Because of the formation of an in-plane polysiloxane network, secondary ions corresponding to the intact immobilized molecule are hardly ever observed, although structurally relevant ions are usually detected. Also in our case no molecular ion peaks were found, but the spectrum contains a prominent peak for CN⁻, and further a series of N-containing hydrocarbons were detected that were probably formed by fragmentation of the immobilized silane molecules. No chlorine signals were found by TOF-SIMS or by XPS, which indicates that full condensation of the silane molecules had taken place in solution or at the surface (see discussion in Chapter 2.2). Brewster angle infrared spectra of a monolayer formed on a double side polished Si wafer (shown in Figure 3.1) revealed C-H stretching bands at 2925 cm⁻¹ and 2854 cm⁻¹, indicative of a liquid crystalline-like order in the SAM.[37-39] In addition, a weak band at 2246 cm⁻¹ was found, characteristic for a nitrile group.

Reduction of the CN SAM with Red Al gave the NH$_2$ SAM (Scheme 3.1). After reduction the nitrile band at 2246 cm⁻¹ disappeared, which suggests that the reduction was complete. Methylene stretching bands were found to remain at a constant wavenumber, implying that the surface reaction did not affect the order in the layer. While the ellipsometric thickness did not change significantly, the advancing

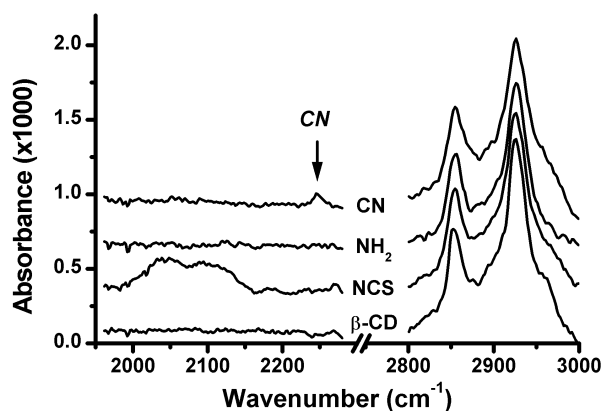contact angle dropped to 60°, indicative of the formation of an amino-terminated surface.[30,40]

Figure 3.1 *Brewster angle FT-IR spectra of monolayers terminated by CN, NH₂, NCS, and β-CD.*

Figure 3.2 shows the high-resolution XPS spectra of the N 1s region for all monolayers. Although the peak intensity is similar to the N 1s peak of the CN SAM, it is clear that for the NH₂ SAM two peaks are present at 399 and 401 eV, which can be assigned to free amine and protonated amine, respectively.[12,31,41,42] The presence of protonated amine after exposing the monolayer to an aqueous 0.5 M NaOH solution does not agree with results found before, but can be easily explained by inadvertent protonation through washing with water afterwards. However, the reported lack of reactivity of these surfaces was not experienced.[31] Reaction of the amino-terminated SAM with DITC to give the NCS SAM (Scheme 3.1) was accompanied by an increase in ellipsometric thickness of ~0.4 nm, which is in good agreement with the dimension of the molecule, and an increase in the advancing contact angle to 68°. Spectroscopic evidence for the successful reaction is shown in Figure 3.1, where a broad band in the IR spectrum is observed around 2070 cm^{-1}, which can be attributed to isothiocyanate groups.[43] Again the methylene stretching bands were unaffected by the surface reactions. In addition, a large decrease in C/N ratio was observed in XPS measurements, which can be explained by the introduction of nitrogen containing DITC molecules. From this change in C/N ratio it was estimated that one out of three amines had reacted with DITC. This seems a reasonable result, since an aromatic ring is more bulky than an alkyl chain and some of the amines were still protonated,

rendering them inactive for reaction with DITC. Table 1 shows the experimentally found value and the calculated value for the introduction of one DITC molecule on three alkyl chains. Finally, TOF-SIMS measurements yielded a prominent NCS peak and several fragments of the DITC molecule in both the positive and negative spectra.
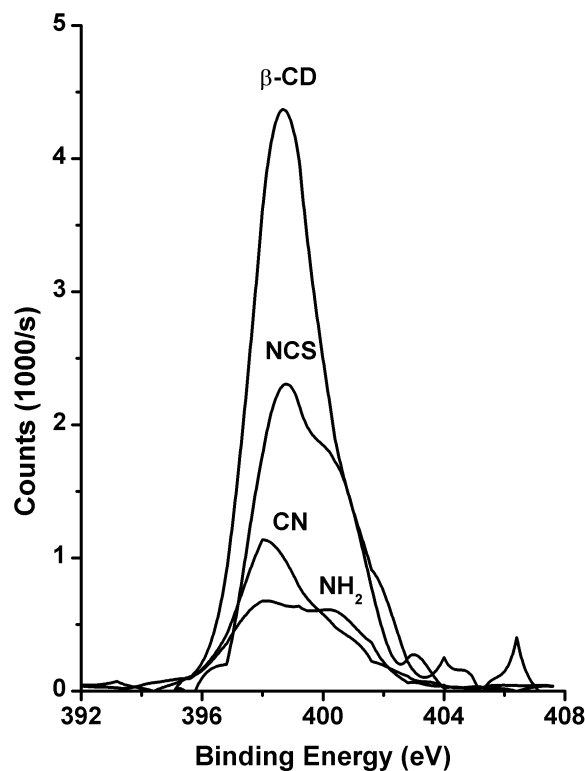

Figure 3.2 *X-ray photoelectron spectra of the N 1s region for monolayers terminated by CN, NH₂, NCS, and β-CD.*

In the final step the β-CD host molecules were introduced by reacting per-6-amino β-CD with the free isothiocyanates on the surface (Scheme 3.1). A clear change in the polarity of the surface was observed as witnessed by the drop in advancing contact angle to 49°. This corresponds to a densely-packed β-CD monolayer with exposed hydroxyl groups and is similar to the advancing contact angle of β-CD SAMs on gold.[12] The ellipsometric thickness increased by ~0.8 nm, as expected for a β-CD lying flat on the surface,[12] and the broad band around 2070 cm^{-1} in the IR-spectrum disappeared, indicating complete reaction of the isothiocyanates. TOF-SIMS did not give a distinct identification of β-CD on the surface, but a range of oxygen-containing hydrocarbons was found, most likely fragments of β-CD. Figure 3.2 shows a marked increase in the N 1s high-resolution XPS spectrum, indicative of the introduction of

N-containing per-6-amino β-CD in the SAM. The reaction caused a decrease in C/N ratio, which can be quantified in terms of how many NCS groups have reacted with a β-CD. It was estimated that if one β-CD cavity was introduced on ca three NCS molecules and thus on ca nine alkyl chains the calculated C/N ratio matched the experimentally found ratio, as shown in Table 1. Experimentally, the area that is occupied by nine close-packed alkyl chains in a SAM is around 2.3 nm^2,[44] and the area occupied by a β-CD molecule is ca 1.9 nm^2.[14] This would imply that using this methodology a densely packed monolayer of β-CDs is formed with a surface coverage of ~80 %. The β-CD molecules are rigidly anchored to the SAM via multiple attachment points, and therefore oriented with the wider secondary side facing upward, accessible for complexation of guest molecules. Tapping mode AFM measurements were performed on all SAMs to inspect the roughness of the substrates (Figure 3.3). Images were generally featureless with a root-mean-square (rms) roughness of ~0.5 nm for all monolayers.

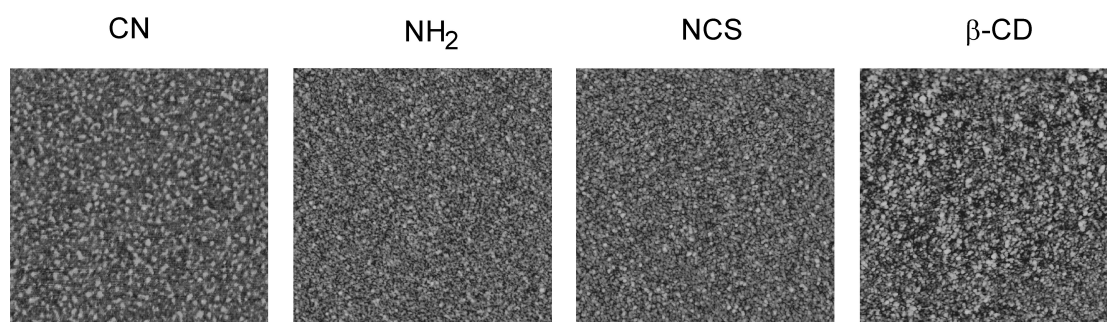| CN	NH$_2$	NCS	β-CD

Figure 3.3 *Tapping mode AFM images (1×1 μm^2) of monolayers terminated by CN, NH$_2$, NCS, and β-CD. Z-scale in all images is 5 nm.*

Although the experiments discussed above indicate the formation of a densely packed β-CD monolayer, our covalent immobilization technique does not allow for any lateral mobility, which is required to achieve closest packing. The closest packing calculated for disks of equal diameter adsorbing onto a flat surface leads to approximately 90 % surface coverage.[45] Speculating on the attachment of the per-6-amino β-CD molecules to the NCS monolayer, it would be reasonable to assume that the first stages of this reaction proceed via *random sequential adsorption* (RSA) configurations.[45] This configuration is generated by sequentially adding disks randomly onto a surface, where a disk is irreversibly adsorbed on the substrate if it

does not overlap any disks already there. This process continues until there is no room left for another disk. At this stage the coverage of the surface is ~55 %.[45] However, we propose that the *β*-CD host molecules can then still react with uncovered parts of the surface by assuming a different conformation with respect to the surface. A tilted conformation effectively reduces the surface area of the *β*-CDs, making immobilization possible albeit via fewer covalent bonds. This additional mode of attachment would lead to a higher surface coverage.

3.2.3 *Reversible binding of a fluorescently labeled guest molecule*

Because of the insulating nature of SiO_2 it is not possible to use techniques such as surface plasmon resonance or electrochemical impedance spectroscopy, which have been typically applied in our group to study the interaction of guest molecules at the *β*-CD SAMs on gold.[14,18,46] Therefore, a desorption experiment was carried out to quantify the interaction of a water-soluble, fluorescently labeled guest molecule **1** (Chart 3.1), bearing two adamantyl units for complexation and a fluorescein dye for fluorescent signaling, with a *β*-CD monolayer on SiO_2.[47] It is expected that **1** binds in a similar fashion as **2**, which has been shown to bind via two interactions with *β*-CD SAMs on gold.
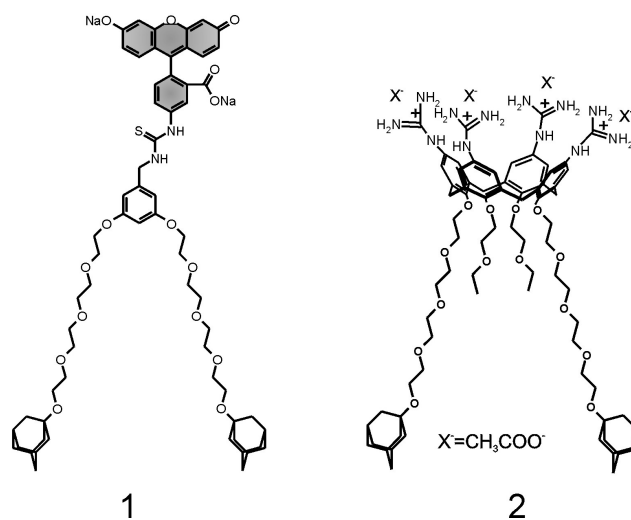

Chart 3.1 *Guest compounds that were used to determine binding constants with β-CD monolayers on SiO₂ (1) and gold (2).*

The desorption experiment is schematically represented in Figure 3.4. First, a *β*-CD monolayer was dipped into an aqueous 10^{-5} M solution of **1**, saturating the host-SAM with guest molecules bound through supramolecular interactions. After that, the substrates were rinsed extensively with an aqueous NaOH solution (pH 9), a 10 mM phosphate buffer solution and water to remove physisorbed material. Next, defined areas of the substrate were exposed to various concentrations of a *β*-CD solution by placing a container on top of the substrate, which was then filled with 100 μl of a *β*-CD solution (0.5 to 10 mM). By exposing the bound guest molecules to a *β*-CD solution, competition is induced between binding to the surface and binding in solution, which in the case of multivalent binding is usually concentration-dependent.[21,48,49] The solution was kept in contact with the SAM for 5 min to allow desorption of **1**. In a time-dependent experiment it was found that 5 min desorption time is sufficient to reach equilibrium. After 5 min, 60 μl of the solution was withdrawn, diluted with an aqueous buffer solution and the fluorescence emission spectrum of the solution was recorded.
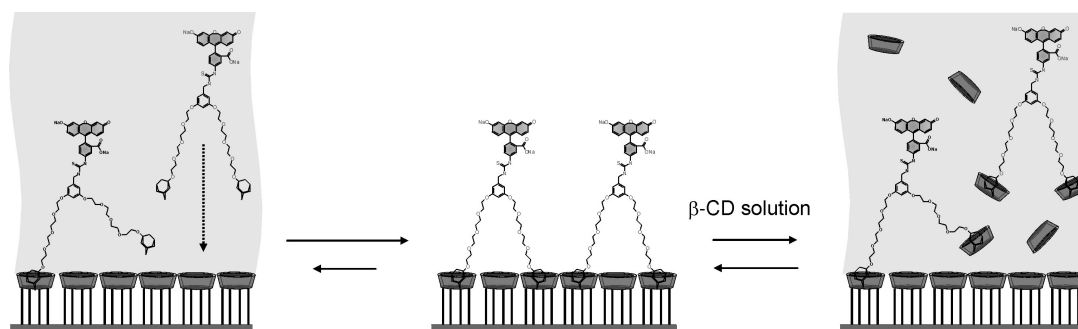

Figure 3.4 *Schematic representation of the β-CD concentration-dependent desorption experiment.*

Figure 3.5A shows the fluorescence spectra for increasing *β*-CD concentrations. It is evident that increasing the *β*-CD concentration in solution results in the desorption of more guest molecules, where maximum desorption is reached around 5 mM. To verify how much of the complexed fluorescent guest molecules had been desorbed, the desorption experiment was repeated on the same spot for the highest *β*-CD concentration (10 mM). The emission maximum was found to be less

than 10% of the initial value, indicating that nearly all of the complexed guest molecules were desorbed during the first experiment (Figure 3.5B).
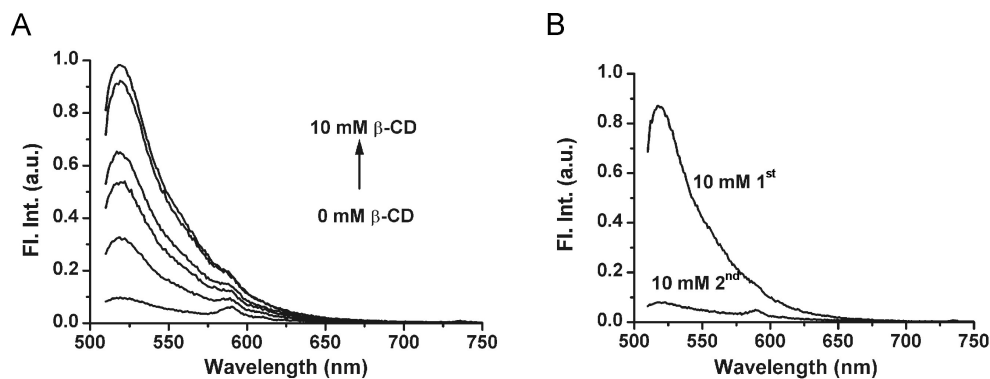

Figure 3.5 *Desorption of guest **1** from the β-CD monolayer by β-CD in solution. (a) Fluorescence spectra of desorbed **1** at β-CD concentrations ranging from 0 to 10 mM. (b) Fluorescence spectra of desorbed **1** at 10 mM β-CD concentration, twice on the same spot.*

The emission maximum (519 nm) obtained for each β-CD concentration is plotted against the β-CD concentration in Figure 3.6. To obtain an estimate of the binding constant of **1** with the β-CD surface, the data points were fitted to a theoretical model.[50] This model describes divalent binding as two consecutive monovalent binding events, i.e. an intermolecular interaction and an intramolecular binding event. The model considers both binding events to be directly related to an intrinsic binding constant ($K_{i,s}$), with an additional effective concentration term (C_{eff}) incorporated for the intramolecular binding event, accounting for the close proximity of the two interacting species. The relation between the observed binding constant (K_{obs}) and intrinsic binding constant is stated in equation 1.

$$K_{obs} = C_{eff} (K_{i,s})^2 \qquad (1)$$

The solid line in Figure 3.6 represents the result of the fitting procedure. The optimal fit resulted in an intrinsic binding constant to the surface $K_{i,s} = 3.3 \times 10^5$ M^{-1}, which gives an observed binding constant $K_{obs} \sim 10^{10}$ M^{-1}. This high binding constant is rationalized by the high effective β-CD concentration at the surface of ~0.2 M. Similar binding constants ($K_{i,s} = 3 \times 10^5$ M^{-1} and $K_{obs} \sim 10^{10}$ M^{-1}) were found by

surface plasmon resonance measurements for the divalent, calix[4]arene-derivatized guest molecule **2** (Chart 3.1) adsorbed on β-CD SAMs on gold,[46,51] indicating that the binding properties of β-CD monolayers on SiO_2 are comparable to those on gold.

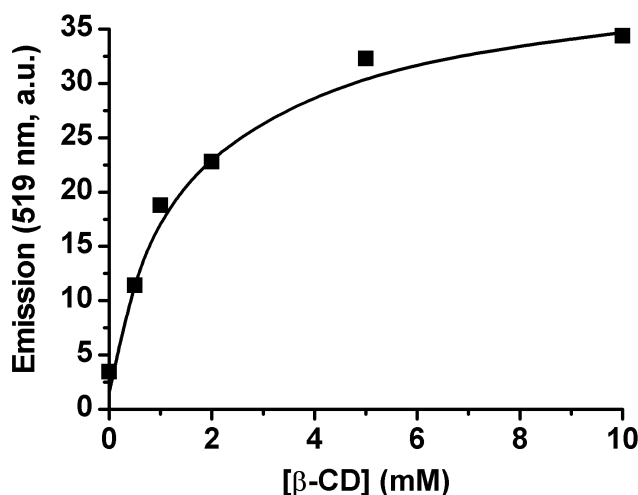***Figure 3.6*** *Fluorescence intensity (519 nm) of desorbed **1** as a function of β-CD concentration (squares) and corresponding fit by a theoretical model (solid line).*

In addition, fluorescence spectroscopy allows for quantification of the number of guest molecules bound to the surface. By comparing the fluorescence intensity of the desorbed solutions with solutions containing known concentrations of **1**, it is possible to determine how many host-guest complexes were formed. In this manner it was found that desorption with the highest β-CD concentration resulted in a 5×10^{-8} M solution of **1**, which means that 3.0×10^{12} molecules were present in 100 μl of solution. As each molecule was bound by two β-CDs, also the number of β-CDs that were involved in binding on the specific area where the container was placed was known (6.0×10^{12}). Combining the surface area that one β-CD occupies (1.9 nm^2),[14] the number of β-CD molecules, and the surface area of the container (3.9×10^{-5} m^2) resulted in a percentage of the surface area that was occupied by β-CDs, complexed with guest molecule **1**. From the data above follows that this percentage was ca. 30 %. This percentage may not seem very high, which could have several reasons. First, after saturating the host SAM with guest molecules from solution the monolayers were rinsed *extensively* with aqueous solutions, as outlined above. This could potentially result in the removal of part of the guest molecules. That this is likely is

shown in Figure 3.5A. Desorption in absence of β-CD resulted in a low fluorescence signal, indicating that some desorption was taking place (although at a low rate). In addition, it is not expected that covalent attachment of the β-CDs leads to the closest packing possible, as was discussed in the Chapter 3.2.2 section.

3.3 Conclusions

The synthesis of monolayers of β-CD host molecules on SiO$_2$ surfaces in four steps starting from a commercially available adsorbate, 1-cyano-11-trichlorosilylundecane, was demonstrated. The cyano-terminated SAMs were successively reduced to their corresponding amines using Red Al as a reducing agent and derivatized with 1,4-phenylene diisothiocyanate as a linker molecule, exposing isothiocyanates that were reacted with per-6-amino β-CD to yield a host SAM. Extensive characterization of these layers indicated the formation of a densely packed β-CD monolayer where the β-CDs are rigidly anchored to the SAM through multiple covalent bonds, with the secondary side of the β-CD cavities facing upward, accessible for complexation of guest molecules. Hence, the β-CD monolayers on SiO$_2$ are similar to the β-CD monolayers on gold with respect to packing and orientation of the host molecules. In a desorption experiment on these SAMs with a fluorescent guest molecule it was shown that the binding properties of the immobilized β-CDs were retained. Moreover, the binding constant of the guest molecule was found to be very similar to the binding constant of a similar guest molecule with β-CD SAMs on gold, indicating that the host monolayers on SiO$_2$ and gold display similar guest binding properties.

The advantage of β-CD monolayers on SiO$_2$ surfaces over β-CD SAMs on gold is that they enable the use of fluorescence techniques, which allow quantification of surface absorption of fluorescent molecules as well as high-resolution visualization of patterns and observation of individual molecules on surfaces. These β-CD monolayers on SiO$_2$ will be employed as a 'molecular printboard' for reversible positioning of guest molecules in the next Chapters, where the position of the guest molecules will be studied with optical techniques such as laser scanning confocal microscopy.

3.4 Experimental Section

General procedures. All moisture sensitive reactions were carried out under nitrogen atmosphere. Reagents were commercial and used without further purification.

Materials and methods. All glassware used to prepare monolayers and to perform subsequent reactions was cleaned by immersion in a Hellmanex or *piraña* solution. **Caution:** *piraña* is a very strong oxidant and reacts violently with many organic materials. Subsequently, the glassware was rinsed with large amounts of Millipore water and dried in an oven. 1-Cyano-11-trichlorosilylundecane was purchased from Gelest Inc, Red Al from Aldrich, and *p*-phenylene diisothiocyanate was purchased from Acros.

Substrate preparation. Four-inch polished, 100-cut, p-doped silicon wafers, cut into 2 x 2 cm samples, and microscope glass slides were used for monolayer preparation. Prior to monolayer formation the substrates were oxidized by immersion in boiling *piraña* (H_2SO_4 (96%): H_2O_2 (30%) 3: 1 v/v) for 15 minutes, rinsed with large amounts of Millipore water and dried in a stream of nitrogen.

Monolayer preparation. Substrates were exposed to a cooled (3-7°C) 0.1-vol% solution of 1-cyano-11-trichlorosilylundecane in freshly distilled toluene for 35 min under N_2. Following monolayer formation the substrates were rinsed with toluene to remove any excess of silanes and subsequently dried in a stream of nitrogen.

Surface reactions. The cyano-terminated SAMs were reduced to the corresponding amines by immersion for 4 h in a 10-vol% solution of Red Al in toluene under nitrogen atmosphere at 40 ˚C. Following the reduction, the substrates were sonicated in a 1 M HCl solution for 5 min to remove the Al salts and sonicated in a 0.5 M NaOH solution for 1 min to deprotonate the amines.[31] The layers were further sonicated in, and rinsed with large amounts of millipore water and finally dried in a stream of nitrogen. Transformation of the amino-terminated SAMs to isothiocyanate-bearing layers was accomplished by exposure to a 0.1 M solution of 1,4-phenylene diisothiocyanate in toluene at 50 °C for 2 h under N_2, followed by rinsing with toluene and drying in a stream of nitrogen. *β*-CD terminated SAMs were finally obtained by reaction of the isothiocyanate-terminated monolayers with per-6-amino *β*-cyclodextrin.[52] The reaction was performed in an aqueous 5 mM per-6-amino *β*-cyclodextrin solution (pH 8.5) at 50 °C for 2 h, after which the substrates were

sonicated in millipore water and finally rinsed with copious amounts of millipore water to remove physisorbed material.

Contact angle goniometry. Contact angles were measured with Millipore water on a Krüss G10 Contact Angle Measuring Instrument, equipped with a CCD camera. Advancing and receding contact angles were determined automatically during growth and shrinkage of the droplet by a drop shape analysis routine.

Ellipsometry. Ellipsometric layer thickness measurements were performed on a Plasmos Ellipsometer (λ = 633 nm) assuming a refractive index of 1.500 for the monolayers and 1.457 for the underlying native oxide. The thickness of the SiO_2 layer was measured separately on an unmodified part of the same wafer and subtracted from the total layer thickness determined for the monolayer covered silicon substrate.

Brewster angle FT-IR. Brewster angle infrared spectra were recorded on a Biorad FTS 60 A spectrophotometer, equipped with a home-built nitrogen-purged glove-box in which the sample holder and MCT detector were situated. Spectra were recorded at an angle of incidence of 73.7° for 512 scans at a resolution of 4 cm^{-1}. A background spectrum was first recorded using a freshly cleaned silicon substrate.

TOF-SIMS. TOF-SIMS spectra were acquired at Tascon GmbH, Münster (Germany) with an ION-TOF "TOF-SIMS IV" instrument with a pulsed primary beam of Au_1^+ and Au_3^+ ions (25 keV) under static conditions. Spectra were taken from an area of 100x100 μm^2 for positively and negatively charged secondary ions.

XPS. XPS spectra were obtained on a Quantera Scanning X-ray Multiprobe instrument, equipped with a monochromatic $Al_{K\alpha}$ X-ray source producing approximately 25 W of X-ray power. Spectra were referenced to the main C 1s peak set at 284.0 eV. XPS-data were collected from a surface area of 1000 μm x 300 μm with a pass energy of 224 eV and a step energy of 0.8 eV for survey scans and 0.4 eV for high resolution scans. For quantitative analysis, the sensitivity factors used to correct the number of counts under each peak were: C 1s, 1.00; N 1s, 1.59.

AFM. AFM measurements were carried out with a Nanoscope III multimode AFM in tapping mode using Si_3N_4 cantilevers (purchased from Nanosensors) with a spring constant of 37-56 Nm^{-1}. Images were acquired in ambient atmosphere.

Fluorescence spectroscopy. Fluorescence spectroscopy was performed on an Edinburgh FS900 fluorospectrophotometer in which a 450 W xenon arc lamp was used as excitation source. M300 gratings with 1800 1/mm were used on both

excitation and emission arms. Signals were detected by a Peltier element cooled, red sensitive, Hamamatsu R928 photomultiplier system. Quartz sample cells of 1 mm were used.

3.5 References

[1]   Ulman, A. *An Introduction to Ultrathin Organic Films*. Academic Press: Boston, 1991.

[2]   Ulman, A. *Chem. Rev.* **1996,** *96*, 1533-1554.

[3]   Rojas, M. T.; Koniger, R.; Stoddart, J. F.; Kaifer, A. E. *J. Am. Chem. Soc.* **1995,** *117*, 336-343.

[4]   Kaifer, A. E. *Isr. J. Chem.* **1996,** *36*, 389-397.

[5]   Kaifer, A. E. *Acc. Chem. Res.* **1999,** *32*, 62-71.

[6]   Nelles, G.; Weisser, M.; Back, R.; Wohlfart, P.; Wenz, G.; Mittler-Neher, S. *J. Am. Chem. Soc.* **1996,** *118*, 5039-5046.

[7]   Weisser, M.; Nelles, G.; Wohlfart, P.; Wenz, G.; Mittler-Neher, S. *J. Phys. Chem.* **1996,** *100*, 17893-17900.

[8]   Weisser, M.; Nelles, G.; Wenz, G.; MittlerNeher, S. *Sens. Actuators B* **1997,** *38*, 58-67.

[9]   Henke, C.; Steinem, C.; Janshoff, A.; Steffan, G.; Luftmann, H.; Sieber, M.; Galla, H. J. *Anal. Chem.* **1996,** *68*, 3158-3165.

[10]   Michalke, A.; Janshoff, A.; Steinem, C.; Henke, C.; Sieber, M.; Galla, H. J. *Anal. Chem.* **1999,** *71*, 2528-2533.

[11]   Janshoff, A.; Steinem, C.; Michalke, A.; Henke, C.; Galla, H. J. *Sens. Actuators B* **2000,** *70*, 243-253.

[12]   De Jong, M. R.; Huskens, J.; Reinhoudt, D. N. *Chem. Eur. J.* **2001,** *7*, 4164-4170.

[13]   Beulen, M. W. J.; Bügler, J.; Lammerink, B.; Geurts, F. A. J.; Biemond, E.; Van Leerdam, K. G. C.; Van Veggel, F. C. J. M.; Engbersen, J. F. J.; Reinhoudt, D. N. *Langmuir* **1998,** *14*, 6424-6429.

[14]   Beulen, M. W. J.; Bügler, J.; De Jong, M. R.; Lammerink, B.; Huskens, J.; Schönherr, H.; Vancso, G. J.; Boukamp, B. A.; Wieder, H.; Offenhauser, A.; Knoll, W.; Van Veggel, F. C. J. M.; Reinhoudt, D. N. *Chem. Eur. J.* **2000,** *6*, 1176-1183.

[15] Schönherr, H.; Beulen, M. W. J.; Bügler, J.; Huskens, J.; van Veggel, F. C. J. M.; Reinhoudt, D. N.; Vancso, G. J. *J. Am. Chem. Soc.* **2000,** *122*, 4963-4967.

[16] Zapotoczny, S.; Auletta, T.; De Jong, M. R.; Schönherr, H.; Huskens, J.; Van Veggel, F. C. J. M.; Reinhoudt, D. N.; Vancso, G. J. *Langmuir* **2002,** *18*, 6988-6994.

[17] Auletta, T.; De Jong, M. R.; Mulder, A.; Van Veggel, F. C. J. M.; Huskens, J.; Reinhoudt, D. N.; Zou, S.; Zapotoczny, S.; Schönherr, H.; Vancso, G. J.; Kuipers, L. *J. Am. Chem. Soc.* **2004,** *126*, 1577-1584.

[18] Huskens, J.; Deij, M. A.; Reinhoudt, D. N. *Angew. Chem., Int. Ed.* **2002,** *41*, 4467-4471.

[19] (a) Chance, R.; Prock, A.; Silbey, R. *Adv. Chem. Phys.* **1978**, *37*, 1-65. (b) Enderlein, J. *Chem. Phys.* **1999**, *247*, 1-9. (c) Kümmerlen, J.; Leitner, A.; Brunner, H.; Aussenegg, F. R.; Wokaun, A. *Mol. Phys.* **1993**, *80*, 1031-1046. (d) Reese, S.; Fox, M. A. *J. Phys. Chem. B* **1998**, *102*, 9820-9824.

[20] Quenching especially hampers fluorescence at continuous metallic films, but is less predominant at metallic nanoparticles or islands, see for example: (a) Chan, V. C. H.; Codd, S. L.; Van der Helm, M.; Spatz, J. P.; Röcker, C.; Nienhaus, G. U.; Levi, S. A.; Van Veggel, F. C. J. M.; Reinhoudt, D. N.; Möller, M. *J. Mater. Res.* **2001**, *676*, Y4.4. (b) Levi, S. A.; Mourran, A.; Spatz, J. P.; Van Veggel, F. C. J. M.; Reinhoudt, D. N.; Möller, M. *Chem. Eur. J.* **2002**, *8*, 3808-3814. (c) Dulkeith, W.; Morteani, A. C.; Niedereichholtz, T.; Klar, T. A.; Feldmann, J.; Levi, S. A.; Van Veggel, F. C. J. M.; Reinhoudt, D. N.; Möller, M.; Gittins, D. I. *Phys. Rev. Lett.* **2002**, *89*, 203002, 1-3. (d) Chumanov, G.; Sokolov, K.; Gregory, B. W.; Cotton, T. M. *J. Phys. Chem.* **1995**, *99*, 9466-9471.

[21] Yang, T. L.; Baryshnikova, O. K.; Mao, H. B.; Holden, M. A.; Cremer, P. S. *J. Am. Chem. Soc.* **2003,** *125*, 4779-4784.

[22] Sagiv, J. *J. Am. Chem. Soc.* **1980,** *102*, 92-98.

[23] Sullivan, T. P.; Huck, W. T. S. *Eur. J. Org. Chem.* **2003**, 17-29.

[24] Moore, L. W.; Springer, K. N.; Shi, J. X.; Yang, X. G.; Swanson, B. I.; Li, D. Q. *Adv. Mater.* **1995,** *7*, 729-731.

[25] Li, D. Q.; Ma, M. *Sens. Actuators B* **2000,** *69*, 75-84.

[26] Yang, X.; Shi, J.; Johnson, S.; Swanson, B. *Sens. Actuators B* **1997,** *45*, 79-84.

[27]   Busse, S.; DePaoli, M.; Wenz, G.; Mittler, S. *Sens. Actuators B* **2001,** *80*, 116-124.

[28]   Deposition below a critical temperature results in the formation of better ordered monolayers: (a) Brzoska, J. B.; Shahidzadeh, N.; Rondelez, F. *Nature* **1992**, *360*, 719-721. (b) Carraro, C.; Yauw, O. W.; Sung, M. M.; Maboudian, R. *J. Phys. Chem. B* **1998**, *102*, 4441-4445. (c) Parikh, A. N.; Allara, D. L.; Ben Azouz, I.; Rondelez, F. *J. Phys. Chem.* **1994**, *98*, 7577-7590. (d) Richter, A. G.; Durbin, M. K.; Yu, C. –J.; Dutta, P. *Langmuir* **1998**, *14*, 5980-5983.

[29]   Red Al, sodium bis(2-methoxyethoxy)aluminum dihydride solution in toluene, is a versatile reducing agent.

[30]   Balachander, N.; Sukenik, C. N. *Langmuir* **1990,** *6*, 1621-1627.

[31]   Lee, M. T.; Ferguson, G. S. *Langmuir* **2001,** *17*, 762-767.

[32]   Persson, H. H. J.; Caseri, W. R.; Suter, U. W. *Langmuir* **2001,** *17*, 3643-3650.

[33]   Wang, D.; Jones, F. R.; Denison, P. *J. Adhes. Sci. Technol.* **1992,** *6*, 79-98.

[34]   Wang, D.; Jones, F. R.; Denison, P. *J. Mater. Sci.* **1992,** *27*, 36-48.

[35]   Hagenhoff, B.; Benninghoven, A.; Stoppeklangner, K.; Grobe, J. *Adv. Mater.* **1994,** *6*, 142-144.

[36]   Butler, J. H.; Cronin, M.; Anderson, K. M.; Biddison, G. M.; Chatelain, F.; Cummer, M.; Davi, D. J.; Fisher, L.; Frauendorf, A. W.; Frueh, F. W.; Gjerstad, C.; Harper, T. F.; Kernahan, S. D.; Long, D. Q.; Pho, M.; Walker, J. A.; Brennan, T. M. *J. Am. Chem. Soc.* **2001,** *123*, 8887-8894.

[37]   MacPhail, R. A.; Strauss, H. L.; Snyder, R. G.; Elliger, C. A. *J. Phys. Chem.* **1982,** *88*, 334-341.

[38]   Snyder, R. G.; Strauss, H. L.; Elliger, C. A. *J. Phys. Chem.* **1982,** *86*, 5145-5150.

[39]   Allara, D. L.; Parikh, A. N.; Rondelez, F. *Langmuir* **1995,** *11*, 2357-2360.

[40]   Flink, S. *Sensing Monolayers on Gold and Glass.* Ph.D. Thesis, University of Twente, Enschede, The Netherlands, 2000.

[41]   Moses, P. R.; Wier, L. M.; Lennox, J. C.; Finklea, H. O.; Lenhard, J. R.; Murray, R. C. *Anal. Chem.* **1978,** *50*, 576-585.

[42]   Kallury, K. M. R.; Thompson, M.; Tripp, C. P.; Hair, M. L. *Langmuir* **1992,** *8*, 947-954.

[43]   IR analysis of the neat compound gives a broad band with maximum at 2074 cm^{-1}.

[44]   Stevens, M. J. *Langmuir* **1999,** *15*, 2773-2778.

[45]   (a) Hinrichsen, E. L.; Feder, J.; Jøssang, T. *J. Stat. Phys.* **1986,** 813. (b) Hinrichsen, E. L.; Feder, J.; Jøssang, T. *Phys. Rev. A* **1990,** *41*, 4199-4209.

[46]   Mulder, A.; Auletta, T.; Sartori, A.; Del Ciotto, S.; Casnati, A.; Ungaro, R.; Huskens, J.; Reinhoudt, D. N. *J. Am. Chem. Soc.* **2004**, *126*, 6627-6636.

[47]   The synthesis of **1** is reported in: Mulder, A. *Multivalent cyclodextrin receptors in solution and at surfaces*. Ph.D. Thesis*,* University of Twente, Enschede, The Netherlands, 2004.

[48]   Horan, N.; Yan, L.; Isobe, H.; Whitesides, G. M.; Kahne, D. *Proc. Natl. Acad. Sci. U. S. A.* **1999,** *96*, 11782-11786.

[49]   Metallo, S. J.; Kane, R. S.; Holmlin, R. E.; Whitesides, G. M. *J. Am. Chem. Soc.* **2003,** *125*, 4534-4540.

[50]   Huskens, J.; Mulder, A.; Auletta, T.; Nijhuis, C. A.; Ludden, M. J. W.; Reinhoudt, D. N. *J. Am. Chem. Soc.* **2004**, *126*, 6784-6797.

[51]   Auletta, T.; Dordi, B.; Mulder, A.; Sartori, A.; Onclin, S.; Bruinink, C. M.; Péter, M.; Nijhuis, C. A.; Beijleveld, H.; Schönherr, H.; Vancso, G. J.; Casnati, A.; Ungaro, R.; Ravoo, B. J.; Huskens, J.; Reinhoudt, D. N. *Angew. Chem., Int. Ed.* **2004,** *43*, 369-373.

[52]   Ashton, P. R.; Königer, R.; Stoddart, J. F.; Alker, D.; Harding, V. D. *J. Org. Chem.* **1996,** *61*, 903-908.

Chapter 4

Patterning of β-Cyclodextrin Monolayers with Divalent Fluorescent Guests[*]

4.1   Introduction

Patterning of surfaces is of prime importance in many fields ranging from microelectronics to biological microarray fabrication and nanotechnology. Lithographic techniques like microcontact printing (μCP) and dip-pen nanolithography (DPN) have been used extensively in recent years to pattern surfaces with sub-100 nm resolution.[1,2] These techniques usually employ the formation of self-assembled monolayers (SAMs), and have mainly been used for the immobilization of monolayer patterns directly onto a bare surface, which can then serve as an etch

---

resist.[3,4] In addition, μCP and DPN can also be used to construct functionalized nanoscale patterns on a surface. This is usually achieved by first depositing a monolayer pattern, which is then derivatized further from solution, or by depositing a monolayer from solution, which is subsequently patterned. Using these methods functional patterns of, for example, biomolecules or metal particles were produced based on non-specific interactions (e.g. electrostatic), or by using covalent chemistry.[5-9] While covalent immobilization results in the formation of robust patterns, it is irreversible and does not allow for self-correction. Non-specific physisorption can be a self-correcting process, allowing the formation of densely packed patterns. However, the adsorption and desorption processes of physisorption are difficult to control due to lack of specificity and due to their sensitivity to many parameters like ionic strength, pH, and temperature. For these reasons it is advantageous to employ supramolecular interactions for the immobilization of molecules on a surface.[10-16] Supramolecular interactions (e.g. host-guest complexes) are specific and directional, and allow for controlled adsorption and desorption of suitable molecules by tuning the number and type of interactions. Monovalent supramolecular interactions generally do not lead to the formation of stable complexes, but when multivalent interactions are employed, stable assemblies can be obtained.[17]

As was discussed in Chapter 3, monolayers of *β*-cyclodextrin (*β*-CD) host molecules can be employed to bind suitable guest molecules, based on host-guest interactions. Such a chemisorbed layer of host molecules can act as a molecular printboard onto which guest molecules can be positioned. In principle, this opens the way to build multilayered supramolecular architectures, based upon specific recognition interactions, in a controlled fashion.[18] This Chapter describes the patterning of the *β*-CD supramolecular printboard with fluorescently labeled guests that bind effectively through a divalent interaction, utilizing readily accessible lithographic techniques like μCP and DPN. Using glass as a substrate enables the use of laser scanning confocal microscopy (LSCM) for direct visualization of the created patterns. In addition, LSCM can be used for identification and quantification of relative amounts of molecules present at the surface, rendering it superior to AFM in this respect.

4.2   Results and Discussion

4.2.1   *Guest molecules*

Four model compounds have been used to study the interaction between multivalent adamantyl-terminated guest molecules and the β-CD printboard on SiO₂ in a qualitative manner. Only the simplest case of multivalency will be discussed in this Chapter: a divalent interaction. The molecules are shown in Chart 4.1.
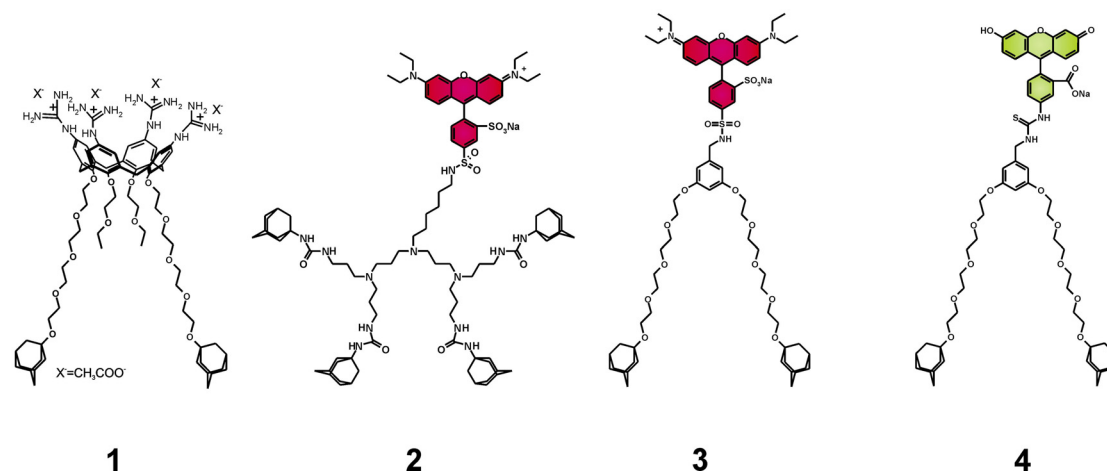

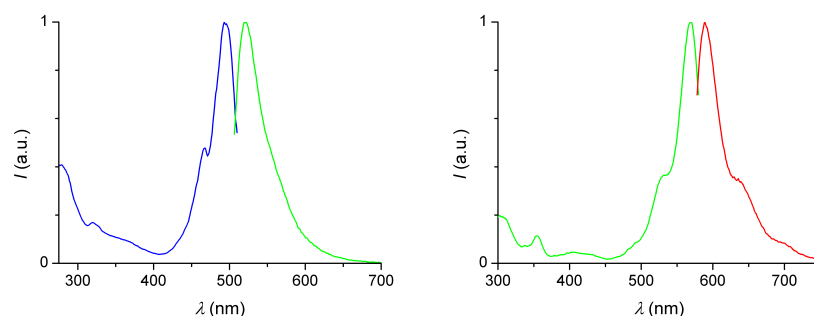**Chart 4.1** *Guest molecules that bind to the β-CD monolayers.*

Figure 4.1 *Emission and excitation spectra (1 μM in water, 298 K) of fluorescein-functionalized wedge **4** (left) and lissamine-functionalized wedge **3** (right).*

Compound **1** uses a calix[4]arene as a synthetic platform.[19] The lower rim is functionalized with adamantyl groups for interaction with β-CDs, which are spaced by poly(ethyleneglycol) (PEG) chains. The reason for employing long PEG chains is twofold: they provide sufficient spacing between the two adamantyl groups to allow a divalent interaction with the monolayer, and in addition prevent non-specific interactions while retaining water solubility. The upper rim is modified with four

guanidinium groups to enhance the water solubility. The other three guest molecules are labeled with a fluorescent group.

Molecule **2** is a PPI dendritic wedge equipped with 4 adamantyls and a lissamine dye. As was shown previously by our group, adamantyl-functionalized PPI dendrimers interact with β-CD SAMs on gold via adamantyl-β-CD interactions.[14] From these studies it was concluded that a second generation PPI wedge was required to allow a divalent interaction with the β-CD SAMs on gold. The spacing of the β-CD cavities on gold does not allow two adamantyl moieties of a single branch to simultaneously bind to the monolayer. As was concluded in Chapter 3, the packing of β-CDs on SiO_2 is not very different from the packing on gold, implying that a second-generation wedge would be sufficient to achieve a divalent interaction.

Molecules **3** and **4** carry long flexible PEG spacers to assure that binding to the β-CD monolayer occurs in a divalent fashion, and are expected to show similar binding behavior as **1**. A phenyl unit was used to couple a fluorescent dye to two adamantyl moieties. Molecule **3** bears the red lissamine dye, whereas the green fluorescein dye is used in molecule **4**. The synthesis and characterization of guest molecules **2-4** was performed by Alart Mulder.[20]

Molecules **1** and **4** displayed a moderate water solubility up to 0.1 mM. Whereas **3** was water soluble in the μm range, **2** was hardly water soluble. The water solubility of both could be increased significantly by complexing the adamantyl moieties with native β-CD.

Figure 4.1 depicts the combined and normalized excitation and emission spectra of molecules **3** (right) and **4** (left). Both excitation and emission spectra are typical of the fluorescent dyes that were incorporated in the molecules. Lissamine-functionalized **3** showed an excitation maximum in aqueous solution at 569 nm with an emission maximum in the red at 589 nm. The spectra recorded for **2** were similar to those of **3**. Fluorescein-functionalized **4** showed an excitation maximum in aqueous solution at 493 nm and an emission maximum in the green at 521 nm.

4.2.2   *Patterning the printboard via microcontact printing*

A readily available technique to prepare patterns on a surface is μCP. Here, *supramolecular* μCP is introduced, which consists of the transfer of molecules from a stamp to a monolayer-modified substrate, where the molecules are held in place by

supramolecular interactions. The process is schematically shown in Figure 4.2 for fluorescent wedge **2**.
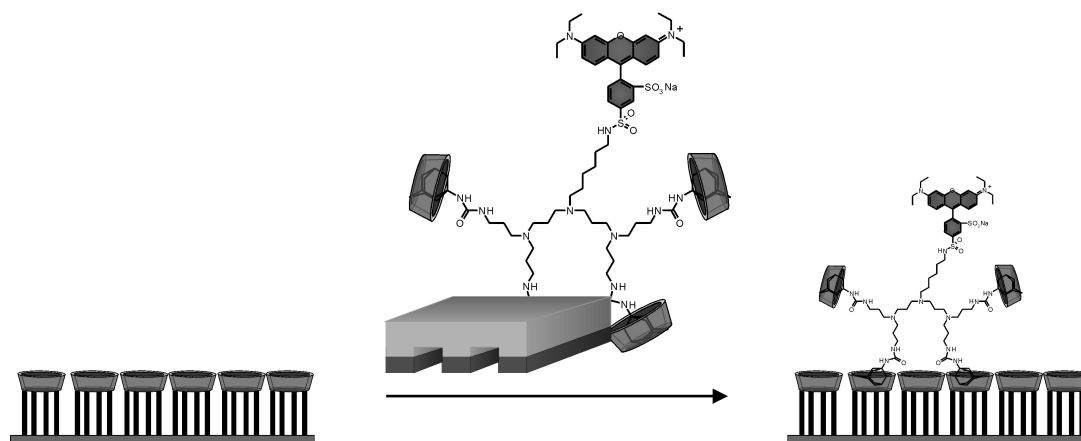

Figure 4.2 *Schematic representation of supramolecular microcontact printing using a fluorescent dendritic wedge molecule.*

Figure 4.3 shows contact mode AFM (CM-AFM) images of β-CD- and PEG-modified SiO$_2$ substrates after μCP of a 0.1 mM solution of compound **1** (left). Printing experiments were performed with PDMS stamps that were oxidized prior to use. Freshly prepared stamps with a feature size of 10 μm, spaced by 5 μm, were mildly oxidized by exposing them to UV/ozone for 30 to 60 min. This procedure renders the stamps hydrophilic, which promotes the adhesion of aqueous ink solutions. The β-CD monolayers were prepared according to the procedure reported in Chapter 3. To verify that supramolecular μCP results in host-guest interactions between the deposited guest molecules and the substrate, the stability of the formed patterns was tested via several rinsing procedures with aqueous solutions. All printing experiments were also performed on a reference layer that does not contain any host sites, which should result in the formation of patterns with only limited stability, caused by the absence of specific interactions. For this reason, monolayers of PEG chains were prepared,[21] which are known to resist non-specific adsorption.[22,23]

It is evident that transfer of molecules from the stamp to the substrate occurred on both monolayers, giving a faithful reproduction of the stamp features, as witnessed by a clear contrast in friction.[24] Rinsing the patterned monolayers with large quantities of aqueous salt solution did not result in noticeable degradation of the patterns on the β-CD monolayer (top, center), while hardly any contrast in friction is observed for the PEG monolayer, reflecting the removal of the patterns (bottom, center). This

difference in pattern stability supports the assumption that supramolecular μCP is governed by host-guest interactions on the *β*-CD monolayer.
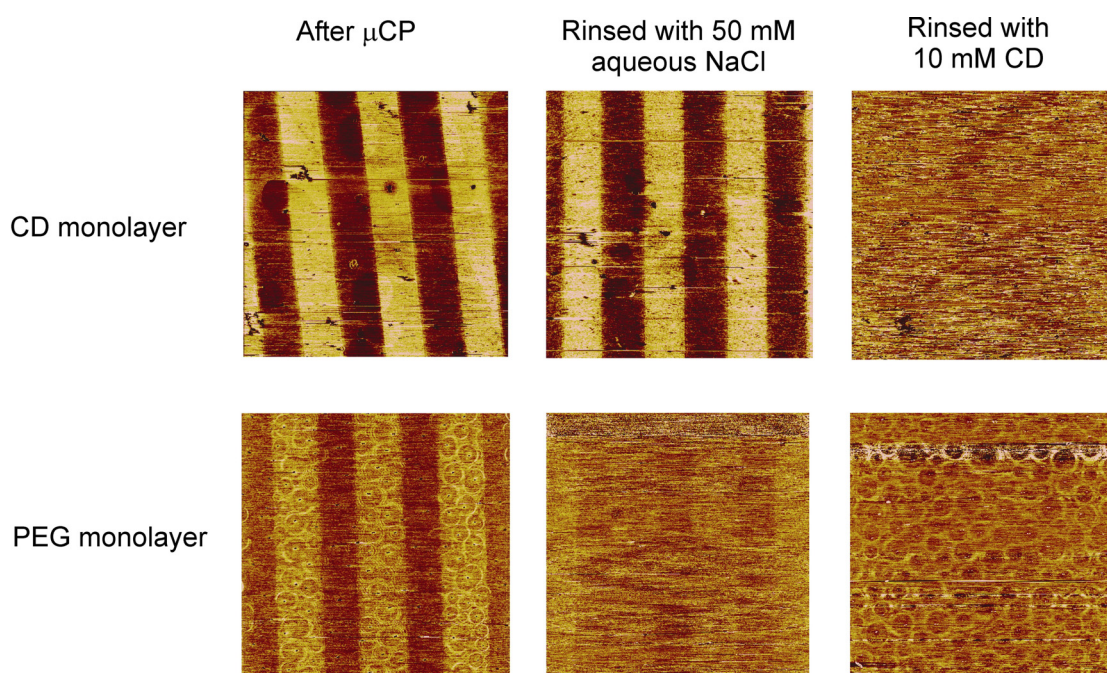

	After μCP	Rinsed with 50 mM aqueous NaCl	Rinsed with 10 mM CD
CD monolayer			
PEG monolayer			

Figure 4.3 *Friction-force AFM images (50×50 μm²) after μCP of molecule **1** on a β-CD monolayer (top) and PEG monolayer (bottom) on SiO₂. Friction forces (a.u.) increase from dark to bright contrast. Images shown after printing, from left to right: without rinsing, after rinsing with 200 ml of 50 mM salt solution, and after rinsing with 200 ml of 10 mM aqueous β-CD solution.*

To examine the reversibility of the supramolecular μCP process, the substrates were additionally rinsed with a concentrated (10 mM) aqueous *β*-CD solution. This induces competition between the surface bound *β*-CDs and those in solution, effectively leading to slow desorption of **1** from the surface, as evidenced by the decrease in friction contrast in Figure 4.3 (right). These findings corroborate the printing experiments of **1** on *β*-CD SAMs on gold, indicating the similarity of *β*-CD monolayers on both surfaces.[25,26]

The reason for working with SiO₂ is the possibility to use fluorescence spectroscopic techniques for visualization of the patterns. Figure 4.4 shows LSCM images of microcontact printed **2** on *β*-CD- and PEG-modified glass slides. To attain sufficient water solubility of **2**, it was employed as the per-*β*-CD complex; a 10^{-5} M

solution was used. Fluorescent patterns are clearly visible giving direct evidence of transfer of ink molecules from the stamp to the surface.
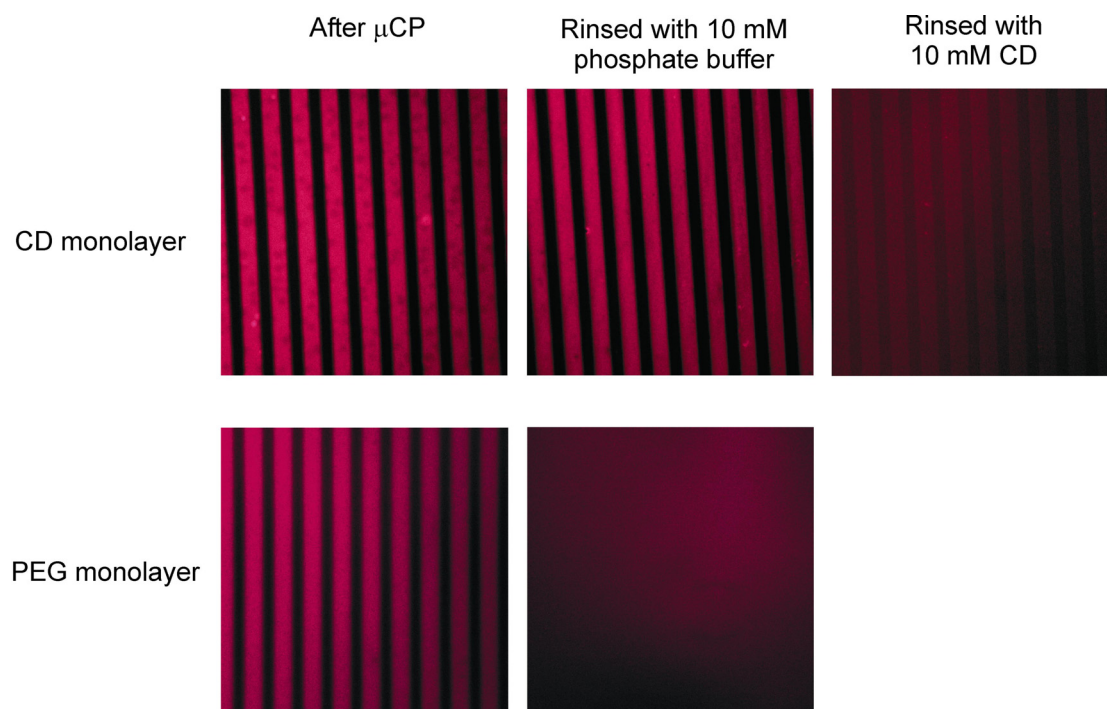

Figure 4.4 *Confocal microscopy images (150×150 μm²) after μCP of fluorescent dendritic wedge **2** on a β-CD monolayer (top) and PEG monolayer (bottom) on SiO₂. **2** was printed as the per-β-CD complex. Images shown after printing, from left to right: without rinsing, after rinsing with 200 ml of a 10 mM phosphate buffer, and after rinsing with 200 ml of a 10 mM aqueous β-CD solution.*

Also here, the printed patterns were rinsed with large amounts of aqueous solutions. The results of the rinsing procedures in Figure 4.4 are similar to the AFM results shown in Figure 4.3 with respect to pattern stability. The fluorescent patterns on β-CD monolayers are hardly affected by rinsing with aqueous buffer solution (top, center), while the same procedure removes the patterns on the reference monolayer (bottom, center). The reversibility of the binding process is shown by rinsing with aqueous β-CD solution, resulting in a significant decrease in fluorescence intensity. These results demonstrate that fluorescent molecule **2** binds in a similar fashion to the β-CD monolayers as **1**, i.e. via multivalent supramolecular interactions. The stability of the patterns is comparable to the stability of patterns of **1**, indicating that only two of the adamantyl groups interact with the β-CD monolayer. Furthermore, it illustrates

that per-β-CD complexes can also be employed in printing experiments. Apparently, the β-CD cavities immobilized at the surface are able to compete with the β-CD molecules that are transferred during the printing process. These findings are in line with a theoretical model that was recently developed in our group, and supports the assumption that a close-packed β-CD surface is prepared following the procedure outlined in Chapter 3.[17]

Additionally, similar µCP experiments were performed for fluorescent wedges **3** and **4**. The confocal microscopy images on β-CD monolayers are depicted in Figure 4.5 (page 80). The top row shows patterns of lissamine-derivatized **3**, and the bottom row depicts patterns of fluorescein-labeled **4**. Patterns produced with both wedges on β-CD and PEG monolayers show similar stabilities to rinsing with aqueous solutions when compared with **1** and **2**, demonstrating that all four guest molecules bind to the β-CD monolayer via a divalent interaction. These results are in agreement with the desorption experiment reported in Chapter 3.2.3, where significant desorption of **4** was only observed for β-CD-containing solutions.

LSCM allows discrimination between similar molecules immobilized on a surface, the only requisite being a different fluorescent group. This gives it an advantage over AFM, which would need a marked difference in size or polarity of the molecules in order to distinguish them.[27,28] Figure 4.6 (page 80) displays confocal microscopy images of a substrate that was patterned with two different guest molecules. First, the β-CD complex of **2** was printed on a monolayer-modified glass slide, followed by dipping of the substrate in an aqueous solution containing **4**. The left image in Figure 4.6 was obtained after exciting at 543 nm and monitoring the emission above 600 nm, typical wavelengths for a lissamine dye. For the center image an excitation wavelength of 488 nm was used and the emission was measured between 500 and 530 nm, a suitable region to monitor fluorescein emission. Simultaneous imaging (right) shows that **2** was only deposited in the regions where the stamp was in contact with the surface, and that **4** adsorbed specifically in the regions where the stamp had not been in contact. This demonstrates that (1) a full monolayer is transferred during the printing process, leaving few or no free binding sites and (2) that there is only limited exchange of the two molecules, resulting in the sharp contrast in the images.

4.2.3 *Quantification of printing and stability of the patterns in time*

Microcontact printing of alkanethiols on gold results in a rapid and clean formation of a monolayer, usually within seconds.[29,30] However, on other surfaces the µCP process can be different, resulting in the formation of submonolayers (under-inking) or multilayers (over-inking) depending mainly on the ink concentration and applied contact time.[31-33] Supramolecular µCP of an 0.1 mM solution of calix[4]arene **1** on β-CD SAMs on gold appeared to result in multilayer formation on the SAM, as evidenced by XPS results.[34] This multilayer could be reduced to approximately a monolayer of guest molecules by rinsing with aqueous solutions.

Here, LSCM is used to compare deposition of fluorescent wedge **3** from solution with deposition via µCP. A droplet of an aqueous solution of **3** (1 µM) was placed on a glass slide modified with a β-CD monolayer, leading to adsorption of **3** onto the SAM. After 5 min of adsorption the substrate was rinsed thoroughly with water to remove physisorbed material, presumably leaving a single layer of guest molecules on the β-CD printboard. Figure 4.7 (page 81) shows the LSCM image of the edge of the droplet (Figure 4.7, left) and the fluorescence intensity profile. In order to compare the amount of molecules on the surface, **3** was also microcontact printed from the same solution. The LSCM image of the printed surface is shown on the right and was captured directly after printing, using identical settings on the confocal microscope as the image on the left. Comparison of the fluorescence intensity profiles indicated that a similar amount of fluorescent molecules was present on both surfaces, demonstrating that printing of **3** from a µM solution resulted in the transfer of approximately one monolayer.

Patterns on β-CD monolayers, generated by µCP, are stable towards rinsing procedures with aqueous solutions and can only be removed by aqueous solutions that induce competition between binding to the surface and in solution. To assess the long-term stability of these patterns, the printed substrates were stored in the dark in a nitrogen atmosphere and imaged after certain time intervals. The identical experiment was also performed on a PEG reference SAM to evaluate the significance of specific interactions for long-term stability. Figure 4.8 (page 81) depicts LSCM images obtained directly after printing (left), after one week of storage (center), and after six weeks of storage (right). The results indicate that stable patterns were formed on the β-CD monolayer, without any noticeable degradation after 6 weeks of storage in the

dark. In contrast, patterns prepared on a reference PEG monolayer started to fade, suggesting that the *β*-CD-adamantyl interaction is required to keep the printed molecules in place.
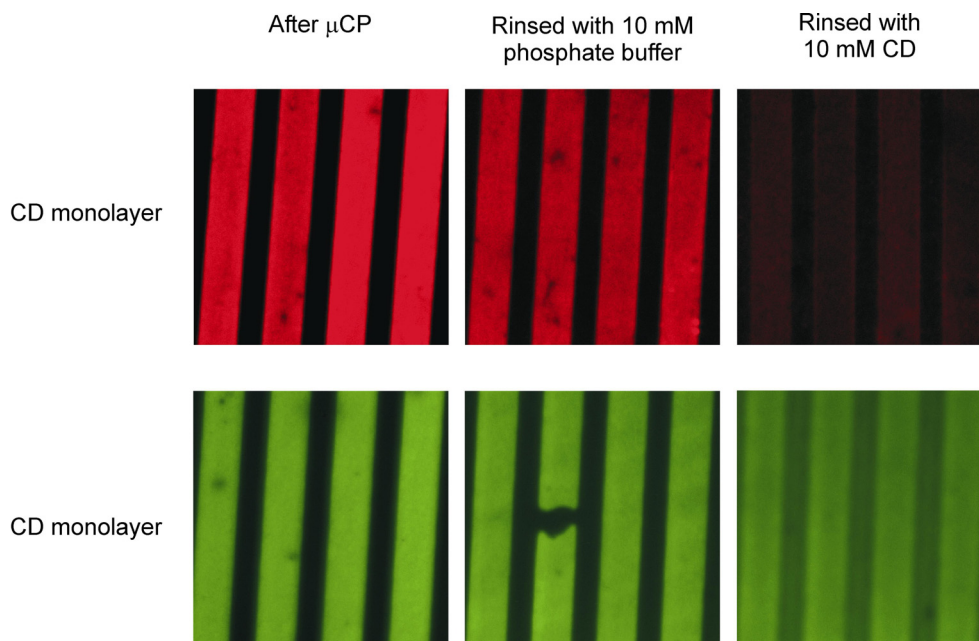

Figure 4.5 *Confocal microscopy images (60×60 μm^2) after μCP of fluorescent dendritic wedges **3** (top) and **4** (bottom) on β-CD monolayers on SiO$_2$. Images shown after printing, from left to right: without rinsing, after rinsing with 200 ml of 10 mM phosphate buffer, and after rinsing with 200 ml of 10 mM aqueous β-CD solution.*
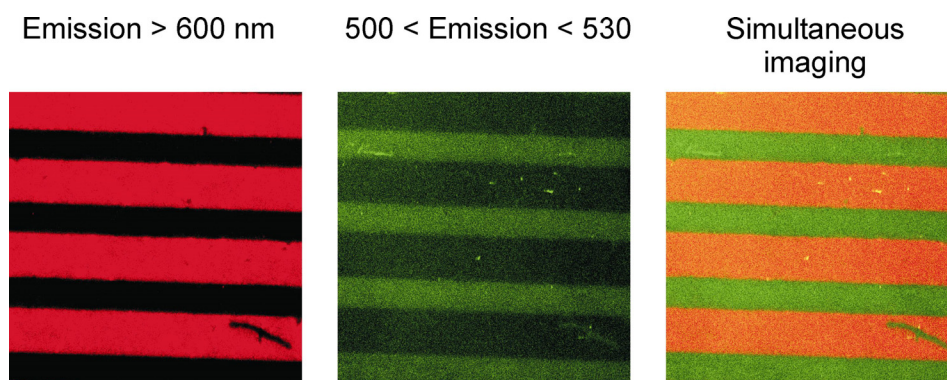

Figure 4.6 *Confocal microscopy images (60×60 μm^2) after μCP of **4** on a β-CD monolayer on SiO$_2$ and subsequent immersion of the glass slide in an aqueous solution of **3**. The substrate was simultaneously excited at 488 and 543 nm and images were recorded by measuring the emission above 600 nm (left) and between 500 and 530 nm (center). The picture on the right shows the combined image.*
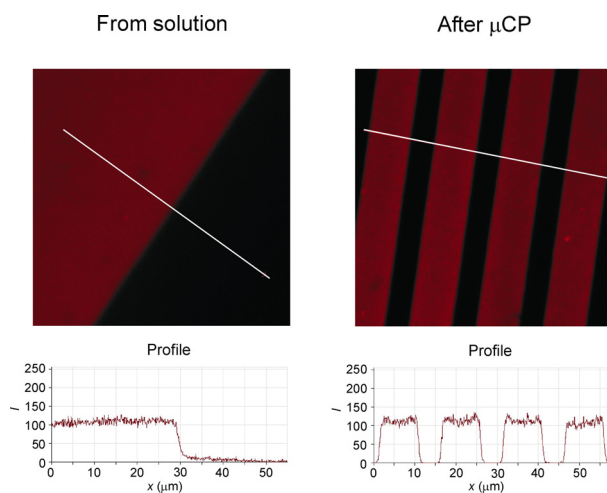
Figure 4.7 *Confocal microscopy images (60×60 μm²) of fluorescent dendritic wedge **3**. Patterning via microcontact printing (right) compared to assembly from an aqueous solution (left). Images were obtained at identical confocal microscope settings.*
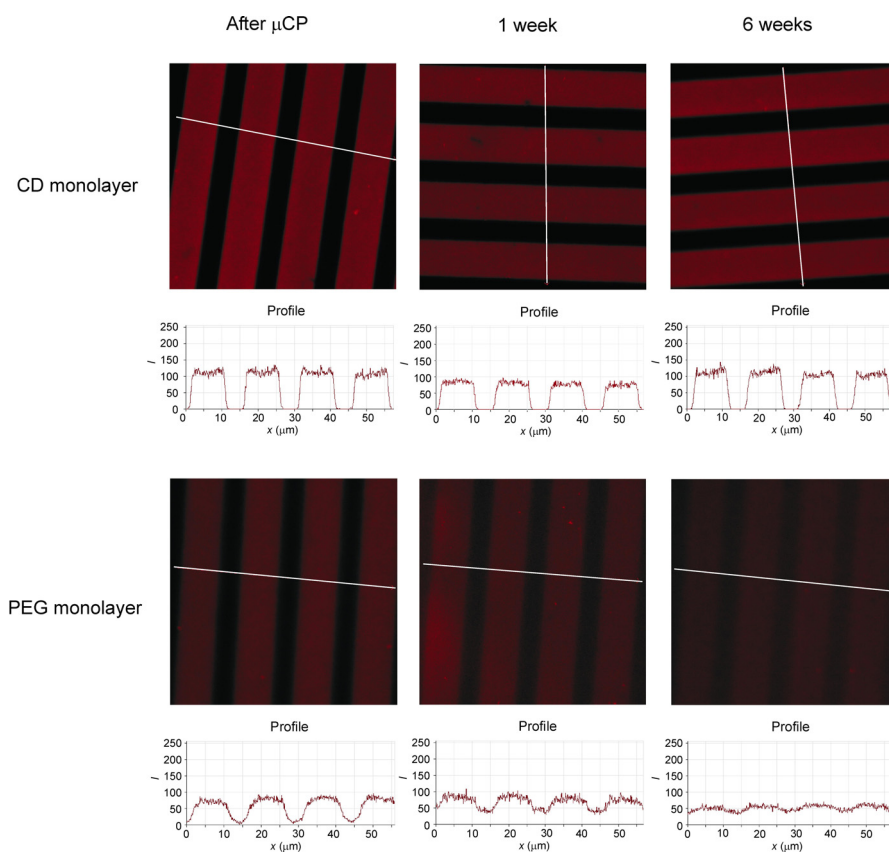

Figure 4.8 *Confocal microscopy images (60×60 μm²) of a β-CD monolayer and a PEG monolayer patterned with **2**. Images were taken: directly after printing (left), after one week of storage in the dark (center), and after six weeks of storage in the dark (right). All images were captured at identical confocal microscope settings.*

81

The principal factors involved in binding guest molecules by CDs are believed to be Van der Waals and hydrophobic interactions.[35] Hydrophobic interactions require water to be present at the *β*-CD interface. As *β*-CD monolayers are moderately hydrophilic, it is likely that water will still be present, even under 'dry' conditions, which could account for the observed stability of microcontact printed patterns under these conditions. In addition, *β*-CD interfaces are known to complex guest molecules in the gas phase.[36-38] The host-guest electronic complementarity, steric complementarity, and the host preorganization are three key elements in determining the stability of a complex in the gas phase.[39] In contrast, such stabilizing factors are not present on the PEG monolayers. In fact, these layers are known to be fully hydrated,[40] which could account for the observed mobility of the guest molecules.

The observation of sharp and stable edges after 6 weeks of storage in the dark corroborates the previous results that at most one monolayer of guest molecules is transferred during printing under these conditions. If a second layer of guest molecules would be present on the printed part of the surface, this layer would not be able to bind via specific interactions and would therefore be mobile on the surface, as observed for the reference monolayer. The fact that this is not observed suggests that all guest molecules interact with the *β*-CD monolayer.

4.2.4 *Patterning the printboard via dip-pen nanolithography*

DPN relies on the transfer of molecules from an inked AFM tip to a substrate by bringing the tip in contact with the substrate. Here we introduce *supramolecular* DPN, of which the procedure is schematically shown in Figure 4.9. An AFM tip is inked with fluorescent guest molecules, which are deposited onto the *β*-CD monolayer by scanning over the monolayer-modified surface.
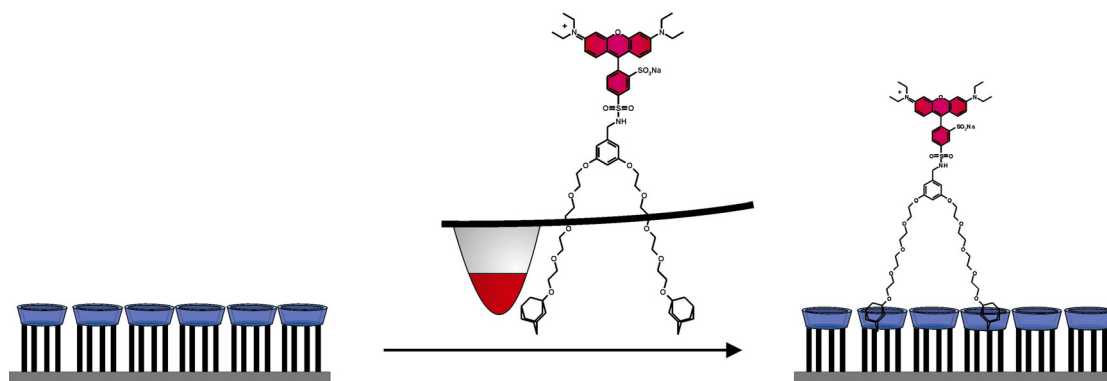
Figure 4.9 *Schematical representation of supramolecular DPN using a fluorescent dendritic wedge molecule.*

To reduce the activation energy required for molecular transport from tip to surface, gold-coated Si_3N_4 tips were covered with an oligo(ethyleneoxy)-terminated SAM.[8,22] Tips were soaked in a 0.1 mM ethanolic solution of **3** for ca 5 min, before being dried in air. It is known that the relative humidity is an important factor in the transport of high-molecular-weight molecules from tip to surface.[41] Therefore, the DPN procedure was carried out at higher relative humidity, typically between 45 and 55%, and at a temperature of ~29 ˚C. A pattern was written across the surface with a scan velocity of ~10 μm/s to produce a cross with lines of 10 μm long and 160 nm wide. Each line was scanned for 10 min. After writing, the glass substrate was imaged by LSCM (Figure 4.10, left), which clearly shows that guest molecules were transferred to the surface. The observed line widths by LSCM are ca. 475 nm for the horizontal line and ca. 400 nm for the vertical line. The deviation from the programmed AFM line width could be explained by a drift in the AFM or by deposition of more than a monolayer of guest molecules. As the horizontal line has the shape of a diamond, it suggests a drift in the AFM during deposition. Although both lines were scanned for equally long periods, the horizontal line, which was scanned first, has a much higher fluorescence intensity, indicative of deposition of more guest molecules. Apparently, the transfer of ink mainly took place during the first 10 min of scanning, leaving little ink for the writing of the second line.
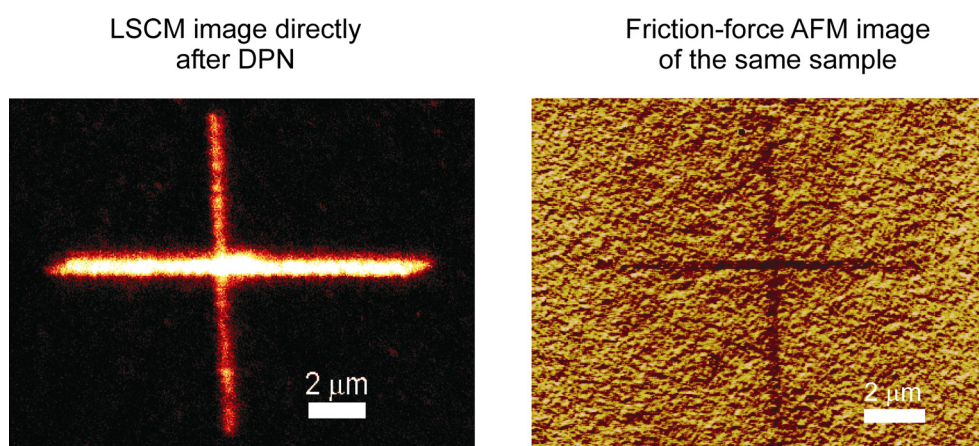
LSCM image directly
after DPN

Friction-force AFM image
of the same sample

Figure 4.10 *Confocal microscopy (left) and friction force AFM images (right) of a pattern of 3 generated by dip-pen nanolithography. Friction forces (a.u.) increase from dark to bright contrast.*

After imaging the glass substrate by LSCM, the same sample was imaged by CM-AFM. Figure 4.10 shows the friction-force image on the right. Clearly, the written pattern is visible. However, the drift resulting in increased line width is not observed by AFM, suggesting that LSCM is a more sensitive method for visualizing DPN-generated patterns.

As a control experiment a β-CD monolayer was scanned with a bare Si_3N_4 tip under similar experimental conditions. Subsequent CM-AFM imaging did not show any visible pattern, indicating that the writing process does not damage the monolayer and that the friction contrast observed in Figure 4.10 is the result of transfer of ink molecules from the tip to the substrate.

To test the stability of written patterns, a rinsing procedure was applied. After imaging of a DPN pattern by LSCM, the substrate was dismounted from the confocal microscope and rinsed with large amounts of water. Following the rinsing it was imaged again. Figure 4.11 shows the LSCM image of the written pattern directly after DPN (top, left) and after rinsing (top, right). The pattern is still visible, indicating that the guest molecules bind to the monolayer via specific supramolecular interactions. The bottom graphs in Figure 4.11 depict the relative (left) and normalized (right) emission intensity line scans taken directly after DPN (red) and after rinsing (blue). It is evident that the fluorescence intensity is dramatically reduced upon rinsing. However, this could also be caused by photobleaching of the lissamine dye, so it is hard to draw conclusions with respect to the amount of fluorescent molecules present

at the surface before and after rinsing. The normalized fluorescence intensity (bottom, right) shows that the line width increased by ca 30% upon rinsing. This broadening might either be caused by migration of **2** over the surface, or by spreading upon washing in case more than a monolayer of guest molecules was deposited.
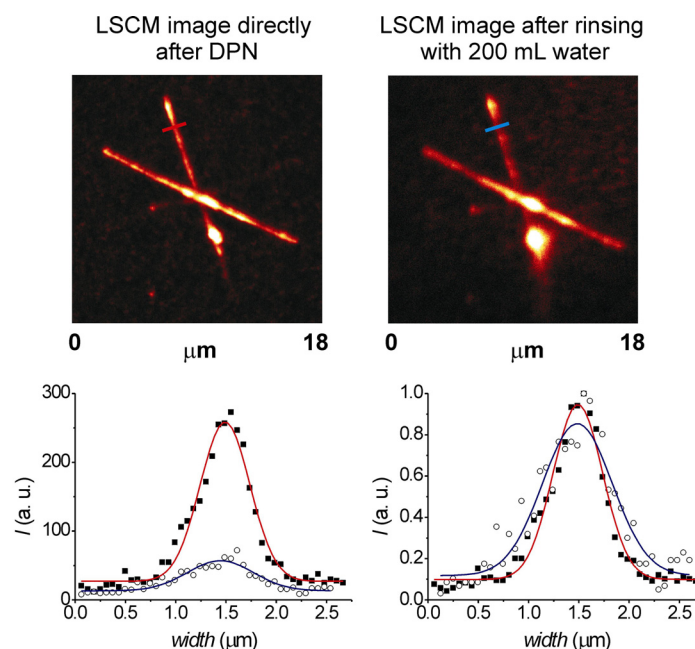

Figure 4.11 *Confocal microscopy images of a DPN generated pattern of **2** obtained directly after writing (top left), and after rinsing with 200 ml of water (top right). The bottom graphs show the relative (left) and normalized (right) emission intensity line scans (markers) and Gaussian fits (solid lines) for the cross-sections before (■) and after (○) rinsing.*

4.3 Conclusions

Lithographic techniques such as μCP and DPN can be employed to position molecules on a monolayer with exposed host molecules. It has been shown that supramolecular μCP of divalent guest molecules leads to the formation of thermodynamically stable patterns. However, the created patterns are reversible and can be erased by rinsing with a solution containing host molecules. This induces competition between binding to the surface and binding in solution and thereby the original host monolayer can be regenerated. Results of the patterning experiments on β-CD monolayers on SiO_2 are comparable to those on β-CD SAMs on gold, reflecting the similarity of the two receptor interfaces.

The principal advantage of patterning β-CD monolayers on SiO_2 is the ability to employ fluorescent techniques like LSCM. Patterns created by supramolecular μCP and DPN were easily visualized using LSCM, providing direct evidence of the transfer of fluorescent guest molecules to the substrate. Moreover, fluorescence techniques allow a more quantitative visualization of the patterns and appear to be more sensitive compared to AFM. Additionally, fluorescent techniques enable straightforward discrimination between different molecules at the interface, providing a handle to monitor the position of different molecules on a surface.

4.4 Acknowledgement

4.5 Experimental section

Materials and methods. For information on the synthesis and characterization of fluorescent guest molecules **1-4**, the reader is referred to the work of Alart Mulder.[19,20]

Substrate preparation. β-CD monolayers were prepared as described in Chapter 3.

Microcontact printing. Stamps were prepared by casting a 10:1 (v/v) mixture of poly(dimethylsiloxane) and curing agent (Sylgard 184, Dow Corning) against a silicon master. After overnight curing at 60˚C, the stamps were mildly oxidized in a UV/ozone reactor for 30 to 60 min and subsequently inked by soaking them into an aqueous adsorbate solution for at least 5 min. Before printing, the stamps were blown dry in a stream of N_2. The stamps were brought into conformal contact with the substrate by hand, without the use of external pressure. Printing on the preformed SAMs was performed for 60 s, after which the stamp was carefully removed. After each printing step the inking procedure was repeated. Microcontact printed substrates were imaged directly after printing, or after thorough rinsing with 200 ml of aqueous solutions of phosphate buffer (10 mM, pH 7), NaCl (50 mM), or native β-CD (10 mM).

AFM. AFM experiments were carried out with a Nanoscope III multimode AFM (Digital Instruments, Santa Barbara, CA, USA) in contact mode using V-shaped Si_3N_4

cantilevers (Nanoprobes, Digital Instruments) with a spring constant of 0.1 N/m. Images were acquired in ambient atmosphere (ca 30-40% relative humidity, 25°C).

Dip-pen nanolithography. Four-inch polished, 100-cut, p-doped silicon wafers, cut into 2×2 cm^2 samples and microscope glass slides were hand-marked with a diamond-tip prior to monolayer preparation. Before the writing procedure was carried out the marked substrates were bleached extensively to reduce background fluorescence. For bleaching, the substrates were exposed to the 435 and 546 nm lines of a mercury lamp with a power of approximately 900 mW. The light was focused on the marker using an oil immersion lens (N.A. 1.4, 63×). The exposure time was at least 30 min.

For the DPN experiments, Si_3N_4 tips coated with 50 nm of gold were used (Ssens BV, The Netherlands). To reduce the activation energy required for molecular transport from tip to surface, gold-coated Si_3N_4 tips were covered with an oligo(ethylene glycol)-terminated SAM.[22] Cleaned gold tips were immersed in a 0.1 mM solution of a thiolated oligo(ethylene glycol) derivative in ethanol overnight, subsequently rinsed with ethanol and dried in a stream of nitrogen. For the writing experiments the tips were inked by soaking them in a 1×10^{-5} M aqueous solution of **2** or a 0.1 mM ethanol solution of **3** for 5 min, and dried in air. The tips were mounted in the AFM head, and the AFM cantilever was positioned within the marker with the use of a CCD camera. Patterns were generated in the vicinity of the marker.

Laser scanning confocal microscopy. Confocal microscopy images of the microcontact printed substrates were taken on a Carl Zeiss LSM 510 microscope. The light was focused on the substrate using an oil immersion lens (N.A. 1.4, 63×). The lissamine-functionalized wedges were excited at 543 nm, while the fluorescein-functionalized wedge was excited at 488 nm. The emitted fluorescence was collected on a PMT R6357 spectrophotometer. All confocal microscopy images were acquired in air.

Fluorescence imaging of the DPN patterns was carried out using an inverted confocal microscope (Zeiss Axiovert) with an oil-immersion lens (N.A. 1.4, 100×). An ArKr ion laser (Spectra Physics Beamlok 2060), operated at 514 nm, was used to excite the fluorophores. The excitation light was filtered using a 514 bandpass filter (Omega 514.5/10). A dichroic mirror (Omega 540DRLP) and a long-pass filter (Omega 550APL) were used to separate the emitted light from the excitation light. The fluorescence signal was detected using an avalanche photodiode (EG&G Electro

Optics SPCM-AQ-14). The sample was scanned over an area, typical 30×30 μm^2 with 512×512 pixels and a pixel dwell time of 1 ms. The excitation power was ~3.5 kW/cm^2. All confocal microscopy images were acquired in air.

4.6   References

[1]   Xia, Y. N.; Whitesides, G. M. *Angew. Chem., Int. Ed.* **1998,** *37*, 551-575.

[2]   Ginger, D. S.; Zhang, H.; Mirkin, C. A. *Angew. Chem., Int. Ed.* **2004,** *43*, 30-45.

[3]   John, P. M. S.; Craighead, H. G. *Appl. Phys. Lett.* **1996,** *68*, 1022-1024.

[4]   Weinberger, D. A.; Hong, S. G.; Mirkin, C. A.; Wessels, B. W.; Higgins, T. B. *Adv. Mater.* **2000,** *12*, 1600-1603.

[5]   Singhvi, R.; Kumar, A.; Lopez, G. P.; Stephanopoulos, G. N.; Wang, D. I. C.; Whitesides, G. M.; Ingber, D. E. *Science* **1994,** *264*, 696-698.

[6]   Hidber, P. C.; Helbig, W.; Kim, E.; Whitesides, G. M. *Langmuir* **1996,** *12*, 1375-1380.

[7]   Sullivan, T. P.; Huck, W. T. S. *Eur. J. Org. Chem.* **2003**, 17-29.

[8]   Lim, J. H.; Ginger, D. S.; Lee, K. B.; Heo, J.; Nam, J. M.; Mirkin, C. A. *Angew. Chem., Int. Ed.* **2003,** *42*, 2309-2312.

[9]   Geissler, M.; Kind, H.; Schmidt-Winkel, P.; Michel, B.; Delamarche, E. *Langmuir* **2003,** *19*, 6283-6296.

[10]   Dietrich, C.; Schmitt, L.; Tampe, R. *Proc. Natl. Acad. Sci. U. S. A.* **1995,** *92*, 9014-9018.

[11]   Arias, F.; Godinez, L. A.; Wilson, S. R.; Kaifer, A. E.; Echegoyen, L. *J. Am. Chem. Soc.* **1996,** *118*, 6086-6087.

[12]   Miura, Y.; Kimura, S.; Imanishi, Y.; Umemura, J. *Langmuir* **1998,** *14*, 2761-2767.

[13]   Fragoso, A.; Caballero, J.; Almirall, E.; Villalonga, R.; Cao, R. *Langmuir* **2002,** *18*, 5051-5054.

[14]   Huskens, J.; Deij, M. A.; Reinhoudt, D. N. *Angew. Chem., Int. Ed.* **2002,** *41*, 4467-4471.

[15]   Thess, A.; Hutschenreiter, S.; Hofmann, M.; Tampe, R.; Baumeister, W.; Guckenberger, R. *J. Biol. Chem.* **2002,** *277*, 36321-36328.

[16] Banerjee, I. A.; Yu, L. T.; Matsui, H. *J. Am. Chem. Soc.* **2003,** *125*, 9542-9543.

[17] Huskens, J.; Mulder, A.; Auletta, T.; Nijhuis, C. A.; Ludden, M. J. W.; Reinhoudt, D. N. *J. Am. Chem. Soc.* **2004,** *126*, 6784-6797.

[18] Spinke, J.; Liley, M.; Guder, H. J.; Angermaier, L.; Knoll, W. *Langmuir* **1993,** *9*, 1821-1825.

[19] Mulder, A.; Auletta, T.; Sartori, A.; Del Ciotto, S.; Casnati, A.; Ungaro, R.; Huskens, J.; Reinhoudt, D. N. *J. Am. Chem. Soc.* **2004,** *126*, 6627-6636.

[20] Mulder, A. *Multivalent cyclodextrin receptors in solution and at interfaces.* Ph.D. Thesis, University of Twente, Enschede, The Netherlands, 2004.

[21] The PEG-terminated SAMs were prepared by exposure of a cleaned and activated SiO_2 substrate to a commercially available mixture of 2-[methoxypoly(ethyleneoxy)-propyl]trimethoxysilane (6 to 9 ethylene glycol units per molecule), according to a procedure given by: Papra, A.; Gadegaard, N.; Larsen, N. B. *Langmuir* **2001,** *17*, 1457-1460.

[22] Pale-Grosdemange, C.; Simon, E. S.; Prime, K. L.; Whitesides, G. M. *J. Am. Chem. Soc.* **1991,** *113*, 12-20.

[23] Lee, S. W.; Laibinis, P. E. *Biomaterials* **1998,** *19*, 1669-1675.

[24] Using a stamp that was not inked did not result in a noticeable friction contrast.

[25] Auletta, T.; Dordi, B.; Mulder, A.; Sartori, A.; Onclin, S.; Bruinink, C. M.; Péter, M.; Nijhuis, C. A.; Beijleveld, H.; Schönherr, H.; Vancso, G. J.; Casnati, A.; Ungaro, R.; Ravoo, B. J.; Huskens, J.; Reinhoudt, D. N. *Angew. Chem., Int. Ed.* **2004,** *43*, 369-373.

[26] Similar experiments on β-CD SAMs on gold showed that guest molecules binding via a monovalent interaction were readily removed from the surface by rinsing with an aqueous salt solution. Guest molecules binding via four interactions were found to be kinetically stable, even upon rinsing with CD solutions.

[27] Hong, S.; Mirkin, C. A. *Science* **2000,** *288*, 1808-1811.

[28] Hong, S.; Zhu, J.; Mirkin, C. A. *Science* **1999,** *286*, 523-525.

[29] Wilbur, J. L.; Kumar, A.; Kim, E.; Whitesides, G. M. *Adv. Mater.* **1994,** *6*, 600-604.

[30]   Larsen, N. B.; Biebuyck, H.; Delamarche, E.; Michel, B. *J. Am. Chem. Soc.* **1997,** *119*, 3017-3026.

[31]   Jeon, N. L.; Finnie, K.; Branshaw, K.; Nuzzo, R. G. *Langmuir* **1997,** *13*, 3382-3391.

[32]   Goetting, L. B.; Deng, T.; Whitesides, G. M. *Langmuir* **1999,** *15*, 1182-1191.

[33]   Arrington, D.; Curry, M.; Street, S. C. *Langmuir* **2002,** *18*, 7788-7791.

[34]   Auletta, T. *New tools for nanotechnology: from single molecule chemistry to surface patterning.* Ph.D. Thesis, University of Twente, Enschede, 2003.

[35]   Rekharsky, M. V.; Inoue, Y. *Chem. Rev.* **1998,** *98*, 1875-1917.

[36]   Moore, L. W.; Springer, K. N.; Shi, J. X.; Yang, X. G.; Swanson, B. I.; Li, D. Q. *Adv. Mater.* **1995,** *7*, 729-731.

[37]   Yang, X.; Shi, J.; Johnson, S.; Swanson, B. *Sens. Actuators B* **1997,** *45*, 79-84.

[38]   Li, D. Q.; Ma, M. *Sens. Actuators B* **2000,** *69*, 75-84.

[39]   Diederich, F., *Cyclophanes*. The Royal Society of Chemistry: UK, 1991.

[40]   Herrwerth, S.; Eck, W.; Reinhardt, S.; Grunze, M. *J. Am. Chem. Soc.* **2003,** *125*, 9359-9366.

[41]   Demers, L. M.; Ginger, D. S.; Park, S.-J.; Li, Z.; Chung, S.-W.; Mirkin, C. A. *Science* **2002,** *296*, 1836-1838.

Chapter 5

Immobilized Dendrimer Boxes for the Encapsulation of Anionic Dyes[*]

5.1   Introduction

Dendrimers are highly branched, well-defined macromolecules consisting of a core, an interior region and numerous end groups. In recent years, this class of molecules has attracted increasing attention because of their molecular recognition properties.[1-4] Moreover, dendrimers can be tailored into biocompatible compounds with low cytotoxicity, which makes them promising candidates as drug delivery systems.[5] The main molecular recognition properties are based on the presence of voids in the interior of the dendrimers or interactions with functionalities at the periphery. Especially higher generation dendrimers, carrying many end groups, are

---

[*] Parts of this Chapter have been published: Auletta, T.; Dordi, B.; Mulder, A.; Sartori, A.; Onclin, S.; Bruinink, C. M.; Péter, M.; Nijhuis, C. A.; Beijleveld, H.; Schönherr, H.; Vancso, G. J.; Casnati, A.; Ungaro, R.; Ravoo, B. J.; Huskens, J.; Reinhoudt, D. N. *Angew. Chem., Int. Ed.* **2004,** *43*, 369-373.

able to encapsulate guests inside their flexible interior as the densely packed end groups 'close' the molecular box. There are numerous examples of guest encapsulation inside dendrimers. One well-known example is the complexation of anionic dyes by dendrimer hosts.[6-13] It is believed that this recognition process is mainly governed by electrostatic interactions between protonated tertiary amines in the dendrimer core and the anionic dyes. However, a recent study suggested that also a good match in shape is required.[11] Dendrimers modified with an apolar periphery can be employed as extractants of anionic dye molecules from water to organic solvents,[6] although there has been some discussion regarding the maximum number of dye molecules that can be encapsulated inside a dendrimer box.[6,8,10,14,15] Neutral molecules can be bound inside dendrimer molecules based on hydrophobic interactions,[16-18] or by employing hydrogen bonds.[19-22]

Studying the complexation behavior of dendrimers on a surface could be of considerable importance for biochip applications and gives a handle to study these molecules at a fixed position in space. This implies that their properties could ultimately be studied at the single molecule level. Immobilization on a surface has been reported based on covalent chemistry,[11,23] physisorption,[24] and via hydrogen-bond formation.[25] Chen *et al.* have even studied the complexation behavior of immobilized dendritic molecules using surface plasmon resonance.[11] Recently, our group has reported the immobilization of single dendrimer molecules on the gold surface via insertion of dendrimer molecules or dendrimer precursors in a monolayer,[26,27] and via host-guest interactions on a molecular printboard on gold.[28] Here, the molecular printboard on glass, which is described in Chapter 3, is used to bind adamantyl-terminated dendrimer molecules via multiple supramolecular interactions. The guest binding properties of the immobilized dendrimers are examined by complexation of fluorescent molecules. The first part of this chapter describes the encapsulation of fluorescent molecules on dendrimer-patterned surfaces. The last part of this chapter deals with isolated immobilized dendrimers, filled with fluorescent dyes. All immobilized dendrimer/dye systems have been studied by laser scanning confocal microscopy (LSCM).

5.2   Results and Discussion

5.2.1   *Immobilization of dendrimers*

Generation 5 poly(propylene imine) (G5 PPI) dendrimers, functionalized with adamantyl groups, have been used for immobilization on *β*-cyclodextrin (*β*-CD) monolayers on glass. The molecular structure of such a dendrimer, carrying 64 adamantyl end groups for complexation with the *β*-CD monolayer, is shown in Chart 5.1. Immobilization of **1** on a *β*-CD monolayer was accomplished via supramolecular microcontact printing (μCP) from aqueous solutions. To solubilize **1** in aqueous solutions, an acidic solution was employed to protonate the tertiary amines. This results in better water solubility and also ensures that the dendrimer adopts a fully extended conformation due to electrostratic repulsion. In addition, the hydrophobic adamantyl groups were complexed with *β*-CD.[29] Via this method, stable aqueous dendrimer solutions could be prepared of up to 0.15 mM.[13] The 62 tertiary amines in the interior of **1** can be employed for complexation of guest molecules, based on electrostatic interactions.
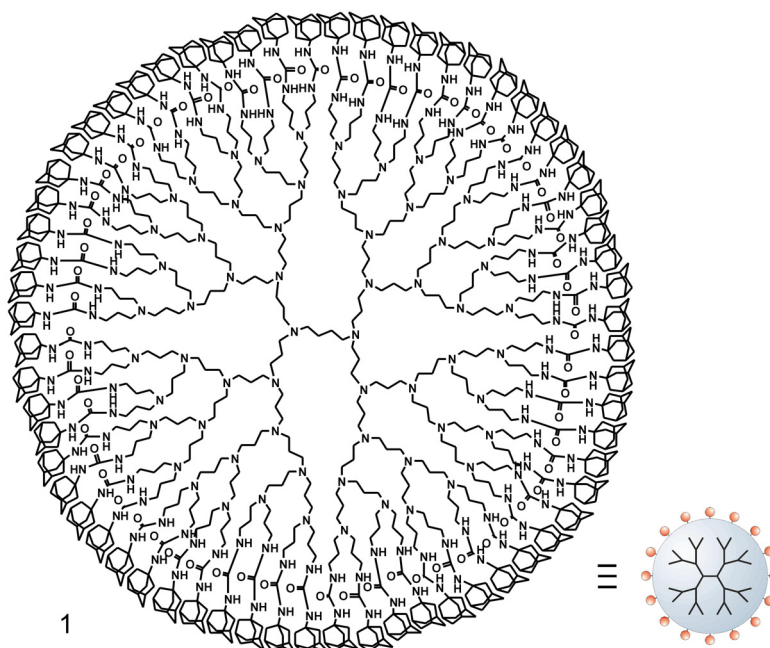

Chart 5.1 *Molecular structure of a fifth generation adamantyl-terminated PPI dendrimer.*

Microcontact printing was performed with oxidized stamps to improve the wettability of the stamp with the aqueous ink solution. Printing was performed from a

0.15 mM aqueous solution at pH 2 containing 10 mM of *β*-CD. Bringing the inked stamps in conformal contact with the molecular printboard resulted in the transfer of dendrimers from the stamp to the surface, as observed by a clear atomic force microscopy (AFM) contrast (Figure 5.1). In this case, the printed pattern could not only be observed in friction-mode, but also in height, implying the transfer of more than a monolayer of dendrimers. Extensive rinsing with an acidic *β*-CD solution resulted in a decrease in height to leave approximately a monolayer of dendrimers. The observed height by AFM was ca. 1 nm, indicating that the dendrimers are in a flattened conformation on the surface, or are flattened by the force of the AFM tip. In contrast to printing experiments with divalent molecules, as discussed in Chapter 4, rinsing with *β*-CD solution did not result in removal of the patterns, even after prolonged rinsing. This is a strong indication that **1** is able to interact via multiple supramolecular interactions, essentially binding in a quasi-irreversible fashion in aqueous solutions. In fact, recent electrochemical measurements in our group, using a G5 PPI dendrimer with 64 ferrocene end groups, suggested that approximately 7 end groups are involved in binding to the molecular printboard on gold.[30]
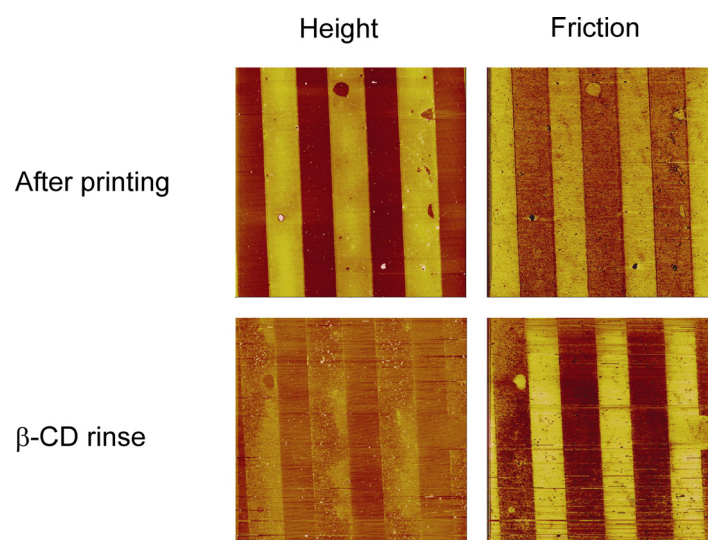

Figure 5.1 Contact-mode AFM images (50×50 μm²) after μCP of the β-CD complex of molecule **1** on a β-CD monolayer. Z-scale in top left image is 20 nm, in the bottom left image 10 nm. Friction forces (a.u.) increase from dark to bright contrast. Images shown after printing: without rinsing (top row) and after rinsing with 300 ml of 10 mM aqueous β-CD solution (bottom row).

5.2.2 *Encapsulation of fluorescent anionic guests*

To encapsulate anionic dye molecules in immobilized dendrimers the dendrimers were printed on *β*-CD monolayers. After printing, the patterns were rinsed extensively with aqueous *β*-CD solutions at pH 2 and subsequently dipped in a 10^{-4} M aqueous dye solution for 1 min. To remove physisorbed dye molecules the substrates were rinsed with an aqueous phosphate buffer solution (pH 7). The procedure is schematically outlined in Figure 5.2.
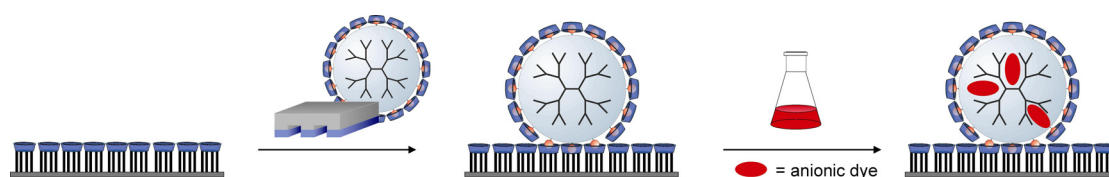

Figure 5.2 *Schematic representation of μCP of* **1** *on a β-CD monolayer, followed by filling of the immobilized molecules with anionic dyes.*

Bengal Rose and fluorescein were chosen for encapsulation in the dendrimer boxes. Both are known to interact with PPI dendrimers modified with apolar groups.[6] Bengal Rose and fluorescein are doubly negatively charged dyes, assuring an electrostatic interaction with the protonated interior of the dendrimers. Both dyes are water-soluble and fluorescent at neutral and high pH values. After the encapsulation process, substrates were imaged under a laser scanning confocal microscope (LSCM). Bengal Rose was excited at 543 nm and fluorescein at 488 nm. The LSCM images in Figure 5.3 show that complexation took place mainly in the parts where the dendrimers were deposited by the stamp, giving a faithful reproduction of the stamp features.

To demonstrate the wide scope of this methodology a more complicated procedure was carried out. After printing the dendrimers on the molecular printboard, a second stamp was inked with an aqueous 10^{-4} M Bengal Rose solution. This stamp was brought into contact with the substrate perpendicular to the printed dendrimer pattern, causing the transfer of Bengal Rose molecules from the stamp to the surface both on the bare *β*-CD monolayer and on the dendrimer-modified monolayer. Next, the substrate was briefly rinsed with water. Following the stamping procedures, the substrate was dipped into an aqueous 10^{-4} M fluorescein solution and finally rinsed

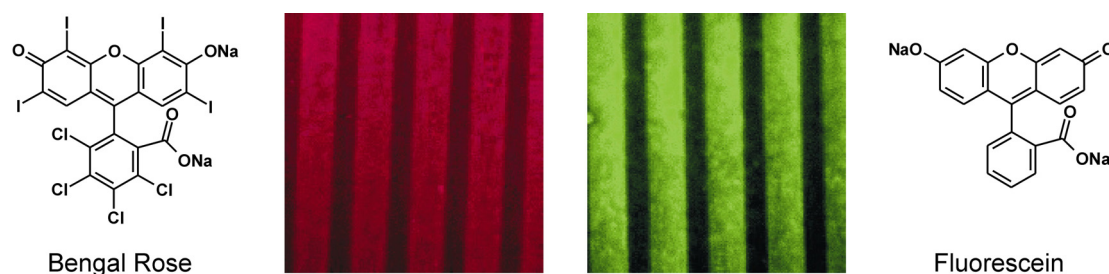with an aqueous phosphate buffer solution (pH 7). The procedure is depicted schematically in Figure 5.4.

Bengal Rose

Fluorescein

Figure 5.3 *Confocal microscopy images (65×65 μm²) after μCP of **1** on a β-CD monolayer, followed by filling of the immobilized dendrimers with Bengal Rose (left) and fluorescein (right).*

Imaging of the substrate, patterned with two dyes, was performed by simultaneously exciting and monitoring the emission at different wavelengths. Figure 5.5 shows the LSCM images of a cross-printed substrate. The left image was obtained by exciting at 543 nm and monitoring the emission above 600 nm, which are suitable wavelengths for Bengal Rose. The image shows that Bengal Rose was selectively deposited in the regions where dendrimers were deposited. The center image was acquired by exciting at 488 nm and monitoring the emission between 500 and 530 nm, where fluorescein emits. It is evident that adsorption of fluorescein took place mainly in the dendrimers and at the parts where Bengal Rose was not deposited. Simultaneous imaging (right) shows alternating parts of dendrimer patterns, selectively filled with the two dyes.
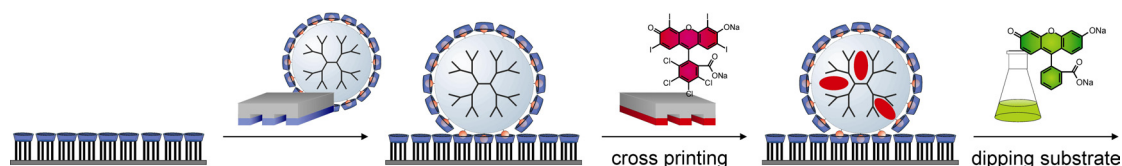

cross printing   dipping substrate

Figure 5.4 *Schematic representation of μCP of **1** on a β-CD monolayer, followed by cross printing of Bengal Rose, and subsequent filling with fluorescein.*
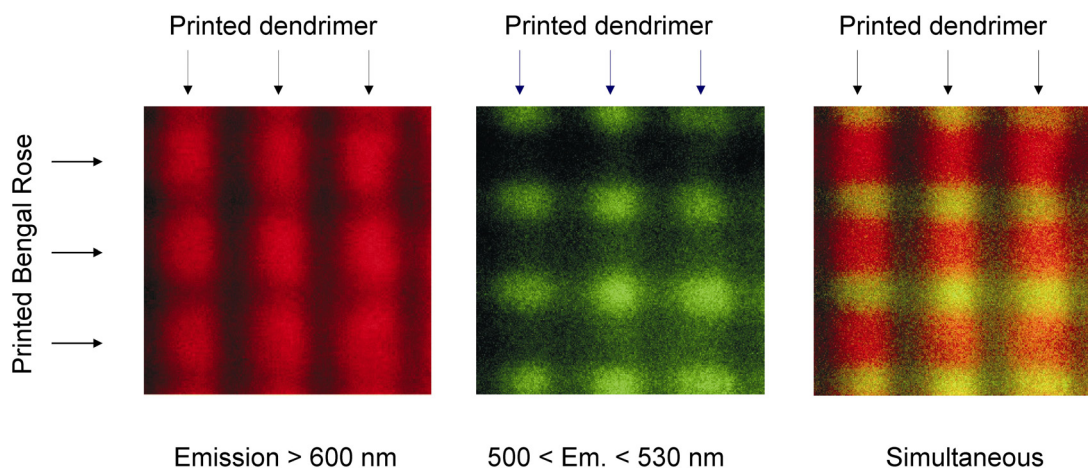
Figure 5.5 Confocal microscopy images (50×50 μm²) after μCP of 1 on a β-CD monolayer, followed by cross printing of Bengal Rose, and subsequent filling with fluorescein. The substrate was simultaneously excited at 488 nm and 543 nm and images were recorded by measuring the emission above 600 nm (left), between 500 and 530 nm (center), and simultaneous (right).
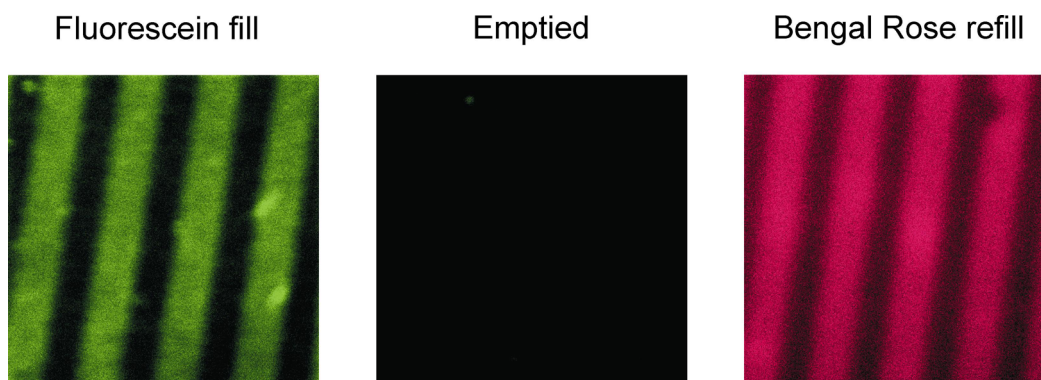

Figure 5.6 Confocal microscopy images (60×60μm²) after μCP of 1 on a β-CD monolayer, followed by filling of the immobilized dendrimers with fluorescein (left). Subsequently, the dendrimers were emptied by rinsing with an aqueous buffer solution at pH 9 (center), reprotonated by rinsing with an HCl solution, and refilled by dipping in a Bengal Rose solution (right). The left and center image were obtained at identical confocal microscope settings.

This experiment demonstrates that in addition to complexation from solution, immobilized dendrimers can also be filled by μCP of anionic dyes. The observation that dipping the substrate in a fluorescein solution results in selective deposition in the

'empty' dendrimers is an indication that Bengal Rose printing resulted in maximum filling of the dendritic molecules. Also, it suggests that the dyes are bound fairly strongly inside the dendrimers, as only limited exchange of the two dyes was observed.

One potential application of dendrimers is in controlled drug release.[5] For this purpose the encapsulation process needs to be reversible and the dendrimers should be able to release their guests upon external stimuli. One clever example was shown by Paleos *et al*. They were able to release encapsulated pyrene molecules from the interior of dendrimers by lowering the pH of the solution.[17] In our case, the reversibility of the encapsulation process was tested on the *β*-CD modified surface. Printed dendrimers were filled with fluorescein by dipping in an aqueous fluorescein solution (Figure 5.6, left image, page 97). Next, the substrate was rinsed with an aqueous 100 mM phosphate buffer solution at pH 9 to deprotonate the dendritic molecules and/or exchange the fluorescein molecules for non-fluorescent salts. LSCM indicated a large decrease in fluorescence intensity (Figure 5.6, center), reflecting the reversibility of the complexation process. Subsequently, the substrate was rinsed with an aqueous HCl solution to reprotonate the tertiary amines in the interior of the dendrimer, and dipped in an aqueous 10^{-4} M Bengal Rose solution. The image on the right (Figure 5.6) shows the substrate after refilling with Bengal Rose. Clearly, Bengal Rose was adsorbed to the dendrimer patterns, demonstrating the reversibility of the guest encapsulation process on a surface. In addition, these experiments demonstrate that the immobilized dendrimer boxes allow many consecutive handling steps without degradation of the microcontact printed pattern.

5.2.3   *Toward single molecule studies*

Single molecule studies offer the possibility to investigate properties of molecules that are often not observed in the bulk due to ensemble averaging.[31] Single molecule studies can lead to a wealth of new information with respect to the interactions of the single entity with its environment.[32] The last part of this chapter describes experiments toward the visualization of immobilized individual dendrimers, filled with anionic fluorescent molecules, by LSCM. Two procedures to observe individual, filled dendrimers on a surface were investigated. In the first approach empty dendrimers were immobilized on a surface, after which they were filled from

solution. In the second procedure the dendrimers were first filled in solution and subsequently transferred to a surface.

As fluorescein and Bengal Rose are not particularly suitable for single molecule studies due to rapid photobleaching, a different dye was chosen. Oregon Green 514 (OG514) is a fluorinated analog of fluorescein, which is known to be more photostable than fluorescein.[33] In addition, it has a high quantum yield (0.96) and a low pK_a of 4.5, making it a suitable reporter dye in biological systems.[34] The molecular structure of the OG514 derivative, used for these studies, is shown in Chart 5.2.
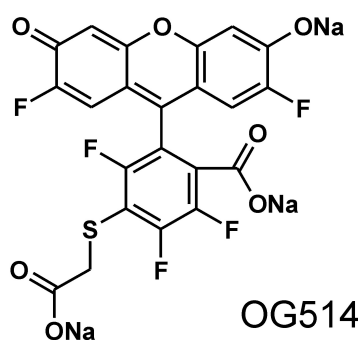

Chart 5.2 *Molecular structure of Oregon Green 514. The hydrolyzed succinimidyl ester derivative was employed in these studies.*

The first approach to visualize isolated, dye-containing dendrimers on a surface consisted of first immobilizing dendrimers on the molecular printboard, which were filled by placing an aqueous dye solution on top of the substrate. Using concentrated dye solutions (10^{-4} – 10^{-6} M) resulted in rapid filling of the dendrimers, as was shown in Chapter 5.2.2. However, OG514 dye molecules also physisorb on the bare β-CD monolayer, albeit to a lesser extent, making conclusive single molecule measurements very difficult to perform since it is not straightforward to discriminate between encapsulated and physisorbed dye molecules. Placing more dilute dye solutions (10^{-7} – 10^{-9} M) on top of substrates patterned with dendrimers resulted in very slow complexation in the molecular boxes, with additional physisorption on the bare monolayer. This implies that the affinity of OG514 for the dendrimers is not high enough to drive selective complexation from aqueous solutions at such low

concentrations. As it was not possible to avoid non-specific adsorption of OG514 dyes using this approach, a different method was explored.

PPI dendrimers modified with an apolar periphery can function as extractants of anionic dye molecules from water to organic solvents like methylene chloride, as has been reported by Meijer and co-workers.[6] This is schematically shown in Figure 5.7. There has been some discussion regarding the maximum number of dye molecules that can be encapsulated inside a dendrimer. For a G5 PPI dendrimer, values ranging from 4 to 50 Bengal Rose molecules have been reported.[6,14] A molecular dynamics study showed that 4 to 6 Bengal Rose molecules could be fitted inside a G5 dendrimer carrying apolar end groups.[15] Another group reported that 25 Bengal Rose molecules could be extracted by a G4 PPI dendrimer, but the same molecule extracted only 1 fluorescein dye.[8]
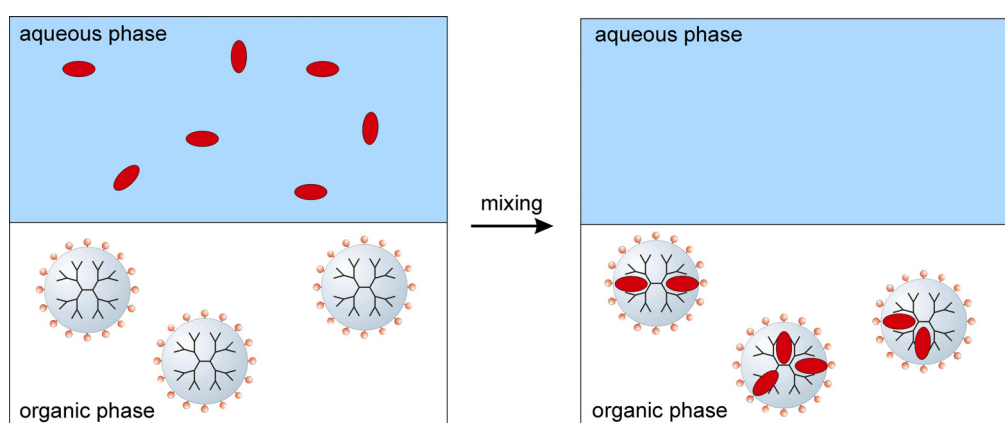

Figure 5.7 Schematic representation of the use of dendrimers as extractants of anionic species from aqueous to organic solutions.

Here, the G5 PPI dendrimers with 64 adamantyl groups, now in an organic solvent not complexed to *β*-CD, were employed to extract OG514 from an aqueous solution. By first filling the dendritic boxes with dyes before depositing them on a surface, the lack of affinity of the dyes that was experienced when filling immobilized dendrimers from aqueous solution is circumvented. Extractions were performed with 1×10^{-5} M aqueous dye solutions, while the dendrimer concentration in the methylene chloride solution was varied. Figure 5.8 shows the UV-Vis absorbances of the OG514 extractions. Extracting the water/dye layer with only methylene chloride did not result in any transfer of dye to the organic phase: the UV-Vis spectrum of the water layer

remained unchanged when compared to a 1×10^{-5} M OG514 stock solution (Figure 5.8, black and red line). However, when dendrimer was added to the organic phase, all fluorescent molecules were extracted into the organic phase up to a ratio of 1 dendrimer to 5 OG514 molecules, as is reflected by the negligible absorbance in the water layer (Figure 5.8, green line). Going to higher ratios resulted in a measurable signal in the water layer, suggesting that not all fluorescent molecules were extracted (Figure 5.8, dark- and light blue lines). This indicates that ca five OG514 molecules fit inside the dendrimer box. The absorbance of encapsulated dye molecules showed a red shift of ca. 20 nm, probably reflecting the transfer of OG514 from a polar aqueous environment to the relatively apolar dendrimer interior.[35]
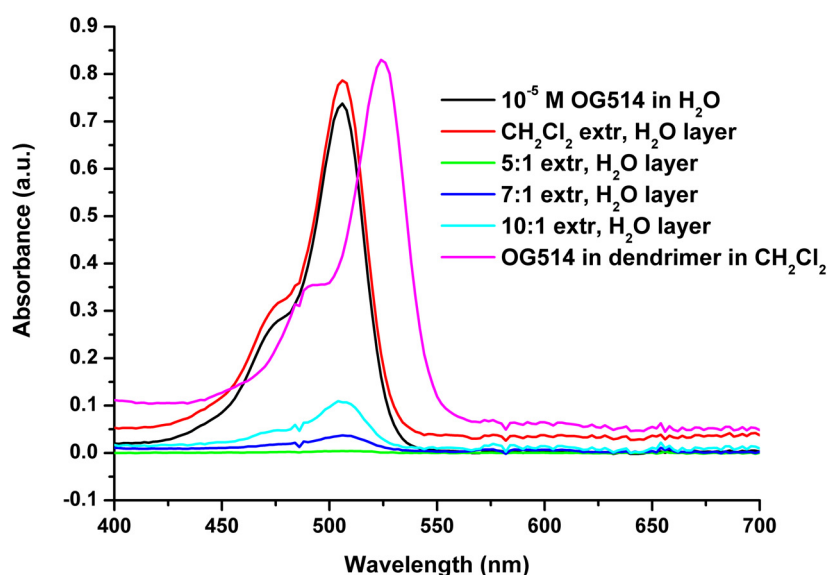

Figure 5.8 UV-Vis spectra of extraction experiments. The Oregon Green 514 concentration was kept constant (1×10^{-5} M). Spectra shown are: 1×10^{-5} M OG514 in water; water layer after extraction with CH_2Cl_2; water layer after extraction with dendrimer, dendrimer: dye ratios 1:5; 1:7; 1:10; CH_2Cl_2 layer with dendrimer after extraction.

The emission spectra before and after extraction are depicted in Figure 5.9. They show a comparable shift in emission maximum from ca 530 nm for OG514 in water to ca 550 nm for the encapsulated dyes. The change in fluorescence intensity upon transfer from the aqueous phase to the organic phase is striking. This large decrease in fluorescence has been observed previously by Balzani and co-workers

upon encapsulation of eosin dyes in PPI dendrimers.[8] They explain the quenching behavior by radiation-less transitions involving hydrogen bonds, which are thought to stabilize the inclusion of the dye inside the dendrimer. Encapsulating more OG514 molecules in a dendrimer reduces the fluorescence intensity even further, an indication that the fluorescent molecules are located close to each other and show self-quenching.
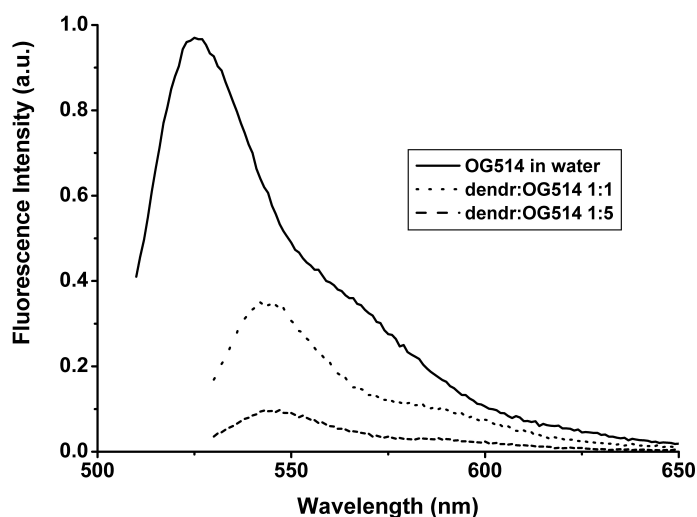

Figure 5.9 *Emission spectra of 1μM solutions of OG514 in water, and encapsulated in dendrimer (1:1 and 1:5).*

Single molecule spectroscopy of a dendrimer host-guest system has been reported by De Schryver *et al*.[36,37] They encapsulated a cyanine dye in poly(phenylene) dendrimers and studied the fluorescence behavior of single assemblies on a surface. Here, the organic solution containing dendrimers and dyes in a 1 to 5 ratio was diluted and spin-coated on a cleaned glass slide to study individual dye-accommodating dendrimer molecules.[38] As a reference, a dilute solution of OG514 in water was spin-coated on a cleaned glass slide. Figure 5.10 (left, page 104) shows a LSCM image after spin coating a 1×10^{-9} M OG514 solution in water at pH 6. Several characteristic features of single molecules were observed. Polarization-sensitive detection allows determination of the orientation of the dipole of single molecules. The red and green false-color coding shows the presence of features with a constant color, which cannot be attributed to ensembles. In addition, abrupt termination of fluorescence on a millisecond timescale (blinking) was observed. A

typical time trace is depicted on the right (Figure 5.10), which shows clearly single step bleaching, indicative of a single molecule.

Figure 5.11 (left, page 104) shows an LSCM image after spin-coating a 10^{-8} M solution of the dendrimer-dye assembly in methylene chloride on a clean glass slide. Several large features were observed. The fluorescent features in the right bottom corner are too large to correspond to single dendrimers, and could be dendrimer clusters. The features in the left top corner are significantly smaller, and might be attributed to single dendrimer molecules. Polarization-sensitive detection does not show features with a constant color, and blinking is also not observed, indicating the absence of single OG514 fluorophores. Figure 5.11 (right) depicts a typical time trace of such a molecule. It is evident that the bleaching behavior differs substantially from single molecule bleaching (Figure 5.10, right). Although it is difficult to observe distinct bleaching steps, the time trace suggests the presence of multiple fluorescent molecules.

These preliminary results suggest that dendrimers filled with anionic OG514 molecules can be transferred successfully from solution to a surface and can be studied with LSCM. Additional proof for the observation of complexed OG514 molecules inside dendrimers might be obtained by comparing single-molecule spectra of free OG514 with encapsulated dyes.

5.3 Conclusions

Fifth generation PPI dendrimers have been immobilized on the molecular printboard on glass. Stability studies with microcontact printed patterns indicated that these dendrimer molecules are anchored to the substrate via multiple supramolecular interactions, forming an essentially irreversible bond when working with aqueous solutions. The guest-binding properties of the immobilized dendrimers were investigated by encapsulating anionic dyes like Bengal Rose and fluorescein, and confocal microscopy images showed that the binding properties were retained. Moreover, more complicated strategies are possible: dyes were delivered to dendrimers by μCP, and the remaining dendrimer parts could be filled selectively with a different dye from solution. Additionally, it was shown that the encapsulation process on the *β*-CD surface is reversible.
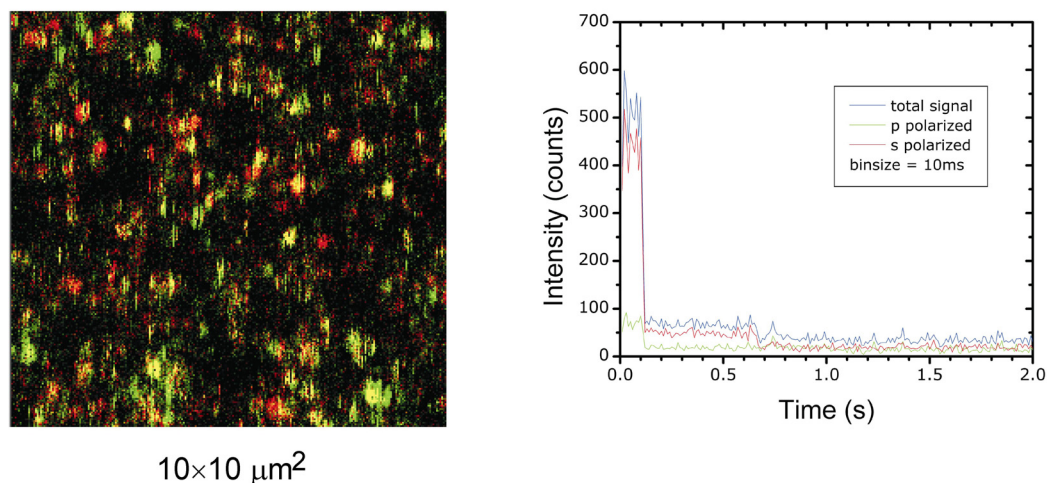
10×10 μm²

Figure 5.10 LSCM image of OG514 dyes on a glass substrate obtained with polarization-sensitive detection (left) and a typical time trace of a single OG514 molecule (right).

10×10 μm²
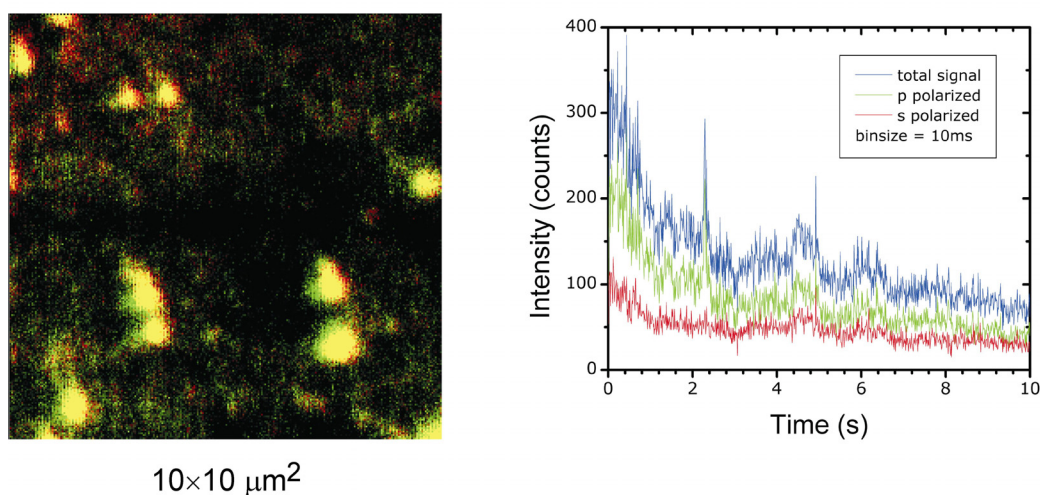
Figure 5.11 LSCM image of filled dendrimers on a glass substrate obtained with polarization-sensitive detection (left) and a typical time trace of such a molecule (right).

Single molecule studies on dendrimers anchored at CD monolayers and filled from aqueous solutions were not successful. Presumably the affinity of the dyes for the dendrimers is not high enough in aqueous solutions and non-specific adsorption could not be prevented. Preliminary studies on the encapsulation of dyes inside the dendrimers by extraction from an aqueous solution to an organic solution, followed by transfer of the filled dendrimers to a surface are promising. LSCM images and time

traces showed a clear difference between immobilized single OG514 molecules and immobilized dendrimers filled with OG514 dyes.

This Chapter shows that dendrimers remain versatile molecules when immobilized onto a surface. As these macromolecules can carry many functionalities, the formed patterns could function as templates for nanofabrication techniques. In addition, the reversibility of the encapsulation process makes these types of immobilized molecular boxes attractive as potential drug delivery systems.

5.4 Experimental Section

Materials and methods. G5 PPI dendrimers with 64 adamantyl groups were prepared by Christian Nijhuis according to a procedure reported by Meijer *et al.*[39] Aqueous dendrimer solutions were made by adding a 10 mM *β*-CD solution of pH 2 to the dendrimers, followed by extensive sonication.[13]

Extraction experiments. Extractions were performed using 1×10^{-5} M of dye in a 10 mM aqueous phosphate buffer solution at pH 6 for OG514, and pH 5 for the Cypher dye. Dendrimer concentrations in methylene chloride were varied from 1×10^{-5} M to 1×10^{-6} M. The extractions were performed by shaking the two phases violently for 1 min, after which the phases were separated. For OG514, an immediate color change took place from green to light-pink upon shaking.

Substrate preparation. *β*-CD monolayers were prepared as described in Chapter 3 with one modification. After *β*-CD attachment, the remaining free amines on the surface were capped by immersion in an aqueous 5 mM methylisothiocyanate solution at pH 9 for 1 h at 50 ˚C. The capped layers were rinsed with water and dried in a stream of nitrogen. Microscope glass slides for spin coating were cleaned in an oxygen plasma for 10 min. Spin-coating was performed at 2500 rpm for 60 s (OG514 in water) or 20 s (dendrimers in methylene chloride).

Microcontact printing. The procedure to prepare PDMS stamps is similar to the one reported in the experimental section of Chapter 4. Before printing, the stamps were mildly oxidized in a UV/ozone reactor for 30 to 60 min to improve wetting by aqueous ink solutions. The stamps were inked in a 0.15 mM dendrimer solution, containing 10 mM *β*-CD, followed by drying in a stream of nitrogen. Printing was performed for 60 s by bringing the stamp in conformal contact with the substrate by hand, without the use of external pressure.

AFM. AFM experiments were carried out with a Nanoscope III multimode AFM (Digital Instruments, Santa Barbara, CA, USA) in contact mode using V-shaped Si_3N_4 cantilevers (Nanoprobes, Digital Instruments) with a spring constant of 0.1 N/m. Images were acquired in ambient atmosphere (ca 30-40% relative humidity, 25˚C).

UV-Vis spectroscopy. UV-Vis spectroscopy was performed on a Hewlett Packard 8452A diode array spectrophotometer using quartz sample cells of 10 mm.

Fluorescence spectroscopy. Fluorescence spectroscopy was performed on an Edinburgh FS900 fluorospectrophotometer in which a 450 W xenon arc lamp was used as the excitation source. M300 gratings with 1800 1/mm were used on both excitation and emission arms. Signals were detected by a Peltier element cooled, red sensitive, Hamamatsu R928 photomultiplier system. Quartz sample cells of 1 mm were used.

Laser scanning confocal microscopy. Confocal microscopy images of the microcontact printed substrates were taken on a Carl Zeiss LSM 510 microscope. The light was focused on the substrate using an oil immersion lens (N.A. 1.4, 63×). Bengal Rose was excited at 543 nm, while fluorescein was excited at 488 nm. The emitted fluorescence was collected on a PMT R6357 spectrophotometer. All confocal microscopy images were acquired in air.

Fluorescence imaging of single molecules was carried out using an inverted confocal microscope (Zeiss Axiovert) with an oil immersion lens (N.A. 1.4, 100×). An ArKr ion laser (Spectra Physics Beamlok 2060), operated at 514 nm, was used to excite the fluorophores. The excitation light was filtered using a 514 bandpass filter (Omega 514.5/10). A dichroic mirror (Omega 540DRLP) and a long-pass filter (Omega 550APL) were used to separate the emitted light from the excitation light. The fluorescence signal was detected using an avalanche photodiode (EG&G Electro Optics SPCM-AQ-14). The sample was scanned over an area, typical $10 \times 10 \ \mu m^2$ with 512×512 pixels and a pixel dwell time of 1 ms. The excitation power was ~3.5 kW/cm^2. All confocal microscope images were acquired in air.

5.5 References

[1]   Baars, M. W. P. L.; Meijer, E. W. *Top. Curr. Chem.* **2000,** *210,* 131-182.

[2]   Smith, D. K.; Diederich, F. *Top. Curr. Chem.* **2000,** *210*, 183-227.

[3]   Zimmerman, S. C.; Lawless, L. J. *Top. Curr. Chem.* **2001,** *217*, 95-120.

[4]   Jansen, J. F. G. A.; De Brabander-Van den Berg, E. M. M.; Meijer, E. W. *Science* **1994,** *266*, 1226-1229.

[5]   Boas, U.; Heegaard, P. M. H. *Chem. Soc. Rev.* **2004,** *33*, 43-63.

[6]   Baars, M. W. P. L.; Froehling, P. E.; Meijer, E. W. *Chem. Commun.* **1997,** 1959-1960.

[7]   Balzani, V.; Ceroni, P.; Gestermann, S.; Gorka, M.; Kauffmann, C.; Maestri, M.; Vogtle, F. *ChemPhysChem* **2000,** *1*, 224-227.

[8]   Balzani, V.; Ceroni, P.; Gestermann, S.; Gorka, M.; Kauffmann, C.; Vogtle, F. *Tetrahedron* **2002,** *58*, 629-637.

[9]   Kleij, A. W.; Van de Coevering, R.; Gebbink, R. J. M. K.; Noordman, A. M.; Spek, A. L.; Van Koten, G. *Chem. Eur. J.* **2001,** *7*, 181-192.

[10]   Teobaldi, G.; Zerbetto, F. *J. Am. Chem. Soc.* **2003,** *125*, 7388-7393.

[11]   Chen, S. F.; Yu, Q. M.; Li, L. Y.; Boozer, C. L.; Homola, J.; Yee, S. S.; Jiang, S. Y. *J. Am. Chem. Soc.* **2002,** *124*, 3395-3401.

[12]   Marchioni, F.; Venturi, M.; Credi, A.; Balzani, V.; Belohradsky, M.; Elizarov, A. M.; Tseng, H. R.; Stoddart, J. F. *J. Am. Chem. Soc.* **2004,** *126*, 568-573.

[13]   Michels, J. J.; Baars, M. W. P. L.; Meijer, E. W.; Huskens, J.; Reinhoudt, D. N. *J. Chem. Soc., Perkin Trans. 2* **2000,** 1914-1918.

[14]   Jansen, J. F. G. A.; Meijer, E. W. *J. Am. Chem. Soc.* **1995,** *117*, 4417-4418.

[15]   Miklis, P.; Cagin, T.; Goddard, W. A. *J. Am. Chem. Soc.* **1997,** *119*, 7458-7462.

[16]   Watkins, D. M.; Sayed-Sweet, Y.; Klimash, J. W.; Turro, N. J.; Tomalia, D. A. *Langmuir* **1997,** *13*, 3136-3141.

[17]   Pistolis, G.; Malliaris, A.; Tsiourvas, D.; Paleos, C. M. *Chem. Eur. J.* **1999,** *5*, 1440-1444.

[18]   Morgan, M. T.; Carnahan, M. A.; Immoos, C. E.; Ribeiro, A. A.; Finkelstein, S.; Lee, S. J.; Grinstaff, M. W. *J. Am. Chem. Soc.* **2003,** *125*, 15485-15489.

[19]   Santo, M.; Fox, M. A. *J. Phys. Org. Chem.* **1999,** *12*, 293-307.

[20]   Boas, U.; Karlsson, A. J.; De Waal, B. F. W.; Meijer, E. W. *J. Org. Chem.* **2001,** *66*, 2136-2145.

[21]   Boas, U.; Sontjens, S. H. M.; Jensen, K. J.; Christensen, J. B.; Meijer, E. W. *ChemBioChem* **2002,** *3*, 433-439.

[22]   Precup-Blaga, F. S.; Garcia-Martinez, J. C.; Schenning, A.; Meijer, E. W. *J. Am. Chem. Soc.* **2003,** *125*, 12953-12960.

[23]   Wells, M.; Crooks, R. M. *J. Am. Chem. Soc.* **1996,** *118*, 3988-3989.

[24]   Tokuhisa, H.; Zhao, M. Q.; Baker, L. A.; Phan, V. T.; Dermody, D. L.; Garcia, M. E.; Peez, R. F.; Crooks, R. M.; Mayer, T. M. *J. Am. Chem. Soc.* **1998,** *120*, 4492-4501.

[25]   Huo, F. W.; Xu, H. P.; Zhang, L.; Fu, Y.; Wang, Z. Q.; Zhang, X. *Chem. Commun.* **2003,** 874-875.

[26]   Friggeri, A.; Schönherr, H.; Van Manen, H. J.; Huisman, B. H.; Vancso, G. J.; Huskens, J.; Van Veggel, F. C. J. M.; Reinhoudt, D. N. *Langmuir* **2000,** *16*, 7757-7763.

[27]   Friggeri, A.; Van Manen, H. J.; Auletta, T.; Li, X.-M.; Zapotoczny, S.; Schönherr, H.; Vancso, G. J.; Huskens, J.; Van Veggel, F. C. J. M.; Reinhoudt, D. N. *J. Am. Chem. Soc.* **2001,** *123*, 6388-6395.

[28]   Huskens, J.; Deij, M. A.; Reinhoudt, D. N. *Angew. Chem., Int. Ed.* **2002,** *41*, 4467-4471.

[29]   For a G5 PPI dendrimer it is not possible to complex all adamantyl groups with cyclodextrin, even in the fully extended conformation, see ref 13.

[30]   Nijhuis, C. A.; Huskens, J.; Reinhoudt, D. N. *J. Am. Chem. Soc.* **2004,** *126*, in press.

[31]   Weiss, S. *Science* **1999,** *283*, 1676-1683.

[32]   Moerner, W. E.; Orrit, M. *Science* **1999,** *285*, 1670-1676.

[33]   Haugland, R. P. *Handbook of fluorescent probes and research products, ninth edition*. Molecular Probes: Eugene, 2002.

[34]   Sun, W.-C.; Gee, K. R.; Klaubert, D. H.; Haugland, R. P. *J. Org. Chem.* **1997,** *62*, 6469-6475.

[35]   Similar extractions were also attempted with a cyanine Cypher dye, but invariably resulted in a precipitate at the water-methylene chloride interface. Apparently, the solubility of this dendrimer-dye system in methylene chloride is very low.

[36]   Kohn, F.; Hofkens, J.; Wiesler, U. M.; Cotlet, M.; Van der Auweraer, M.; Müllen, K.; De Schryver, F. C. *Chem. Eur. J.* **2001,** *7*, 4126-4133.

[37]   Kohn, F.; Hofkens, J.; Gronheid, R.; Cotlet, M.; Müllen, K.; Van der Auweraer, M.; De Schryver, F. C. *ChemPhysChem* **2002,** *3*, 1005-1013.

[38]   Due to time limitations, this procedure has not yet been attempted on the cyclodextrin host monolayer.

[39]   Baars, M. W. P. L.; Karlsson, A. J.; Sorokin, V.; De Waal, B. F. W.; Meijer, E. W. *Angew. Chem., Int. Ed.* **2000,** *39*, 4262-4265.

Chapter 6

Immobilized Dendrimers as Template for the Electroless Deposition of Metals

6.1   Introduction

Electroless deposition (ELD) of metals offers a fast and low-cost method to generate metal patterns on a surface. ELD is based on the deposition and reduction of metal ions from a solution to a surface without applying an electrical potential. This redox process generally takes place on a surface that can catalyze the process, or on a non-catalytic surface that is activated with a metal catalyst. One of the attractive features of ELD is the large choice of metals and surfaces that can be employed for deposition. Metal patterns of copper, silver, gold, nickel, and cobalt have been fabricated onto either metallic or insulating substrates.[1-6] The principal technological application of ELD lies in the production of metal patterns in printed circuits.[7] Techniques that have been used to create suitably patterned surfaces include photolithography[1,4,8] and e-beam lithography,[9] but in recent years microcontact

printing (μCP) has become the technique of choice. μCP can be used to either passivate parts of a catalytic surface,[3] or activate parts of a non-catalytic surface.[7] A widely used approach to activate non-catalytic surfaces employs the metal-ligand binding motif between a ligating monolayer and metal colloids that catalyze ELD.[10] By either printing the monolayer and subsequent dipping in a colloid solution, or printing the colloids on a homogeneous monolayer submicrometer metal patterns have been fabricated.[7,11-16]

Metal colloids are interesting materials for use in catalysis and nano-devices.[17] Dendritic molecules possess amino ligand sites that allow preorganization of metal ions and it has been shown that upon reduction monodisperse dendrimer-stabilized nanoparticles are formed. Because of the open structure of dendrimers the metal clusters are not shielded from the surrounding solution, which means that the catalytic site remains active.[18] Poly(amido amine) (PAMAM) dendrimers have been used to stabilize nanoparticles of copper,[17-19] gold,[20,21] silver,[22] platinum,[23,24] and palladium.[23,24] Also poly(propylene imine) (PPI) dendrimers have been shown to stabilize colloids of copper,[25] palladium,[26] gold,[27] and platinum.[27] In recent years, these composite materials have been investigated intensely and were found to catalyze a range of reactions.[28]

Dendritic molecules can be functionalized with a variety of groups at their periphery, which can be used to immobilize dendrimer-containing nanoparticles on a surface. Dendrimer-gold nanocomposites have been immobilized via electrostatic interactions using the layer-by-layer technique,[29] and dendrimer-stabilized palladium nanoparticles have been deposited on a mica surface and imaged with AFM.[30] Bittner and co-workers have shown that it is possible to first deposit a dendrimer on a surface, followed by adsorption of metal ions in the immobilized dendrimers from solution. These metal-loaded dendrimers were subsequently used for ELD of copper and cobalt.[31,32] Combining this with μCP resulted in cobalt structures with a lateral size of several hundred nanometers.[32]

In this chapter, specific supramolecular interactions between adamantyl-functionalized dendrimers and the *β*-CD monolayers on glass have been employed to produce stable dendritic patterns on a surface. These surface-confined dendrimers have been used to template the ELD of copper and cobalt following two different strategies. The first consisted of patterning the molecular printboard with dendrimer-

stabilized colloids using µCP and dip-pen nanolithography (DPN). These patterns acted as nuclei for the ELD of copper. In the second strategy empty dendrimers were printed on the printboard, which were filled with metal ions from solution, and subsequently used to direct ELD of cobalt.

6.2   Results and Discussion

6.2.1   *Dendrimer-stabilized gold colloids*

The preparation of dendrimer-stabilized gold colloids in modified PPI dendrimers has been reported previously by our group.[27] Fifth generation PPI dendrimers, derivatized with adamantyl groups for host-guest interactions with β-CD monolayers, were dissolved in an aqueous solution containing 10 mM of β-CD, as was reported in Chapter 5. An acidic solution was used, fully protonating the dendrimer-β-CD assembly. To this solution an $HAuCl_4$ solution was added in such quantities that the amine : metal ratio was 2 : 1. Driven by electrostatic interactions, the $AuCl_4^-$ anions migrate into the dendritic assemblies, where they are subsequently reduced upon addition of an aqueous solution of $NaBH_4$. This procedure yields stabilized gold nanoparticles with a narrow size distribution and an average diameter of ca 2 nm, as observed by transmission electron microscope (TEM) measurements.[27] A schematic representation of this procedure is depicted in Figure 6.1.
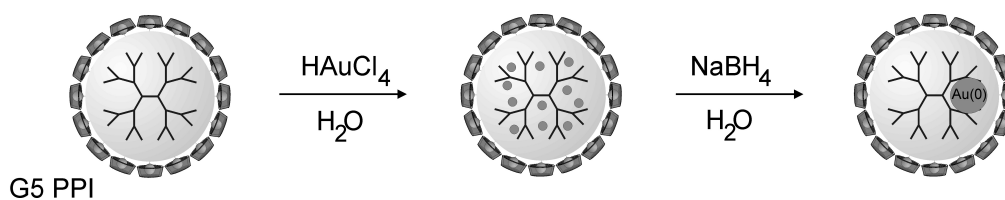

Figure 6.1 *Schematic representation of the preparation of dendrimer-stabilized Au colloids.*

In addition to TEM measurements, where the stabilized colloids are deposited on a copper grid, it was attempted to visualize the nanoparticles on the molecular printboard on glass by high-resolution scanning electron microscope (SEM) measurements. Figure 6.2 shows a SEM image of dendrimer-stabilized gold colloids, which were deposited onto the β-CD monolayer during a 1 min dip in an aqueous dendrimer-stabilized colloid solution. The gold particles are clearly visible as a result of the contrast with the silicon substrate. The smallest features that are visible have a

diameter between 2 and 3 nm, which indicates that these are individual metal particles inside a dendrimer. Larger features are most likely aggregates of metal clusters. Colloids with a diameter smaller than 2 nm were not observed. This could have two reasons: either the stabilized particles have clustered into larger aggregates, or the smaller particles could not be observed due to the resolution limit of the SEM.
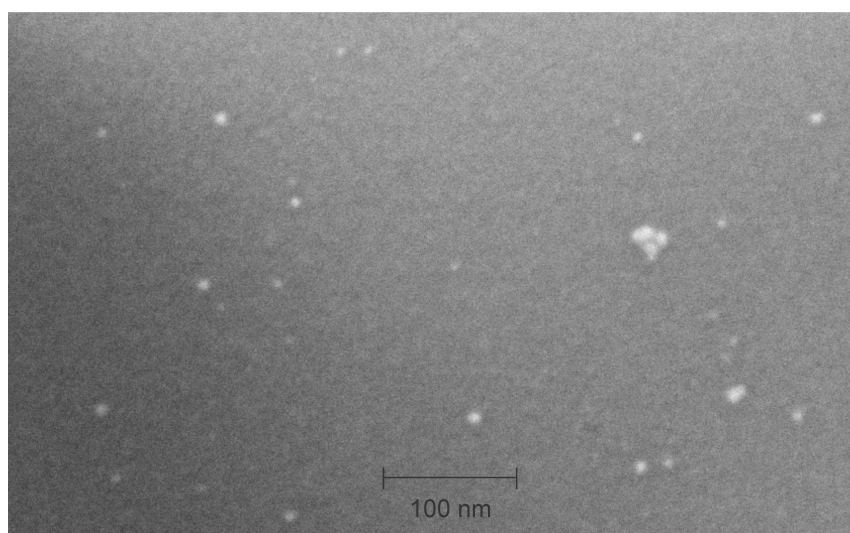

Figure 6.2 *High-resolution SEM image of dendrimer-stabilized Au colloids on the molecular printboard.*

6.2.2   *Electroless copper deposition on dendrimer-stabilized gold colloids*

To obtain metal patterns on a substrate, μCP of the dendrimer-stabilized colloids was combined with ELD of copper. Inking of the stamp was accomplished by soaking it in an aqueous solution containing the nanocomposite material. Prior to inking, the stamps were oxidized in a UV-ozone reactor for 30 to 60 min to promote adhesion between the ink and the stamp. The inked stamp was dried with nitrogen and brought into conformal contact with the *β*-CD monolayer for 1 min, without the use of external pressure. After printing, the substrate was immediately dipped into a freshly prepared copper ELD bath for ca 5 min. The main components of the ELD bath were $CuSO_4$, EDTA as a chelating agent, and formaldehyde as the reducing agent. During copper deposition hydrogen bubbles were observed at the surface, indicative of copper deposition. The overall reaction at the surface is:[33]

$$CuEDTA^{2-} + 2\ C_2HO + 4\ OH^- \longrightarrow Cu^0 + H_2 + 2\ H_2O + 2\ HCOO^- + EDTA^{4-}$$
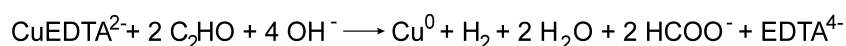
Following ELD of copper, the substrate was rinsed briefly with water and dried. The printing and ELD procedure is schematically shown in Figure 6.3.
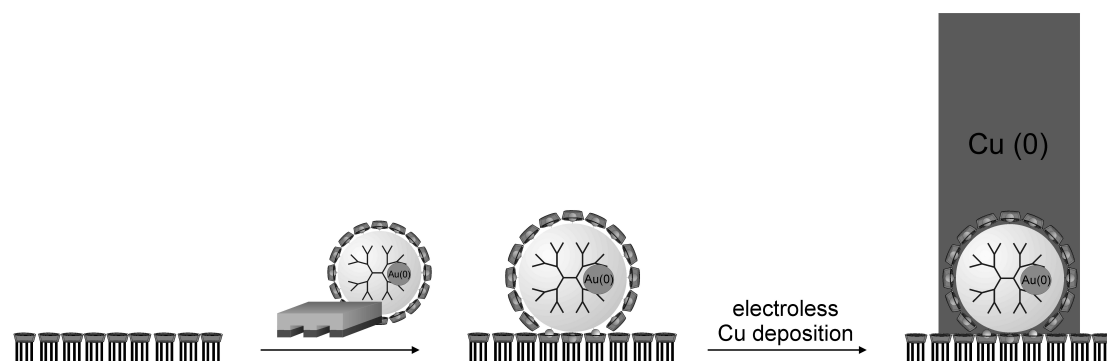

Figure 6.3 *Schematic representation of μCP of dendrimer-stabilized Au colloids, followed by electroless Cu deposition.*

After ELD the patterned substrates had a reddish color, indicative of copper deposition. Inspection of the substrates with contact mode AFM (CM-AFM) showed that copper was deposited on the printed dendritic gold colloids. Figure 6.4 shows the CM-AFM results after ELD. The top row shows the height (left) and friction (right) images, while the average height profile in the marked section is shown at the bottom. The ELD process is very selective. Copper was only deposited in the regions where the stamp was in contact with the surface, yielding metal wires of around 85 nm in height.

Although copper deposition is a very selective process, as no copper growth was observed in between the stamped regions, parts of the substrate remained uncovered. A possible explanation for this observation could be that not enough colloidal material was transferred in these regions during printing to start the copper growth, as a minimum amount of catalyst is known to be necessary to initiate ELD.[34]
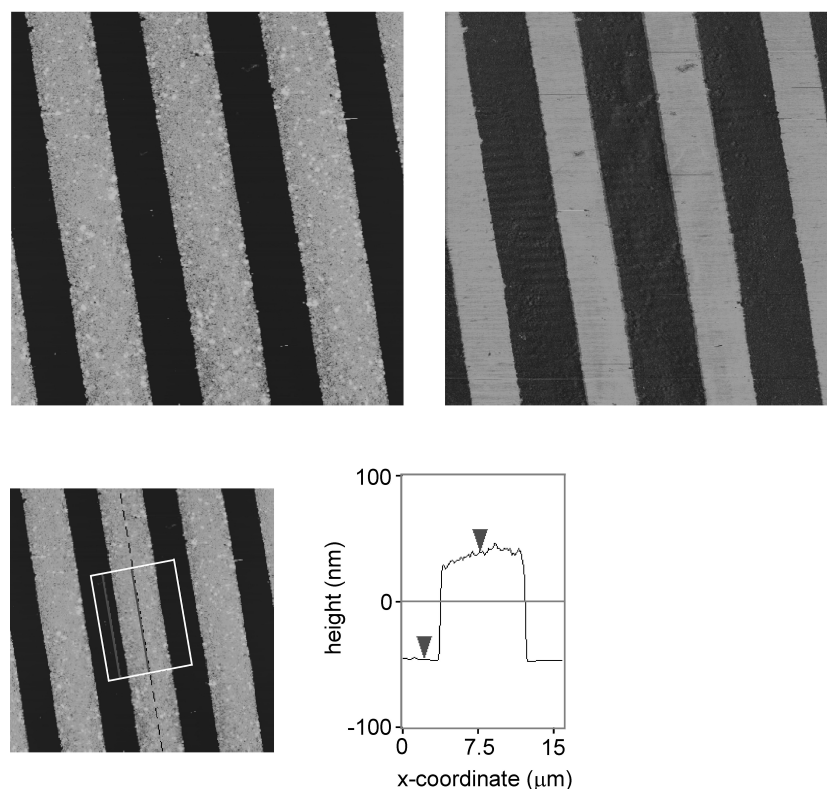
Figure 6.4 *CM-AFM results (50×50 μm²) of electroless Cu depostion on microcontact printed dendrimer-stabilized Au colloids. Depicted images are height (top, left) and friction (top, right). Z-scale is 200 nm and friction forces (a.u.) increase from dark to bright contrast. Bottom images show the average height profile in the marked section.*

The same method of depositing the nanocomposite material, followed by vertical amplification of the patterns was also attempted using dip-pen nanolithography. Writing molecules with an AFM tip on a surface allows the creation of patterns with sub-100 nm dimensions.[35] An unmodified Si_3N_4 AFM tip was inked in an aqueous dendrimer-stabilized gold colloid solution, dried, and scanned slowly over the *β*-CD surface. A scan speed of 10 μm s⁻¹ was used and the area was scanned 5 times. Following the writing procedure, the substrates were dipped in the ELD bath for ca. 5 min. Figure 6.5 shows CM-AFM images after writing and after ELD. Figure 6.5A was obtained in friction-force after writing a 10×10 μm² box on the substrate, followed by zooming out and imaging the written pattern at higher scan speed. A clear contrast in friction was observed, suggesting that molecules were deposited.[36] The height image in Figure 6.5B shows a similar substrate after ELD.[37] Copper deposition took place, as witnessed by the 55 nm high features on the substrate. The observed

features fit the 10×10 μm^2 box that was written, but only parts of the written box were enhanced by copper deposition. Possibly, material was not deposited equally over the entire written pattern, resulting in metal deposition only in the areas where enough stabilized colloids were transferred from the tip to the monolayer.
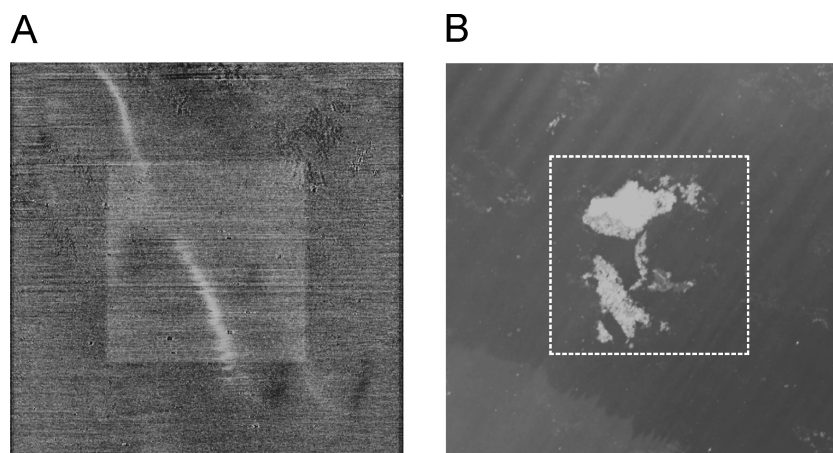

Figure 6.5 (a) CM-AFM friction image (20×20 μm²) after DPN of dendrimer-stabilized Au colloids. Friction forces (a.u.) increase from dark to bright contrast. (b) CM-AFM height image (20×20 μm²) after electroless Cu deposition on DPN-written pattern. Z-scale is 60 nm. The dotted square corresponds to the written 10×10 μm area.

Optimization of the writing process was attempted by coating the AFM tip with a poly(ethylene-glycol) monolayer to reduce the activation energy for molecular transport from tip to surface.[38] In addition, DPN was performed at elevated humidity (50-60%), which is known to facilitate transport of high-molecular weight molecules to the substrate.[38] However, none of these optimizations resulted in reproducible ELD on written patterns. Perhaps the kinetic processes involved in the transfer of a dendrimer-stabilized colloid from the surface of an AFM-tip, via the water meniscus between the tip and substrate, to the *β*-CD monolayer are too slow to reach sufficient deposition to initiate ELD.

6.2.3 Electroless cobalt deposition on PAMAM dendrimers

Poly(amido amine) (PAMAM) dendrimers constitute another class of commercially available dendrimers. PAMAM dendrimers possess a more open structure compared to PPI dendrimers as a result of the longer spacing between the

branches of the dendritic molecules, which potentially makes them more suitable for ELD. Here, fourth generation PAMAM dendrimers modified with 64 adamantyl groups were employed for attachment to β-CD monolayers. A similar procedure as described by Bittner and co-workers, who immobilized OH-terminated G4 PAMAM dendrimers on bare silicon wafers, was followed.[32] The procedure is schematically shown in Figure 6.6.
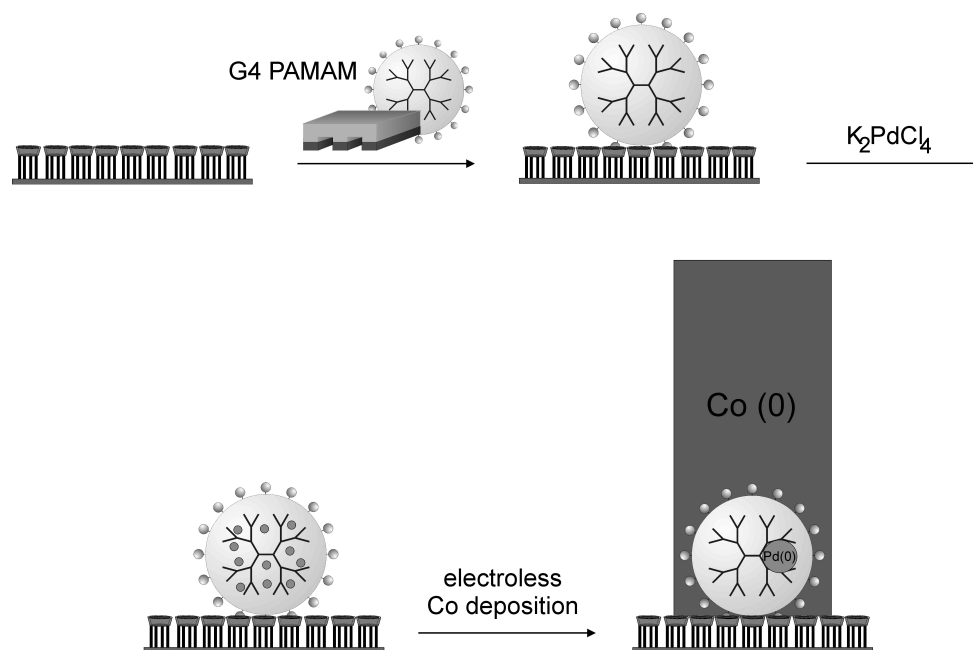

Figure 6.6 *Schematic representation of the electroless Co deposition process. G4 PAMAM dendrimers were immobilized on a β-CD monolayer to hosts Pd ions. The Pd ions were reduced to Pd particles, which acted as nucleation centers for electroless Co deposition.*

A 0.1 mM solution of G4 adamantyl-PAMAM dendrimer in ethanol was prepared. PDMS stamps were cleaned in ethanol and inked by soaking in the dendrimer solution. Printing was performed by bringing the stamp in conformal contact with the β-CD monolayer for 2 min without the use of external pressure. Directly after printing, a drop of an aqueous K_2PdCl_4 solution at pH 5, containing 0.1 M NaCl, was put on the substrate for 15 min. In contrast to the procedure to prepare dendrimer-stabilized gold colloids, the tertiary amines are not protonated. The tertiary amines and amide groups in the dendrimer can bind Pd^{2+} ions, provided that they possess at least one weakly bound ligand. In this case, Cl^- is the labile ligand. At pH 5 the amount of chloropalladate species is over 90%,[34] indicating that complexation

from this solution should preferentially take place inside the dendrimers. After palladium complexation, the substrates were rinsed with water and immersed in an electroless cobalt deposition bath for 2-3 min. The main components of this bath were $CoCl_2$, a ligating compound, and dimethylaminoborane as the reductant. Finally, the substrates were rinsed with water and dried.

Inspection of the substrate with an optical microscope showed that deposition of cobalt took place on all contacted areas. Figure 6.7 shows CM-AFM images of a patterned surface. Around 60 nm of cobalt was selectively deposited on the printed parts, demonstrating that dendrimers immobilized on functionalized surfaces can be filled selectively with metal ions from solution, which in turn direct electroless metal deposition.

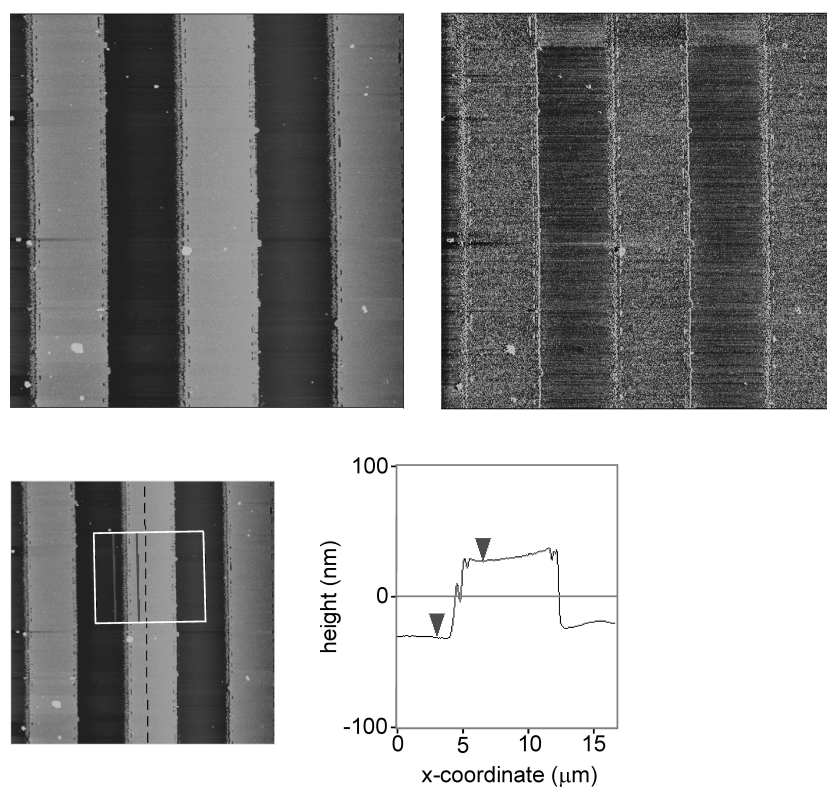***Figure 6.7*** *CM-AFM results (40×40 μm²) of electroless Co deposition on microcontact printed PAMAM dendrimers, which were filled with Pd ions. Depicted images are height (top, left) and friction (top, right). Z-scale is 200 nm and friction forces (a.u.) increase from dark to bright contrast. Bottom images show the average height profile in the marked section.*

6.3 Conclusions

Dendrimers, confined to a surface through multiple host-guest interactions, have been used to direct the ELD of metals. It was shown that PPI dendrimer-stabilized colloids could be employed to pattern the molecular printboard using lithographic techniques like μCP and DPN. Amplification of the colloidal patterns was accomplished by electroless deposition of copper. Microcontact printing, followed by ELD resulted in μm wide copper lines of ca 80 nm in height. However, DPN did not yield reproducible results, possibly because of slow transport of the dendrimer-colloid assembly from the tip to the surface.

In a second procedure, adamantyl-derivatized PAMAM dendrimers were immobilized on the *β*-CD surface using μCP. On these functionalized glass surfaces it was possible to selectively fill the immobilized dendrimers with Pd^{2+} ions, which were employed to direct ELD of cobalt. Using this method, substrates were selectively patterned with cobalt lines of ca 60 nm in height. For DPN followed by ELD this second procedure might be more suitable, as the metal deposition is very uniform and dendrimers of lower mass (without nanoparticle) need to be transported from the AFM tip to the surface.

Combining readily accessible lithographic techniques like DPN with the molecular printboard and ELD could ultimately result in the fabrication of metal wires with sub-100 nm dimensions. As the dendrimers bind strongly to the *β*-CD monolayer, the writing process will not be hampered by mobility of molecules over the surface.

6.4 Experimental Section

Materials and methods. G5 PPI dendrimers with 64 adamantyl groups were prepared by Christian Nijhuis, according to a procedure reported by Meijer *et al.*[39] Aqueous dendrimer solutions were made by adding a 10 mM *β*-CD solution pH 2 to the dendrimers, followed by extensive sonication. G4 PAMAM dendrimers with 64 adamantyl groups were prepared by Christian Nijhuis, according to a similar procedure as the PPI dendrimers.

Substrate preparation. *β*-CD monolayers were prepared as described in Chapter 5.

SEM. SEM measurements were performed on a LEO 1550 FEG SEM with a redesigned high-efficiency *in-lens* detector. EDX system: Thermo NORAN

Instruments, model Vantage. PBS: Thermo NORAN's Extended-range MAXray wavelength-dispersive X-ray analysis system.

AFM. AFM experiments were carried out with a Nanoscope III multimode AFM (Digital Instruments, Santa Barbara, CA, USA) in contact mode using V-shaped Si_3N_4 cantilevers (Nanoprobes, Digital Instruments) with a spring constant of 0.1 N/m. Images were acquired in ambient atmosphere (ca 30-40% relative humidity, 25˚C).

Preparation of dendrimer-stabilized gold colloids. This procedure has been reported previously.[27] Briefly, 0.5 ml of a 0.15 mM aqueous dendrimer solution was diluted to 2 ml. 0.5 ml of a 0.01 M aqueous $HAuCl_4$ solution was slowly added with vigorous stirring. Subsequently, 0.2 ml of a 0.1 M solution of $NaBH_4$ in water was added at once, while stirring vigorously. A clear brownish-red solution was obtained.

Microcontact printing. *PPI dendrimer procedure*: The procedure is similar to the one reported in Chapter 5. Instead of a dendrimer solution, a dendrimer-stabilized colloid solution was used as the ink.

PAMAM dendrimer procedure: PDMS stamps were cleaned with EtOH and inked by soaking in a 0.1 mM G4 PAMAM dendrimer solution in EtOH. After drying with nitrogen a stamp was brought in conformal contact with the *β*-CD substrate for 2 min, after which the stamp was carefully removed.

Dip-pen nanolithography. Four-inch polished, 100-cut, p-doped silicon wafers, cut into 2×2 cm^2 samples and microscope glass slides were hand-marked with a diamond-tip prior to monolayer preparation. For the DPN experiments, bare Si_3N_4 tips or Si_3N_4 tips coated with 50 nm of gold were used (Ssens BV, The Netherlands). To reduce the activation energy required for molecular transport from tip to surface, gold coated Si_3N_4 tips were covered with an oligo(ethylene glycol)-terminated SAM.[40] Cleaned gold tips were immersed in a 0.1 mM solution of a thiolated oligo(ethylene glycol) derivative in ethanol overnight, subsequently rinsed with ethanol and dried in a stream of nitrogen. For the writing experiments the tips were inked by soaking them in the dendrimer-stabilized colloid solution for 5 min and dried in air. The tips were mounted in the AFM head, and the AFM cantilever was positioned within the marker with the use of a CCD camera. Patterns were generated in the vicinity of the marker at relative humidities between 25 and 60%.

Loading of immobilized PAMAM dendrimers. This procedure has been reported previously.[32] Briefly, one drop of an aqueous solution containing 0.36 mM K_2PdCl_4,

0.1 M NaCl, and 0.01 M 2-morpholinoethanesulfonic acid (MES, pH = 4.9) as a buffer was put on the substrate for 15 min. Finally, the substrate was rinsed with water.

Electroless deposition. *Cu deposition*: Substrates patterned by μCP or DPN were immersed in an electroless copper deposition bath for 5 min. The bath consisted of an aqueous solution of 40 mM $CuSO_4$, 140 mM Na_2SO_4, 120 mM Na_4EDTA, 300 mM NaHCOO, 30 mM CH_2O in water, adjusted to pH 13 with NaOH.

Co deposition: This procedure has been reported previously.[32] Briefly, the metallization solution was prepared immediately prior to use by mixing three parts of Co stock solution, two parts of reductant, and five parts of water. The Co stock solution was prepared by adjusting a 50 ml aqueous solution with 0.5 g NH_4Cl, 0.3 g $CoCl_2$, and 0.4 g of Na_2EDTA to pH 7 with 2 M NaOH. The reductant consisted of a solution of 1.7 g of dimethylaminoborane in 50 ml of water. The patterned substrate was immersed in the argon-bubbled metallization solution at 310 K for 2-3 min to grow a metallic film.

6.5   References

[1]   Dulcey, C. S.; Georger, J. H.; Krauthamer, V.; Stenger, D. A.; Fare, T. L.; Calvert, J. M. *Science* **1991,** *252*, 551-554.

[2]   Vargo, T. G.; Gardella, J. A.; Calvert, J. M.; Chen, M. S. *Science* **1993,** *262*, 1711-1715.

[3]   Gorman, C. B.; Biebuyck, H. A.; Whitesides, G. M. *Chem. Mater.* **1995,** *7*, 252-254.

[4]   Porter Jr., L. A.; Choi, H. C.; Schmeltzer, J. M.; Ribbe, A. E.; Elliot, L. C. C.; Buriak, J. M. *Nano Lett.* **2002,** *2*, 1369-1372.

[5]   Hrapovic, S.; Liu, Y. L.; Enright, G.; Bensebaa, F.; Luong, J. H. T. *Langmuir* **2003,** *19*, 3958-3965.

[6]   Zangmeister, C. D.; Van Zee, R. D. *Langmuir* **2003,** *19*, 8065-8068.

[7]   Hidber, P. C.; Helbig, W.; Kim, E.; Whitesides, G. M. *Langmuir* **1996,** *12*, 1375-1380.

[8]   Dressick, W. J.; Dulcey, C. S.; Georger, J. H.; Calvert, J. M. *Chem. Mater.* **1993,** *5*, 148-150.

[9]   Carr, D. W.; Lercel, M. J.; Whelan, C. S.; Craighead, H. G.; Seshadri, K.; Allara, D. L. *J. Vac. Sci. Technol., A* **1997,** *15*, 1446-1450.

[10]   Dressick, W. J.; Kondracki, L. M.; Chen, M. S.; Brandow, S. L.; Metijevic, E.; Calvert, J. M. *Coll. Surf. A* **1996,** *108*, 101-111.

[11]   Kind, H.; Bittner, A. M.; Cavalleri, O.; Kern, K.; Greber, T. *J. Phys. Chem. B* **1998,** *102*, 7582-7589.

[12]   Chen, M. S.; Brandow, S. L.; Dulcey, C. S.; Dressick, W. J.; Taylor, G. N.; Bohland, J. F.; Georger, J. H.; Pavelchek, E. K.; Calvert, J. M. *J. Electrochem. Soc.* **1999,** *146*, 1421-1430.

[13]   Delamarche, E.; Geissler, M.; Magnuson, R. H.; Schmid, H.; Michel, B. *Langmuir* **2003,** *19*, 5892-5897.

[14]   Geissler, M.; Wolf, H.; Stutz, R.; Delamarche, E.; Grummt, U. W.; Michel, B.; Bietsch, A. *Langmuir* **2003,** *19*, 6301-6311.

[15]   Delamarche, E.; Donzel, C.; Kamounah, F. S.; Wolf, H.; Geissler, M.; Stutz, R.; Schmidt-Winkel, P.; Michel, B.; Mathieu, H. J.; Schaumburg, K. *Langmuir* **2003,** *19*, 8749-8758.

[16]   Carmichael, T. B.; Vella, S. J.; Afzali, A. *Langmuir* **2004,** *20*, 5593-5598.

[17]   Balogh, L.; Tomalia, D. A. *J. Am. Chem. Soc.* **1998,** *120*, 7355-7356.

[18]   Zhao, M. Q.; Sun, L.; Crooks, R. M. *J. Am. Chem. Soc.* **1998,** *120*, 4877-4878.

[19]   Ottaviani, M. F.; Montalti, F.; Turro, N. J.; Tomalia, D. A. *J. Phys. Chem. B* **1997,** *101*, 158-166.

[20]   Esumi, K.; Suzuki, A.; Aihara, N.; Usui, K.; Torigoe, K. *Langmuir* **1998,** *14*, 3157-3159.

[21]   Grohn, F.; Bauer, B. J.; Akpalu, Y. A.; Jackson, C. L.; Amis, E. J. *Macromolecules* **2000,** *33*, 6042-6050.

[22]   Esumi, K.; Suzuki, A.; Yamahira, A.; Torigoe, K. *Langmuir* **2000,** *16*, 2604-2608.

[23]   Zhao, M. Q.; Crooks, R. M. *Angew. Chem., Int. Ed.* **1999,** *38*, 364-366.

[24]   Ye, H.; Scott, R. W. J.; Crooks, R. M. *Langmuir* **2004,** *20*, 2915-2920.

[25]   Floriano, P. N.; Noble, C. O.; Schoonmaker, J. M.; Poliakoff, E. D.; McCarley, R. L. *J. Am. Chem. Soc.* **2001,** *123*, 10545-10553.

[26]   Yeung, L. K.; Crooks, R. M. *Nano Lett.* **2001,** *1*, 14-17.

[27]   Michels, J. J.; Huskens, J.; Reinhoudt, D. N. *J. Chem. Soc., Perkin Trans. 2* **2002**, 102-105.

[28]   Crooks, R. M.; Lemon, B. I.; Sun, L.; Yeung, L. K.; Zhao, M. Q. *Top. Curr. Chem.* **2001,** *212*, 81-135.

[29]   He, J. A.; Valluzzi, R.; Yang, K.; Dolukhanyan, T.; Sung, C. M.; Kumar, J.; Tripathy, S. K.; Samuelson, L.; Balogh, L.; Tomalia, D. A. *Chem. Mater.* **1999,** *11*, 3268-3274.

[30]   Sun, L.; Crooks, R. M. *Langmuir* **2002,** *18*, 8231-8236.

[31]   Bittner, A. M.; Wu, X. C.; Kern, K. *Adv. Funct. Mat.* **2002,** *12*, 432-436.

[32]   Wu, X. C.; Bittner, A. M.; Kern, K. *Langmuir* **2002,** *18*, 4984-4988.

[33]   Schumacher, R.; Pesek, J. J.; Melroy, O. R. *J. Phys. Chem.* **1985,** *89*, 4338-4342.

[34]   Dressick, W. J.; Dulcey, C. S.; Georger, J. H.; Calabrese, G. S.; Calvert, J. M. *J. Electrochem. Soc.* **1994,** *141*, 210-220.

[35]   Ginger, D. S.; Zhang, H.; Mirkin, C. A. *Angew. Chem., Int. Ed.* **2004,** *43*, 30-45.

[36]   In the height image no pattern was observed.

[37]   Imaging the written pattern by zooming out was not followed by ELD. ELD was only performed on samples that were not zoomed out.

[38]   Lim, J. H.; Ginger, D. S.; Lee, K. B.; Heo, J.; Nam, J. M.; Mirkin, C. A. *Angew. Chem., Int. Ed.* **2003,** *42*, 2309-2312.

[39]   Baars, M. W. P. L.; Karlsson, A. J.; Sorokin, V.; De Waal, B. F. W.; Meijer, E. W. *Angew. Chem., Int. Ed.* **2000,** *39*, 4262-4265.

[40]   Pale-Grosdemange, C.; Simon, E. S.; Prime, K. L.; Whitesides, G. M. *J. Am. Chem. Soc.* **1991,** *113*, 12-20.

Chapter 7

Monolayer-Functionalized Microfluidics Devices for Optical Sensing of Acidity[*]

7.1   Introduction

If one word were to describe the technological advances in the last two decades it would be miniaturization. In many fields the advances in fabrication technology have led to a reduction in size of devices by several orders of magnitude. One area that benefits in particular from this trend is the area of micro total analysis systems (μTAS), also called "lab on a chip".[1] Microfabricated systems are of great current interest in biological and life sciences for the analysis of biological macromolecules,[2,3] as well as for the development of sensors and chemical synthesis on-chip.[4] Microfluidics devices are characterized by a high surface-to-volume ratio: surface effects become dominant in fluid handling and surface properties play a

---

crucial role in chip-based applications. One straightforward method to generate modified surfaces is by using self-assembled monolayers (SAMs). Deposition of SAMs is amenable to implementation in microfluidics devices, since it only requires the flow of a solution or a gas stream of adsorbate molecules through the channels. Many of the microfluidics systems are based on glass or silicon, implying that trichloro- or trialkoxysilane derivatives can be employed for surface modification. SAMs have been used in glass microfluidics networks to engineer surface properties with the aim of controlling liquid motions,[5] confining and aligning of biological macromolecules and liquid crystals,[6,7] stabilizing the liquid interface in an extraction system,[8] controlling electroosmotic flow,[9,10] preventing cell adhesion[10,11] and protein adsorption,[12] and creating zones for specific immobilization of proteins.[13]

When derivatized with fluorescent groups, SAMs can function as optical sensors. This has been shown on flat surfaces,[14-17] and also in microfluidics networks.[17,18] This Chapter describes the immobilization of two molecular switches in a microfluidics device. Molecular switches are systems capable of reversible interconversion between two or more states.[19,20] Among the different families of switches, chemically driven switches are especially interesting for applications in sensing and biology,[21,22] and have even been studied at a single molecule level.[23,24] Immobilization of such a molecular switch in a microfluidics network could potentially be used to probe solutions inside the microfluidics network, to monitor processes inside the channel, or to control processes in the channel.

The first part of this Chapter describes the surface confinement of a molecular switch in a glass microfluidics network by attaching it to a monolayer. The molecular switch interconverts between a fluorescent and non-fluorescent state, based on the acidity of organic solutions that are in contact with the monolayer. To demonstrate the wide scope of this methodology, a second molecular switch is immobilized, which is able to sense differences in pH of *aqueous* solutions by a change in fluorescence response. In this case, a hybrid microfluidics system, consisting of glass and PDMS, is employed. PDMS networks represent a useful alternative for the fabrication of microfluidics devices. They are easy to fabricate, transparent in the UV-vis region, chemically inert, compatible with aqueous solutions,[25] and have a low cost of fabrication.[26] In addition, PDMS shows a strong adhesion to glass surfaces, allowing easy assembly of such hybrid systems.

7.2   Results and Discussion

7.2.1   A Rhodamine B molecular switch

Rhodamine B (RhB) derivatives containing primary amide groups at the 2'-position can be switched reversibly between a fluorescent amide form and a non-fluorescent spirolactam upon addition of acid or base.[27] A molecular switch (shown in Figure 7.1) was synthesized in two steps from RhB. First, RhB was reacted with oxalyl chloride to yield RhB acid chloride, which was subsequently reacted with propylamine to give **1** in 87% yield. Upon addition of base, **1a** converts to its lactam form causing interruption of the electron resonance in the dye. Upon acid addition, the amide moiety in **1b** is protonated and **1a** is formed by opening of the lactam. This reaction results in the recovery of the aromaticity of the system. The UV-vis spectrum in Figure 7.1 clearly shows the difference in absorbance for the two species.
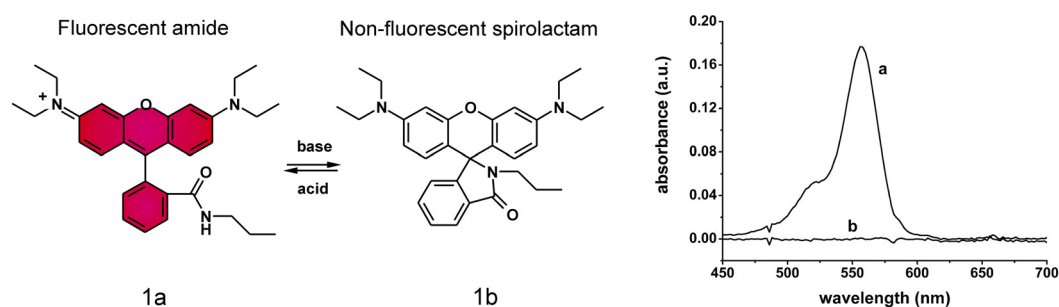

Figure 7.1 *Molecular structures of the RhB-derivatized molecular switch and corresponding UV-vis spectra of a 10^{-5} M solution of **1** in methylene chloride.*

Titrating small amounts of acetic acid to a diluted solution of **1b** results in a marked increase of the fluorescence. Figure 7.2 shows the titration curve for additions of 1 to 25% of acetic acid to a 10^{-6} M RhB lactam solution. The system is sensitive enough to detect the addition of 1% of acetic acid and reaches maximum fluorescence intensity after addition of ca. 20% of acetic acid. Adding base to a solution of **1a** results in quenching of the fluorescence.
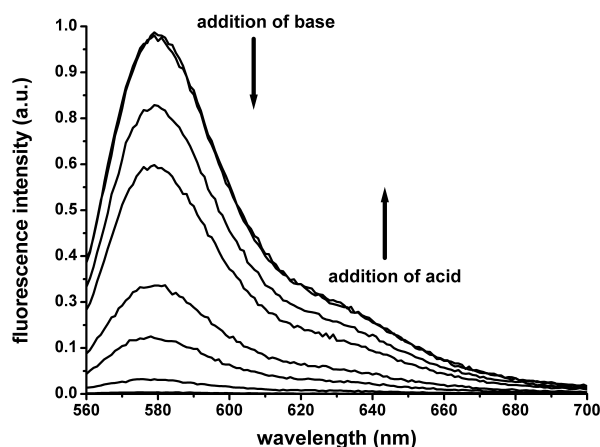
Figure 7.2 Emission spectra of 1 in methylene chloride as a function of added acetic acid or triethylamine.

7.2.2 Immobilization of the molecular switch

RhB was attached to the SiO_2 surface through reaction with a preformed amino monolayer. RhB was first activated by reaction with oxalyl chloride, generating the acid chloride derivative, which can be used to react with the amino monolayer. To limit the number of attached dye molecules to the surface and simultaneously cap the remaining free amines, the reaction was performed in the presence of a 10-fold excess of a non-fluorescent competitive reagent, acetyl chloride. The process is schematically shown in Scheme 7.1.
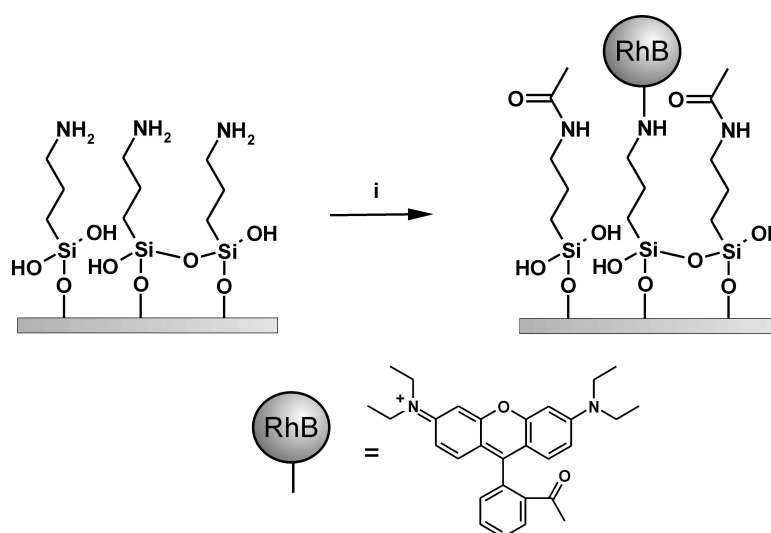
Scheme 7.1 Immobilization of the RhB molecular switch on a preformed amino SAM and capping of the remaining free amines: (i) RhB acid chloride, acetyl chloride, CH_2Cl_2.

The procedure to immobilize the RhB molecules was performed on planar silicon wafers and in microchannels. The planar substrates were used to characterize the monolayer formation and subsequent reaction. Exposing the cleaned substrates to a toluene solution containing 3-aminopropyl triethoxysilane (APTES) resulted in an ellipsometric thickness of 0.6 nm and an advancing contact angle of 63°, corresponding to an amino-terminated monolayer.[28] After reaction with RhB acid chloride and acetyl chloride the ellipsometric thickness increased to 1.2 nm and the advancing contact angle to 69°, indicating a successful surface attachment.

7.2.3   *Optical sensing of acidity inside a microchannel*

Functionalization of the glass surface and subsequent immobilization of RhB inside the microfluidics network was performed by pumping the reagents by means of syringes. A schematic representation of the chip and the network layout is depicted in Figure 7.3. All reagents were introduced at reservoir 4. After functionalization with APTES, the channels were rinsed extensively using pressure driven flows of methylene chloride and ethanol to remove physisorbed material from the walls of the microfluidics network. Subsequently, a solution containing RhB acid chloride and acetyl chloride was flowed through the channels after which the channels were rinsed extensively with methylene chloride.
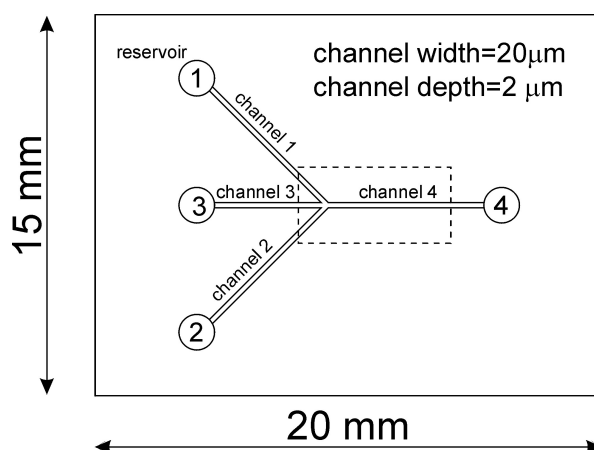

Figure 7.3 Schematic representation of chip layout. The dotted rectangle corresponds to the area inspected with confocal microscopy.

The fluorescence responses of the sensing molecules were monitored by mounting the microfluidics network on a laser scanning confocal microscope (LSCM). The setup is schematically shown in Figure 7.4. A laser light beam was focused on the bottom of the microchannel by an objective lens, exciting the immobilized molecules. The mixture of reflected light and emitted light was captured by the same objective and focused on an Avalanche Photo Diode (APD) via a dichroic mirror. Only the emitted fluorescent light passed through the dichroic mirror and was collected by the APD.
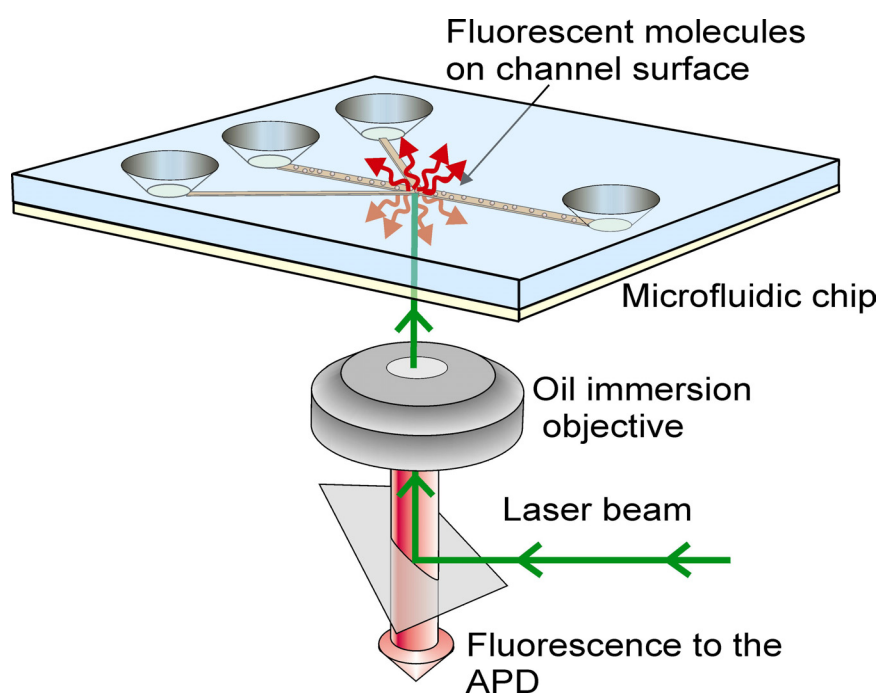
Figure 7.4 *Schematic setup of microfluidics network mounted on an LSCM.*

Figure 7.5 (page 132) shows an example of the fluorescence signal of the RhB monolayer after inspection with an LSCM, and the mean fluorescence intensity measured over 10 line scans. The microfluidics channel is clearly visible and the emitted fluorescence appeared to be uniform throughout the whole device. The enhanced fluorescence intensity at the edges of the channel can be explained by the presence of RhB molecules on the sidewalls of the channel.

To verify if the surface-confined RhB is able to switch in a similar manner as the solution counterpart, a fixed area of the network (70×70 μm^2) was inspected with LSCM while flowing acidic and basic solutions through the channels. Solvents were fed into channels 1 and 2 by means of syringes. Channels 3 and 4 were used as outlets. A flow of acetic acid in methylene chloride (20% v/v) was pumped into the network via inlets 1 and 2 by pressure and the fluorescence intensity of the layer was recorded (Figure 7.6, scan 1). Subsequently, a solution of triethylamine in methylene chloride (20% v/v) was flowed through the channels and the same area of the network was imaged again (Figure 7.6, scan 2). The fluorescence intensity was reduced to approximately 30% of the intensity under acidic conditions, implying that fluorescent molecules were converted from the fluorescent amide form to the non-fluorescent spirolactam form. The fact that less than 100% decrease in fluorescence intensity was observed might be caused by steric constraints of the immobilized dyes in the monolayer. The RhB dye must change its conformation to form the spirolactam. In addition, the high local concentration of dye molecules could result in energy transfer processes that change the fluorescence properties. Reintroducing the acidic solution at inlet 2 showed that the switching process is reversible: the fluorescence emission of the RhB molecules was completely recovered (Figure 7.6, scan 3).

Employing the laminar flow of fluids inside microfluidics networks allowed studying the mixing of fluids of different acidity along the microchannel. Introducing the triethylamine solution at inlet 1 and the acetic acid solution at inlet 2 gave a clear gradient in fluorescence intensity across the channel width, representing the difference in acidity of both solutions (Figure 7.6, scan 3). The effect of diffusion-controlled mixing could be monitored along the microchannel towards outlet 4 (Figure 7.6, scan 4), and at a more downstream position the fluorescence intensity of the solution was found to be uniform across the channel width, indicating complete mixing of the two fluids (Figure 7.6, scan 5). Both solutions are 20% in volume, which means that more acetic acid molecules than triethylamine molecules are present in solution, accounting for the observed fluorescence intensity.[29] Replacing the base in reservoir 1 with the acidic solution created the starting conditions again, and the emission of the layer was fully recovered (Figure 7.6, scan 6).
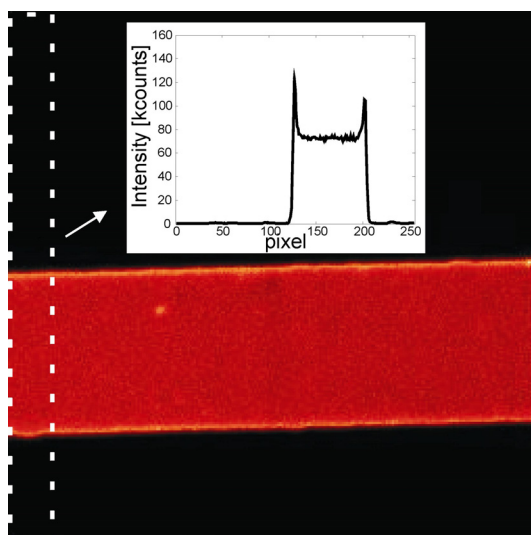
Figure 7.5 *Typical confocal microscopy image (70×70 μm²) and mean fluorescence intensity (inset) measured over 10 scan lines.*

Condition	Inlet 1	Inlet 2
scan1	acid	acid
scan2	base	base
scan3,4,5	base	acid
scan6	acid	acid

Figure 7.6 *Confocal microscopy images of the RhB-functionalized microfluidics chip at different positions along the channel, using various conditions (see Table), and mean fluorescence intensity profiles for each scan averaged over 10 scan lines.*

The reproducibility and stability of the fluorescence signal were further tested by repeated acid/base cycles over a time period of 5.5 h. The normalized fluorescence intensity values are depicted in Figure 7.7 and demonstrate that the system is stable over this time period. The immobilized RhB molecules respond to changes in acidity with a clear and reproducible change in fluorescence emission.
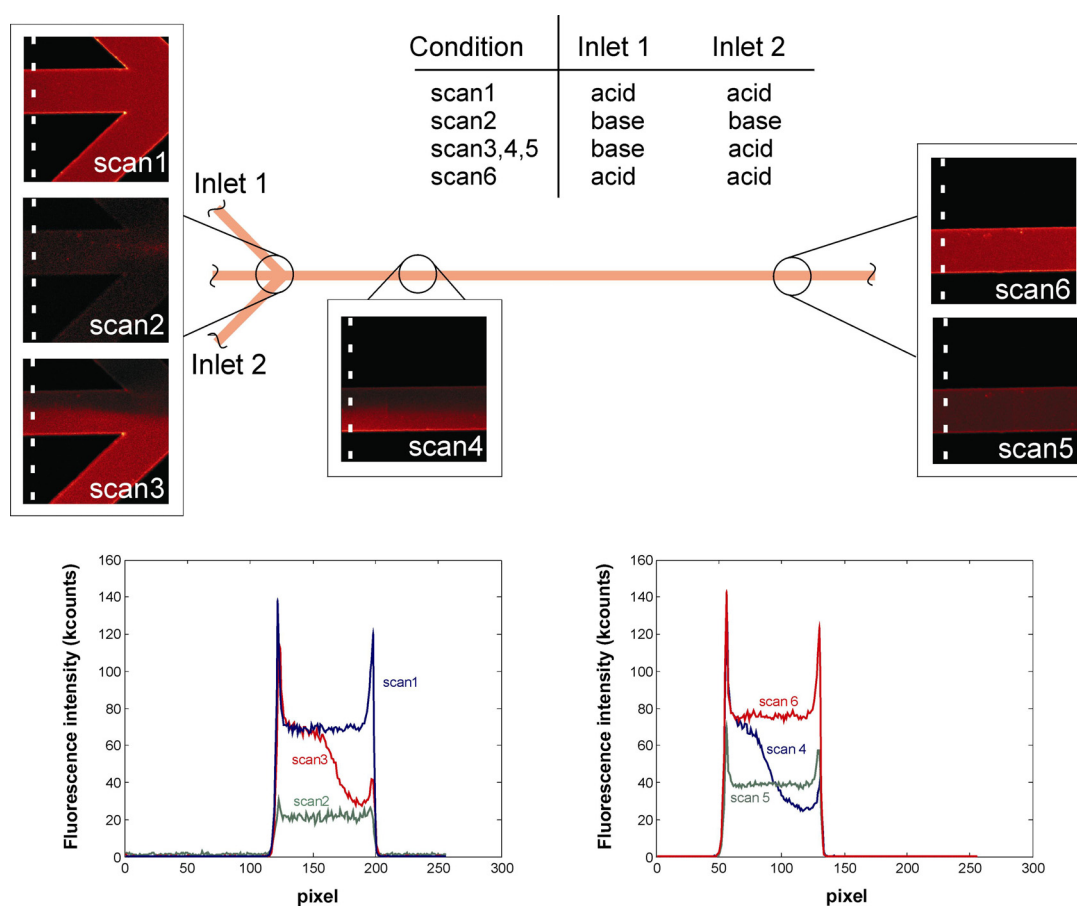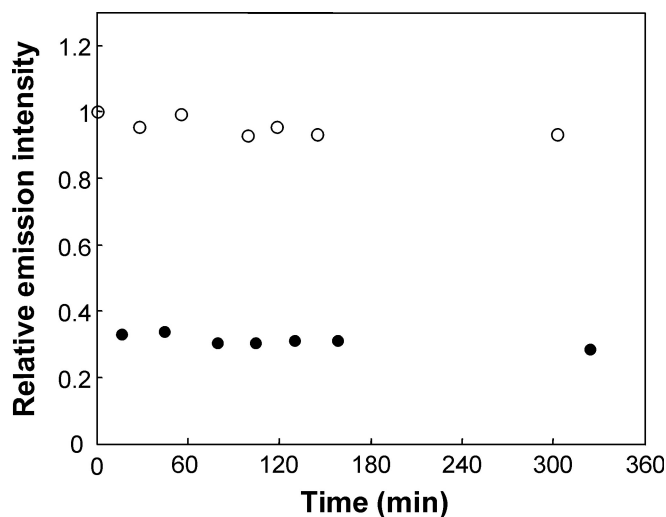

Figure 7.7 *Repeated on-off switching of the RhB molecules in the microfluidics channel. Relative mean fluorescence intensity after alternating exposure to acid (open dots) and to base (solid dots). In between acid/base cycles the channels were rinsed with methylene chloride.*

The possibility of autofluorescence causing the observed changes in fluorescence intensity was ruled out by performing control experiments in a microfluidics network without a functionalized monolayer. The channels were cleaned with the same procedure used prior to functionalization, and acidic and basic solutions were alternatively flown through the channels. The measured autofluorescence of the solvents was ca three orders of magnitude lower than the fluorescence detected in RhB-functionalized channels using the same solvents.

7.2.4 pH sensing in aqueous solution

To broaden the scope of optical sensing from organic solutions to aqueous solutions, a second molecule was used that displays pH-dependent fluorescence.[30] Oregon Green dyes are fluorinated analogs of fluoresceins and are considered to be

better pH sensors than fluorescein because of their higher photostability.[31] One application of this probe is to trace the pH in different cellular compartments.[32]

Here, a functionalized derivative of Oregon Green 514 (OG514) was immobilized onto a preformed monolayer to sense the pH of solutions in microfluidics networks. Instead of using glass-fabricated networks a hybrid system consisting of a microscope glass slide and a poly(dimethylsiloxane) (PDMS) stamp was employed.

To attach OG514 to a monolayer, the succinimidyl ester derivative was reacted with a preformed amino SAM, after which the remaining free amines were capped by reaction with butyl isothiocyanate. The procedure is shown schematically in Scheme 7.2. For this system a monolayer containing a long alkyl chain was employed instead of APTES, as APTES monolayers display only a limited stability in aqueous solution, which is probably caused by a lack of well-defined structure in the siloxane networks of this difunctional reagent.[33]
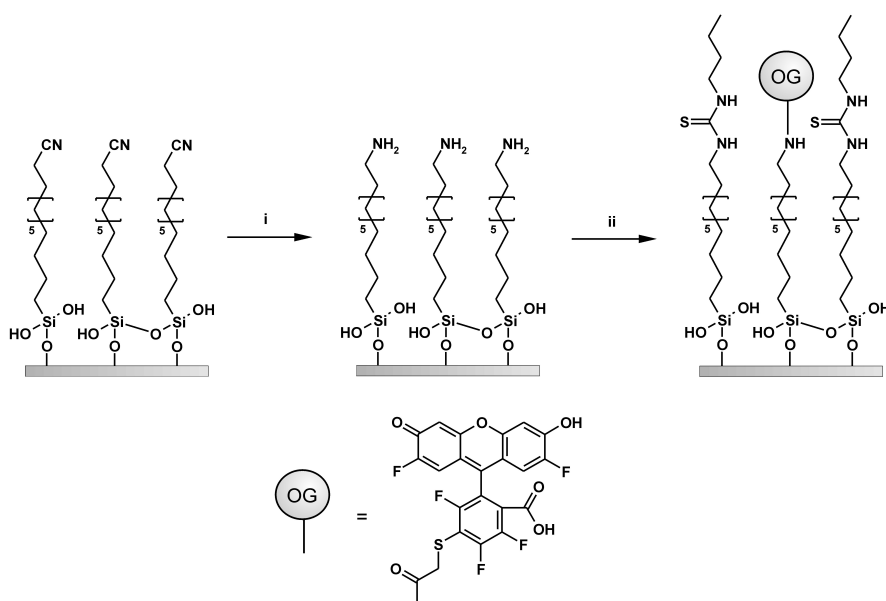
Scheme 7.2 *Immobilization of the OG514 molecular switch on a preformed amino SAM, followed by capping of the remaining free amines: (i) Red Al, toluene, 40 ˚C; (ii) (a) OG 514 succinimidyl ester, diisopropylethylamine, acetonitrile; (b) butyl isothiocyanate, diisopropylethylamine, acetonitrile.*

The procedure to prepare amino SAMs was reported in Chapter 3. First, a cyano-terminated monolayer is prepared from 1-cyano-11-trichlorosilylundecane, which is subsequently reduced to the corresponding amine. The advancing contact angle of the amino monolayer was 61˚ and had an ellipsometric thickness of 2.0 nm.

After attachment of OG514, followed by capping of the remaining free amines with butylisothiocyanate, the advancing contact angle increased to 74° and the ellipsometric thickness to 2.7 nm, indicative of a successful surface attachment.

Microchannels fabricated in PDMS and monolayer-modified microscope glass slides were placed in a custom-made holder onto which tubing was connected for pressure driven flows. A schematic representation of the hybrid system is depicted in Figure 7.8. The bonding between PDMS and the glass was not very strong, probably due to the presence of the sensing layer, but allowed the flowing of aqueous solutions through the channels. A possible solution for this problem could be found in the use of epoxy glue to seal the two components of the device.[34]

The microfluidics system was flushed with four aqueous solutions of different pH value in a random order. Figure 7.9A shows LSCM images of a fixed area (40×40 μm^2) of the microchannel when flowing the four different solutions through the channel. It is evident that the fluorescence intensity depends on the pH of the solution. Figure 7.9B depicts the relative fluorescence intensity as a function of the pH of the solution. The measured data (solid points) were fitted to a sigmoidal curve (solid line), and from this curve a pK_a value was obtained of ca 4.9, which matches the reported pK_a value of 4.8 for OG514 in aqueous solution.[32,35]

The observed increase in fluorescence intensity of a factor two upon going from acidic to basic pH values is modest when compared to similar measurements in solution,[35] but this behavior has been observed before for immobilized Oregon Green dyes.[36] Immobilization results in a high local concentration of dye molecules, which could result in energy transfer processes that change the fluorescence properties of OG514. In addition, part of the dye molecules might be buried within the hydrophobic alkyl chains of the monolayer, rendering them inaccessible to the aqueous solution and therefore unable to switch between the fluorescent and non-fluorescent forms.
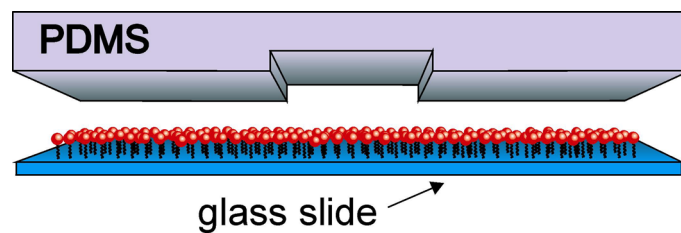
Figure 7.8 *Schematic representation of hybrid microfluidics system: A PDMS stamp on top of a monolayer-modified microscope glass slide.*
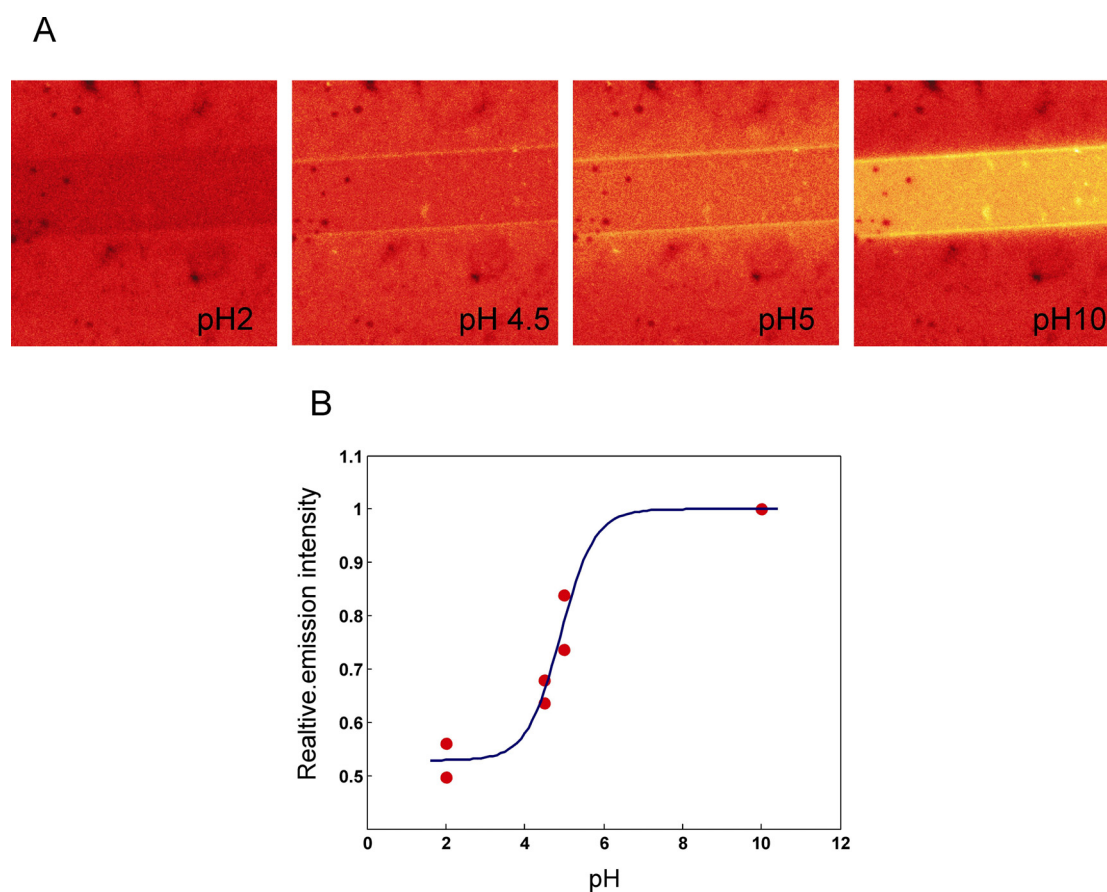
Figure 7.9 *(a) Confocal microscopy images (40×40 μm²) of a PDMS channel on the functionalized microscope glass slide at four different pH values. (b) Relative emission intensities as a function of pH value: experimental data (solid dots) obtained from the Oregon Green 514 functionalized layers and fitted curve (solid line).*

7.3   Conclusions

Monolayers bearing fluorescent groups that are able to sense changes in acidity of the surrounding solution have been immobilized in microfluidics devices. Rhodamine B-derivatized monolayers were confined to the walls of glass-fabricated microchannels and were able to switch between a fluorescent and a non-fluorescent state reversibly, depending on the acidity of the organic solution inside the microchannel. In addition, a hybrid system, consisting of glass and PDMS, was employed to attach Oregon Green 514 to the glass surface. This system was able to sense the pH of aqueous solutions that flowed through the fluidic network by a change in fluorescent properties.

This approach of immobilizing sensing molecules inside microfluidics networks could find widespread application for monitoring processes inside a fluidic network. The main advantage of using fluorescence spectroscopy as an analysis tool is that integration with analysis equipment is not necessary, enabling real-time monitoring of processes inside the fluidic network. The benefit of using SAMs to confine the sensing molecules is their ease in preparation and the short response times, since the sensing molecules are in direct contact with the medium to be analyzed.

7.4   Experimental Section

General procedures. All moisture-sensitive reactions were carried out under nitrogen or argon atmosphere. Reagents are commercially available and were used without further purification, unless stated otherwise. Toluene was distilled from Na, and methylene chloride was purified over active aluminum oxide and stored over molecular sieves. ^{1}H NMR spectra were recorded at 25˚C using a Varian Inova 300 spectrometer. ^{1}H NMR chemical shifts (300 MHz) are given relative to residual CHCl$_3$ (7.25 ppm). FAB-MS spectra were recorded on a Finnigan Mat 90 spectrometer with *m*-nitrobenzylalcohol as a matrix.

Materials and methods. All glassware used to prepare monolayers and to perform subsequent reactions was cleaned by immersing in a *piraña* solution. **Caution:** *piraña* is a very strong oxidant and reacts violently with many organic materials. Subsequently, the glassware was rinsed with large amounts of Millipore water and dried in an oven.

Rhodamine B acid chloride. Rhodamine B (laser grade) (50 mg, 0.104 mmol) was dissolved in 10 ml of dry methylene chloride. A large excess of oxalyl chloride (3 ml) was added to the solution, and the reaction mixture was stirred under argon for 30 min at room temperature. The color of the reaction mixture changed from red to purple. The solvent was evaporated under reduced pressure. The excess of oxalyl chloride was removed by evaporating with a vacuum pump. The obtained purple solid was used without further purification.

Rhodamine B propylamine. Rhodamine B acid chloride was dissolved in 20 ml of dry methylene chloride. Subsequently, 10 equivalents of propylamine were added (61 mg, 1.04 mmol) and the reaction mixture was stirred overnight. The solvent and propylamine were evaporated under reduced pressure. The remaining solid was taken up in dichloromethane and washed with 0.1 N HCl, brine and water. The solvent was removed under reduced pressure to give Rhodamine B propylamine as a pink solid (47 mg, 0.091 mmol, 87%. ^{1}H NMR (CDCl$_3$): δ 7.91 (m, ArH, 1H), 7.43 (m, ArH, 2H), 7.09 (m, ArH, 1H), 6.26-6.48 (m, ArH, 6H), 3.36 (q, 8H, NCH_2CH$_3$), 3.12 (t, 2H, NCH_2CH$_2$), 1.58 (m, 2H, CH$_2$CH_2CH$_3$), 1.19 (t, 12H, CH$_2$CH_3), 0.71 (t, 3H, CH$_2$CH_3); MS (FAB): *m/z* calcd for [M-Cl]$^+$ 484.3; found 484.3.

Substrate preparation. The inside of microfluidics channels, glass slides, and silicon wafers were cleaned in boiling *piraña* (H$_2$SO$_4$ (96%): H$_2$O$_2$ (30%) 3: 1 v/v) for 15 min, rinsed with copious amounts of millipore water and dried in a stream of nitrogen.

Monolayer preparation and surface reactions. *Coupling of RhB to APTES monolayers*: Cleaned channels or silicon wafers were placed in a dry glove box and brought in contact with a 0.25% (v/v) solution of APTES in freshly distilled toluene at room temperature for 2.5 h, after which they were rinsed extensively with toluene and methylene chloride. Finally they were dried in a stream of nitrogen. The functionalized glass substrates were brought in contact with a 10^{-6} M solution of RhB acid chloride in methylene chloride, containing a 10-fold excess of acetyl chloride, for 1.5 h at room temperature. Acetyl chloride was used as a non-fluorescent competitive reagent to limit the number of fluorescent RhB molecules that are linked to the amino-functionalized glass surface. After anchoring RhB acid chloride and acetyl chloride to the surface via amide formation, the substrates were rinsed extensively with methylene chloride and ethanol and finally dried in a stream of nitrogen.

Amino monolayers from 1-cyano-11-trichlorosilylundecane: This procedure is reported in Chapter 3.

Coupling of Oregon Green 514 succinimidyl ester to amino SAMs, and subsequent capping: Oregon Green 514 carboxylic acid, succinimidyl ester (OG 514, Molecular Probes, Inc. Eugene, OR, USA)) was covalently coupled to the amino SAMs by immersion of the substrates in a 10^{-5} M solution of OG 514 in acetonitrile containing 0.05 ml of diisopropylethylamine (DIPEA) for 2.5 h at room temperature. After attachment, the substrates were rinsed and sonicated in acetonitrile and chloroform and dried in a stream of nitrogen. The remaining free amines were capped by immersing the substrates in a solution containing 0.1 ml of butyl isothiocyanate and 0.05 ml of DIPEA in acetonitrile for 2.5 h at room temperature. Finally, the glass slides were rinsed and sonicated in acetonitrile and chloroform and finally in a stream of nitrogen.

UV-vis spectroscopy. UV-vis spectroscopy was performed on a Hewlett Packard 8452A diode array spectrophotometer using quartz sample cells of 10 mm. UV-vis measurements were performed in 10^{-5} M methylene chloride solutions.

Laser scanning confocal microscopy. The confocal set up used for detection of the fluorescent signals is a home-built setup based on a Zeiss Axiovert 135 TV microscope. The microscope is equipped with a home-built scanning stage (80 × 80 μm^2 maximal scan area). Light from an Ar:Kr laser (Spectra Physics, BeamLok 2060) has been used in the experiments (λ_{exc}= 514.4nm). Circularly polarized light has been achieved with a combination of a λ/2 and a λ/4 wave plate. The beam is then coupled into the back aperture of a 63 × Olympus 1.4 NA immersion oil objective via a dichroic mirror (Omega 540DRLP) and focused onto the bottom surface of the channel. The fluorescence emitted from the illuminated volume is separated from the residual excitation light by using a rejection band filter (514.5 Raman) directed onto two glass fibers that serve as pinholes and sent to two avalanche photo diodes (SPCM-AQ-14, EG&G Electro Optics). Fluorescence data recording was performed using an interface card *PCI-MIO-16E4* (National Instruments, USA) and software written in *LabVIEW 6.1* (National Instruments, USA). Areas of 70×70 and 40×40 μm^2 were scanned. Each scan area consisted of 256×256 pixels, photons were collected for 1ms on each pixel, the excitation power was within the range 0.05-0.15 kW/cm^2. Post-processing of the data was also done with software written in *LabVIEW 6.1*.

Microfluidics network fabrication. *Glass networks*: microchips were fabricated with conventional wet-etch technology at MESA$^+$ cleanroom facilities. One side of a 1.1

mm thick Borofloat glass wafer (SCHOTT GLAS, Mainz Germany) was covered with a 0.7 μm thick amorphous silicon (a-Si) layer by means of Plasma Enhanced Chemical Vapor Deposition (PECVD). A layer of photoresist Olin907/17 (Olin Microelectronic Materials Norwalk, CT, USA) was spin-coated on top of the a-Si layer and patterned to act as mask for the Reactive Ion Etching (RIE) of the a-Si layer which served then as a mask for the etching of the channels in the glass substrate. Etching for 12 min in a 10% HF solution resulted in 2 μm deep channels. Access holes to the channels were made in the same substrate by powder blasting. The wafer was then cleaned in acetone by ultrasound and subsequently in fuming HNO_3. The a-Si layer was dissolved in KOH. After rinsing in DI-water and drying, the wafer was fusion-bonded to a 0.5 mm thick Pyrex wafer (Pyrex® 7740, Corning, NY, USA). The Pyrex wafer was then thinned down to 170 μm (required for the confocal microscope) by HF etching, having previously protected the Borofloat side with dicing foil.

PDMS networks: The PDMS microchannels were fabricated using a replica molding method on a silicon wafer patterned by conventional lithography. First the silicon wafer was spun with Ti35 SE image reversal photoresist (Olin Microelectronic Materials Norwalk, CT, USA), and exposed through the same mask used for the glass network fabrication. After development, the resist appeared patterned as a network on the silicon surface. The silicon was then etched to a depth of 2 μm with Reactive Ion Etching (RIE) using SF6 plasma (12 sccmSF6, 50 mTorr, 75 Watt). The photoresist was stripped in acetone, and the silicon surface spincoated with a fluorocarbon solution (1:1 FC40:FC722, 3M Netherlands, Leiden, NL) to prevent the PDMS from sticking to the silicon. PDMS prepolymer and curing agent (Sylgard 184, Dow Corning) were mixed in a 10:1 ratio (v/v), degassed under vacuum, poured onto the master, and cured at 80 ˚C for two hours. The PDMS replica was then carefully peeled off.

Both fabrication techniques resulted in chips with outer dimensions of 15×20 mm². Each chip fits inside a Delrin custom-made holder (Dupont) onto which tubing is connected to create pressure driven flows. In the base of the holder, magnets are placed in order to fix the holder on a stainless steel platform mounted on the scanning stage of the confocal microscope and guarantee in this way a fixed relative position between the chip and the objective.

7.5 References

[1] Harrison, D. J.; Fluri, K.; Seiler, K.; Fan, Z. H.; Effenhauser, C. S.; Manz, A. *Science* **1993,** *261*, 895-897.

[2] Reyes, D. R.; Iossifidis, D.; Auroux, P. A.; Manz, A. *Anal. Chem.* **2002,** *74*, 2623-2636.

[3] Auroux, P. A.; Iossifidis, D.; Reyes, D. R.; Manz, A. *Anal. Chem.* **2002,** *74*, 2637-2652.

[4] Feng, X. Z.; Haswell, S. J.; Watts, P. *Curr. Top. Med. Chem.* **2004,** *4*, 707-727.

[5] Zhao, B.; Moore, J. S.; Beebe, D. J. *Science* **2001,** *291*, 1023-1026.

[6] Li, Y.; Pfohl, T.; Kim, J. H.; Yasa, M.; Wen, Z.; Kim, M. W.; Safinya, C. R. *Biomed. Microdevices* **2001,** *3*, 239-244.

[7] Pfohl, T.; Kim, J. H.; Yasa, M.; Miller, H. P.; Wong, G. C. L.; Bringezu, F.; Wen, Z.; Wilson, L.; Kim, M. W.; Li, Y.; Safinya, C. R. *Langmuir* **2001,** *17*, 5343-5351.

[8] Hibara, A.; Nonaka, M.; Hisamoto, H.; Uchiyama, K.; Kikutani, Y.; Tokeshi, M.; Kitamori, T. *Anal. Chem.* **2002,** *74*, 1724-1728.

[9] Sui, Z. J.; Schlenoff, J. B. *Langmuir* **2003,** *19*, 7829-7831.

[10] Kirby, B. J.; Wheeler, A. R.; Zare, R. N.; Fruetel, J. A.; Shepodd, T. J. *Lab Chip* **2003,** *3*, 5-10.

[11] Cox, J. D.; Curry, M. S.; Skirboll, S. K.; Gourley, P. L.; Sasaki, D. Y. *Biomaterials* **2002,** *23*, 929-935.

[12] Munro, N. J.; Huhmer, A. F. R.; Landers, J. P. *Anal. Chem.* **2001,** *73*, 1784-1794.

[13] Xiong, L.; Regnier, F. E. *J. Chromatogr., A* **2001,** *924*, 165-176.

[14] Flink, S.; Van Veggel, F. C. J. M.; Reinhoudt, D. N. *Adv. Mater.* **2000,** *12*, 1315-1328.

[15] Van der Veen, N. J.; Flink, S.; Deij, M. A.; Egberink, R. J. M.; Van Veggel, F. C. J. M.; Reinhoudt, D. N. *J. Am. Chem. Soc.* **2000,** *122*, 6112-6113.

[16] Crego-Calama, M.; Reinhoudt, D. N. *Adv. Mater.* **2001,** *13*, 1171-1174.

[17] Basabe-Desmonts, L.; Beld, J.; Zimmerman, R. S.; Hernando, J.; Mela, P.; García Parajó, M. F.; Van Hulst, N. F.; Van den Berg, A.; Reinhoudt, D. N.; Crego-Calama, M. *J. Am. Chem. Soc.* **2004,** *126*, 7293-7299.

[18] Rudzinski, C. M.; Young, A. M.; Nocera, D. G. *J. Am. Chem. Soc.* **2002,** *124,* 1723-1727.

[19] Lehn, J.-M., *Supramolecular Chemistry, Concepts and Perspectives.* Wiley VCH: Weinheim, 1995.

[20] Balzani, V.; Gomez-Lopez, M.; Stoddart, J. F. *Acc. Chem. Res.* **1998,** *31*, 405-414.

[21] Stellwagen, A. E.; Craig, N. L. *Trends Biochem. Sci.* **1998,** *23*, 486-490.

[22] Coe, B. J. *Chem. Eur. J.* **1999,** *5*, 2464-2471.

[23] Brasselet, S.; Moerner, W. *Single Mol.* **2000,** *1*, 17-23.

[24] Levi, S. *Supramolecular Chemistry at the Nanometer Level.* Ph.D. Thesis, University of Twente, Enschede, The Netherlands, 2001.

[25] Lee, J. N.; Park, C.; Whitesides, G. M. *Anal. Chem.* **2003,** *75*, 6544-6554.

[26] Ng, J. M. K.; Gitlin, I.; Stroock, A. D.; Whitesides, G. M. *Electrophoresis* **2002,** *23*, 3461-3473.

[27] Adamczyk, M.; Grote, J. *Bioorg. Med. Chem. Lett.* **2000,** *10*, 1539-1541.

[28] Flink, S. *Sensing monolayers on gold and glass.* Ph.D. Thesis, University of Twente, Enschede, The Netherlands, 2000.

[29] Both solutions are 20% in volume, which means that 2.4 times more acetic acid molecules are present.

[30] The RhB molecule used in Chapter 7.2.1 does not switch in aqueous solution.

[31] Haugland, R. P. *Handbook of fluorescent probes and research products, ninth edition.* Molecular Probes: Eugene, 2002.

[32] Lin, H. J.; Szmacinski, H.; Lakowicz, J. R. *Anal. Biochem.* **1999,** *269*, 162-167.

[33] Lee, M. T.; Ferguson, G. S. *Langmuir* **2001,** *17*, 762-767.

[34] Li, S. F.; Chen, S. C. *IEEE Transactions on Advanced Packaging* **2003,** *26*, 242-247.

[35] Delmotte, C.; Delmas, A. *Bioorg. Med. Chem. Lett.* **1999,** *9*, 2989-2994.

[36] Ji, J.; Rosenzweig, N.; Griffin, C.; Rosenzweig, Z. *Anal. Chem.* **2000,** *72*, 3497-3503.

Summary

Functionalized monolayers of alkylsilanes on silicon oxide have been employed as well-defined platforms for surface patterning and sensing. Host monolayers of β-cyclodextrins (β-CDs) were prepared and characterized in detail. These host monolayers have been utilized as molecular printboards by patterning them with suitable guest molecules using lithographic techniques. Fluorescent guest molecules that could bind to the β-CD monolayer via two host-guest interactions created stable, yet reversible fluorescent patterns. The patterns were visualized using confocal fluorescence microscopy. Employing dendrimers that bind via multiple interactions resulted in very stable patterns on the molecular printboard. The immobilized dendrimers function as 'molecular boxes' for anionic dye molecules. Vertical amplification of the patterns was accomplished by electroless deposition of metals on dendrimer-stabilized colloids, generating metal lines of less than 100 nm high on an insulating surface. In addition, monolayers have been applied in microfluidics networks for sensing purposes. Monolayers carrying fluorescent groups were immobilized inside microchannels, where they could sense the acidity of fluids by their fluorescent properties.

A literature overview of self-assembled monolayers (SAMs) on silicon oxide is presented in Chapter 2, which covers the aspects of monolayer formation and subsequent derivatization. The last part of this chapter focuses on the application of SAMs on silicon oxide in nanotechnology. Lithographic techniques that may utilize SAMs, such as photolithography, soft lithography, and dip-pen nanolithography are included.

Chapter 3 describes the preparation of β-CD host monolayers on silicon oxide. An ordered and stable cyano-terminated monolayer was modified in three consecutive surface reactions. Detailed characterization of all monolayers by contact angle measurements, ellipsometric thickness measurements, Brewster-angle infrared spectroscopy, X-ray photoelectron spectroscopy, and time-of-flight secondary ion mass spectrometry indicated the formation of a densely-packed cyclodextrin surface.

The *β*-CD monolayer binds suitable guest molecules in a reversible manner as was shown by adsorption and subsequent desorption of a divalent fluorescent guest molecule. From the desorption data a binding constant was obtained, which corresponds well to previously obtained results with a divalent guest molecule on *β*-CD monolayers on gold, reflecting the similarity between *β*-CD monolayers on gold and on glass.

Chapter 4 deals with the use of *β*-CD monolayers on silicon oxide as molecular printboard. Several fluorescent guest molecules, effectively binding through a divalent interaction, have been used for patterning the molecular printboard via lithographic techniques such as microcontact printing and dip-pen nanolithography. Patterns of (sub-)micrometer dimensions were produced, and the stability of the patterns toward rinsing with aqueous solutions was investigated by monitoring with laser-scanning confocal microscopy (LSCM). In addition, fluorescence microscopy was employed to assess the long-term stability of the patterns, and to quantify the relative amount of molecules that was transferred to the surface upon microcontact printing.

Chapter 5 describes how the molecular printboard is patterned with 5th generation poly(propylene imine) (PPI) dendrimers, which bind in a quasi-irreversible fashion from aqueous solutions. Like in solution, the immobilized dendrimers can be used as a 'molecular box' for the encapsulation of anionic dye molecules such as Fluorescein and Bengal Rose. The encapsulation process is reversible, which was demonstrated by emptying the dendrimers and subsequently filling them with a different dye molecule. In addition, immobilized individual dendrimers, filled with fluorescent molecules, were studied by LSCM. Preliminary single-molecule experiments were performed by extracting Oregon Green 514 (OG514) dyes into the dendrimers in solution, after which they were spin-coated on a glass surface. LSCM images of single OG514 dyes are clearly different from dendrimer images, suggesting that single dendrimer molecules filled with OG514 dyes were observed.

Chapter 6 describes the use of immobilized dendrimers as templates for the electroless deposition of metals. Two procedures to generate less than 100 nm high metal wires on an insulating surface are presented. The first employs electrostatic interactions between the protonated PPI-dendrimer core and aurate anions to prepare dendrimer-stabilized gold colloids in solution. Patterning the molecular printboard with these dendrimer-stabilized colloids, followed by electroless deposition of copper

resulted in the selective growth of copper on the patterned areas. In the second procedure poly(amido amine) (PAMAM) dendrimers are immobilized on the *β*-CD monolayer and subsequently Pd-containing ions are coordinated to the amino and amido groups of the dendrimers. Selective electroless deposition of cobalt yielded cobalt lines of ca 60 nm in height.

SAMs can be implemented in microfluidics devices. Chapter 7 describes the use of monolayers bearing fluorescent groups for optical sensing of acidity in microfluidics devices. SAMs carrying a Rhodamine derivative were prepared inside glass microchannels. It is shown that the fluorescence from the monolayer can be switched 'off' or 'on' by flowing basic or acidic organic solutions through the microfluidics network, respectively. When acidic and basic solutions were introduced simultaneously, the mixing of the two solutions could be monitored by LSCM. In addition, a different fluorescent group was attached to a monolayer to monitor the pH of *aqueous* solutions in microfluidics devices. In this case, a hybrid system consisting of glass and PDMS was employed.

The results presented in this thesis demonstrate the ability of SAMs to create functional surfaces that can be employed as molecular platforms. Employing non-covalent interactions between guest molecules and a host monolayer allows the formation of stable, yet reversible patterns depending on the number of interactions. These immobilized guest molecules may act as templates for further functionalization, providing new strategies for nanofabrication. Combining SAMs with microfluidics devices exploits the high surface to volume ratio to create robust functional interfaces that may find application in fields like sensing or catalysis.

Samenvatting

Dit proefschrift beschrijft het gebruik van functionele monolagen op siliciumoxide (glas) voor oppervlaktepatronering en sensordoeleinden. β-Cyclodextrine (β-CD) gastheermonolagen werden gemaakt en zorgvuldig gekarakteriseerd. Deze gastheermonolagen kunnen dienen als een moleculaire printplaat door ze te patroneren met geschikte gastmoleculen met behulp van lithografische technieken. Fluorescente moleculen, die via twee gast-gastheer interacties binden aan de β-CD monolaag, werden gebruikt om stabiele, maar reversibele patronen te maken. Deze patronen zijn zichtbaar gemaakt met behulp van een confocale microscoop. Immobiliseren van dendrimeermoleculen, die via meer interacties aan de gastheermonolaag kunnen binden, leidde tot de vorming van zeer stabiele patronen. De geïmmobiliseerde dendrimeermoleculen kunnen gebruikt worden als een 'moleculaire doos'. Dit is zichtbaar gemaakt door ze te vullen met fluorescente moleculen. Aan de tweedimensionale patronen werd een derde dimensie toegevoegd door middel van depositie van metalen. Op deze manier werden metaaldraden van minder dan 100 nm hoog gemaakt. Ook zijn monolagen toegepast in geminiaturiseerde chemische systemen om als sensor te kunnen dienen. Monolagen met fluorescente groepen werden vastgezet in kanaaltjes met micrometer dimensies, waar ze de zuurgraad van vloeistoffen konden meten door middel van een verandering in fluorescentie.

Een literatuuroverzicht van zelf-assemblerende monolagen op glas wordt gepresenteerd in hoofdstuk 2. De meeste aspecten van de vorming van monolagen en verdere functionalisering komen aan bod. Het laatste deel van dit hoofdstuk gaat in op de toepassingen van zelf-assemblerende monolagen op glas in de nanotechnologie. Enkele lithografische technieken waarbij monolagen een rol spelen worden behandeld.

Hoofdstuk 3 beschrijft de vorming van β-CD monolagen op siliciumoxide. Uitgaande van een cyanide-getermineerde monolaag worden de β-CD lagen gemaakt in drie achtereenvolgende stappen. Alle monolagen zijn uitgebreid gekarakteriseerd

met behulp van randhoekgoniometrie, diktemetingen, infraroodmetingen, röntgen-foto-electronspectroscopie en "time-of-flight" secundaire-ionen-massaspectrometrie. Deze technieken duiden op een dicht-gepakt β-CD oppervlak. Adsorptie- en desorptie-experimenten met een gastmolecuul dat via twee interacties bindt lieten zien dat de binding met de β-CD monolagen reversibel is. Uit deze desorptie-experimenten werd een bindingsconstante afgeleid, die overeen komt met de bindingsconstante van een soortgelijk gastmolecuul met β-CD monolagen op goud. Hieruit blijkt dat β-CD monolagen op glas en goud sterke overeenkomsten vertonen.

In hoofdstuk 4 wordt het concept van een moleculaire printplaat op glas geïntroduceerd. Verschillende fluorescente gastmoleculen, die via een tweevoudige interactie binden, zijn gebruikt om de moleculaire printplaat te patroneren. Hiervoor zijn lithografische technieken als microcontact-printen en "dip-pen"-nanolithografie gebruikt. Patronen met (sub-)micrometer dimensies werden gecreëerd. De stabiliteit van deze patronen met betrekking tot wasprocedures met waterige oplossingen werd gecontroleerd door middel van confocale microscopie. Tevens werd confocale microscopie aangewend om de stabiliteit van de patronen op lange termijn te bepalen en om de hoeveelheid overgedragen gastmoleculen tijdens het microcontact-printen te vergelijken met adsorptie uit oplossing.

Hoofdstuk 5 beschrijft het patroneren van de moleculaire printplaat met vijfdegeneratie poly(propyleen imine) (PPI) dendrimeren. Deze moleculen binden quasi-irreversibel aan de β-CD monolaag. Net als in oplossing blijken de geïmmobiliseerde dendrimeren te kunnen functioneren als een 'moleculaire doos' voor geschikte moleculen, zoals negatief geladen fluorescente moleculen. Zo werden patronen van dendrimeren selectief gevuld met fluoresceïne en Bengaals rood. Ook kunnen gevulde dendrimeren weer leeggemaakt worden door middel van wasprocedures en vervolgens gevuld worden met een ander molecuul. Eveneens werd getracht individuele, gevulde dendrimeren te visualiseren met confocale microscopie. Daarvoor werden de dendrimeren in oplossing gevuld met fluorescente moleculen (oregon green 514). Na "spin-coaten" op een glasoppervlak was duidelijk het verschil te zien tussen confocale microscopieplaatjes van individuele fluorescente moleculen en van dendrimeren. Dit suggereert dat individuele dendrimeermoleculen inderdaad waargenomen zijn.

Hoofdstuk 6 beschrijft het gebruik van geïmmobiliseerde dendrimeren voor de selectieve depositie van metalen. Twee procedures om metaaldraden van enkele

tientallen nanometers hoog te verkrijgen worden gepresenteerd. De eerste maakt gebruik van electrostatische interacties tussen de geprotoneerde dendrimeerkern en goud-bevattende anionen, om zo dendrimeer-gestabiliseerde colloïden in oplossing te verkrijgen. Wanneer de moleculaire printplaat gepatroneerd werd met deze dendrimeer-gestabiliseerde colloïden, kon selectief koper worden neergeslagen op de patronen. De tweede procedure gebruikt poly(amido amine) (PAMAM) dendrimeren, die op het oppervlak vastgezet werden. Vervolgens werden palladium-bevattende ionen gecoördineerd aan de amine- en amidegroepen van de dendrimeren, die na reductie als katalysator voor cobaltdepositie konden dienen.

Zelf-assemblerende monolagen kunnen toegepast worden in geminiaturiseerde chemische systemen. Hoofdstuk 7 toont aan dat monolagen met fluorescente groepen als optische sensor in geminiaturiseerde systemen kunnen dienen. Monolagen met rhodamine groepen werden bereid in microkanalen van glas. De fluorescentie van deze monolagen kon aan- en uitgeschakeld worden door respectievelijk zure of basische organische vloeistoffen door het microkanaal te laten stromen. Wanneer de zure en basische vloeistoffen tegelijk toegevoerd werden kon het mengen van de twee vloeistoffen gevolgd worden met een confocale microscoop. Ook werd een ander fluorescent molecuul vastgezet aan een monolaag om zo de pH van *waterige* vloeistoffen te meten. Hiervoor werd een hybride systeem, bestaande uit glas en een polymeer (PDMS), gebruikt.

De resultaten die beschreven staan in dit proefschrift laten zien dat zelf-assemblerende monolagen kunnen dienen als een moleculair platform. Door het gebruiken van niet-covalente interacties tussen gastmoleculen en een gastheer-monolaag kunnen stabiele, maar toch reversibele patronen gemaakt worden, afhankelijk van het aantal interacties. Deze geïmmobiliseerde gastmoleculen kunnen als uitgangspunt dienen voor verdere functionalisering, wat zou kunnen leiden tot nieuwe nanofabricatietechnieken. Door gebruik te maken van zelf-assemblerende monolagen in geminiaturiseerde systemen kan de grote oppervlakte/volume verhouding benut worden om zo chemische grensvlakken te verkrijgen die toepassing zouden kunnen vinden als sensoren of katalysatoren.

Dankwoord

Een regenachtige vrijdagmiddag, nog een paar uurtjes tot de borrel, prima omstandigheden voor een dankwoord! Als geboren Groninger, opgegroeid Fries en inmiddels zo'n beetje genaturaliseerd Tukker is het dan mijn tijd om afscheid te nemen van het AIO bestaan.

Het is ontzettend moeilijk om alle mensen die de afgelopen 4 jaar een bijdrage hebben geleverd aan de totstandkoming van dit boekje in een paar bladzijden te bedanken. Ik ga het toch proberen. Als eerste wil ik mijn promotor David Reinhoudt bedanken. David, bedankt voor het vertrouwen dat je altijd in mij hebt gehad, zelfs op momenten dat ik het zelf niet echt meer had. Ook wil ik je bedanken voor de vrijheid binnen mijn project die je me gegeven hebt, ik denk dat de switch naar CD-monolagen op glas niet verkeerd heeft uitgepakt.

Ook mijn co-promotor Bart Jan Ravoo wil ik bedanken. Bart Jan, jij werd mijn dagelijks begeleider op een moment dat alles net begon te rollen. Bedankt voor je enthousiasme, de sturing die je gaf wanneer nodig, de etentjes bij jou thuis (een goed organisch chemicus kan ook goed koken!), maar vooral voor de frisse blik die je meenam uit Ierland. Tevens heeft jouw snelheid in manuscripten corrigeren zeker bijgedragen aan de snelheid waarin mijn proefschrift tot stand kwam. Frank van Veggel wil ik bij deze bedanken voor de begeleiding tijdens de eerste twee jaar van mijn onderzoek. Ook al waren het niet de meest produktieve, daar leer je misschien nog wel het meest van.

Dan Jurriaan, of 'de Huskens', je bent nooit officieel mijn begeleider geweest, maar toch heb ik veel aan je te danken. Jij overzag de mogelijkheden van de CD-monolagen op glas al voordat ik wist hoe ik ze moest maken! Jouw enthousiasme (Hihihiiaaaaarrr!!!) was zelfs aanstekelijk voor nuchtere noorderlingen.

In het bijzonder wil ik bedanken mede nuchtere noordeling Alart Mulder. Toen jij voorstelde "laten we eens proberen CD-monolagen op glas te maken" had ik geen idee dat dat de basis voor mijn proefschrift zou worden. Naast ons eendrachtig samenwerken in het lab heb ik me ook altijd zeer vermaakt tijdens onze competatieve

bezigheden. Of dit nu ging om bier/cola drinken, tafeltennissen, snookeren, kaarten, tennissen of voetballen, verliezen was geen optie!

Als full-time monolagen-bakker heb je natuurlijk niet voldoende tijd (en kwaliteiten) om zelf ingewikkelde syntheses uit te voeren. Daarom ben ik Hans Beijleveld, Jurjen ter Maat en Andrea Sartori erg dankbaar dat ik hun moeizaam verkregen gastmoleculen mocht gebruiken. Een speciaal woord van dank verdient daarbij ook Christian Nijhuis, die zonder morren vele grammen dendrimeer en CD-heptaamine aan mij afstond, zonder ook maar éénmaal te vragen of ie daar nog wat voor terug kreeg!

For operating the world smallest pen, the help of Mária Péter was essential. Mária, thank you for the countless hours you spent behind the AFM, imaging, writing, and re-imaging. Echter, kleine geschreven patroontjes moeten ook weer teruggevonden worden. Samenwerken met de Optische Technieken groep van prof. Niek van Hulst was daarbij onontbeerlijk. In het bijzonder wil ik Jacob Hoogenboom bedanken. Jacob, als die microscoop maar eenmaal uitgelijnd is, is het imagen van elk sample een peulenschil voor jou.

Eén van de doelstellingen waar ik vier jaar geleden mee begon was het combineren van monolagen en geminiaturiseerde systemen. Hoewel dit een stuk lastiger bleek dan verwacht is er toch een mooi hoofdstuk uitgekomen. Hiervoor heb ik hulp gekregen van Petra Mela. Petra, thank you for your efforts to get this damn monolayer chemistry inside the channels and for all the time you spent imaging them. Ook wil ik bij deze prof. Albert van den Berg bedanken voor zijn toch niet aflatende enthousiasme tijdens de MiCS meetings.

Een mens heeft maar twee handen en een dag maar 24 uur. Daarom wil ik de volgende personen bedanken voor het uit handen nemen van taken waarin zij veel beter zijn dan ik: Albert van den Berg voor de XPS metingen, Mark Smithers voor het SEMen, Birgit Hagenhoff voor de TOF-SIMS metingen, Marcel de Bruine voor amanuensele ondersteuning, Carla Weber-van der Ploeg en Izabel Katalanc voor de administratieve zaken en Tieme Stevens voor de massaspectrometrie (er is er toch nog eentje in m'n proefschrift terecht gekomen).

I am greatly indebted to Jurriaan Huskens, Alart Mulder, and Becky Zimmerman who took the time to struggle their way through my concept-thesis looking for mistakes.

During the grand total of five years I have spent in the SMCT group, many people from all over the world (but particularly from the Mediterranean region) came and went. The following people, who are listed in complete random order, I would like to thank for making these past years very enjoyable: Emiel & Monica, Wiljan, Venkat, Fijs, Mattijs, Francesca, Becky, Lourdes, Marta, Richard, Miguel, Olga, and many others.

Mijn paranimfen Alart Mulder en Christian Nijhuis bedank ik alvast voor de zware ceremoniële taken die zij op zich hebben willen nemen.

De laatste regels zijn gereserveerd voor een aantal mensen die niets met chemie te maken hebben. Pa en ma, bij deze wil ik jullie bedanken voor het geven van alle vrijheid die ik me maar kan wensen. Toen ik vertelde dat ik een promotieonderzoek wilde gaan doen was dat waarschijnlijk een groot mysterie voor jullie. Hoewel ik vrees dat er na vier jaar op dat gebied nog niet veel is veranderd, waardeer ik jullie continue vertrouwen toch heel erg. Lieve Cornelie, gelukkig zijn er buiten het werk nog zoveel andere dingen te doen. Die doe ik het allerliefst met jou. De afgelopen stressvolle tijd heb ik jouw flexibiliteit enorm bewonderd. Ik kan alleen maar hopen dat jij over ruim twee jaar hetzelfde kunt zeggen.

Steffen Onclin

Curriculum Vitae

Steffen Onclin werd geboren op 11 februari 1975 te Groningen. Na het behalen van zijn VWO-diploma aan het Bogerman College te Sneek, begon hij in 1994 aan de studie Chemische Technologie aan de Universiteit Twente. In het kader van deze studie werkte hij vier maanden op het NatLab van Philips in Eindhoven. In 2000 studeerde hij af binnen de vakgroep Supramoleculaire Chemie en Technologie onder leiding van prof. dr. ir. David N. Reinhoudt. Zijn afstudeerwerk betrof de synthese van metaal-complexerende calixarenen die toegepast zouden kunnen worden als optische sensoren. Vanaf juli 2000 tot en met juli 2004 werd zijn promotieonderzoek uitgevoerd binnen dezelfde vakgroep onder supervisie van prof. dr. ir. David N. Reinhoudt en dr. Bart Jan Ravoo. De resultaten van dit promotieonderzoek staan beschreven in dit proefschrift.